NIO/SP-30/2017
SSP 3055

DISTRIBUTION RESTRICTED

Studies on extreme waves, extreme water levels, storm surge, tsunami height and coastal morphology for Coastal Road project

Sponsored by

Municipal Corporation Greater Mumbai (MCGM)
Mumbai

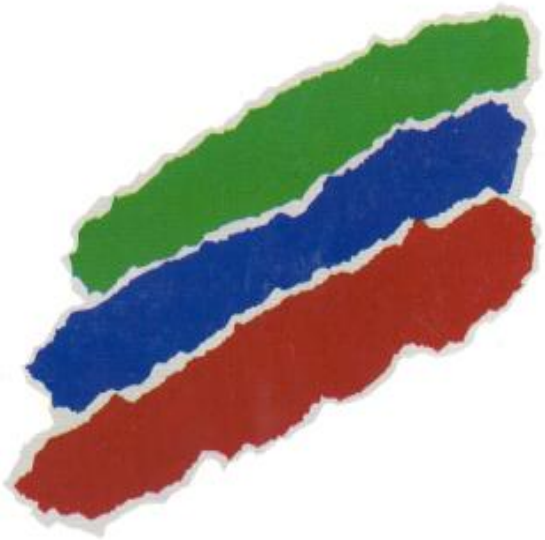

July 2017

सीएसआईआर – राष्ट्रीय समुद्र विज्ञान संस्थान
CSIR-NATIONAL INSTITUTE OF OCEANOGRAPHY
(वैज्ञानिक तथा औद्योगिक अनुसंधान परिषद**)**
(COUNCIL OF SCIENTIFIC & INDUSTRIAL RESEARCH)
दोना पावला, गोवा भारत **/ DONA PAULA, GOA - 403004 India**
फ़ोन/**Tel : 91(0)832-2450450/ 2450327**
फैक्स **/Fax: 91(0)832-2450602**
इ-मेल/**e-mail : ocean@nio.org**
http:// www.nio.org

NIO/SP-30/2017
SSP 3055

Studies on extreme waves, extreme water levels, storm surge, tsunami height and coastal morphology for Coastal Road project

Sponsored by

Municipal Corporation Greater Mumbai (MCGM)
Mumbai

July 2017

सीएसआईआर – राष्ट्रीय समुद्र विज्ञान संस्थान
CSIR-NATIONAL INSTITUTE OF OCEANOGRAPHY
(वैज्ञानिक तथा औद्योगिक अनुसंधान परिषद)
(COUNCIL OF SCIENTIFIC & INDUSTRIAL RESEARCH)
दोना पावला, गोवा भारत / DONA PAULA, GOA - 403004 India
फ़ोन/Tel : 91(0)832-2450450/ 2450327
फैक्स /Fax: 91(0)832-2450602
इ-मेल/e-mail : ocean@nio.org
http:// www.nio.org

PROJECT TEAM

Jaya Kumar Seelam Project leader

Jyoti P. Kerkar

Mani Murali R.

Pednekar, P.S.

List of Figures

List of tables

Chapter 1

1 INTRODUCTION

1.1 Background

Municipal Corporation of Greater Mumbai (MCGM) has proposed a coastal road along the Mumbai coast to ease the vehicular traffic. The proposed coastal road, approximately 35.6 km long, comprises a combination of the road based on reclamation, bridges, elevated roads and tunnels along the western side of Mumbai. The entire length is divided into two parts, i.e., North Part and Southern Part. The south part is approximately about 9.98 km from Princess Flyover to Worli Sea Link, and north part is 25.62 km from Bandra Sea Link to Kandivali Junction. It includes constructions Tunnels, Bridges, Road on stilts, Land fill Road; Land fill road without obstructing Mangroves and Elevated roads. The southern part comprises of 2 tunnels each of about 3.452 km in length. A total reclamation area for the southern part will be about 90 ha.

This proposed road improves the quality of life by providing easy access to essential services and various products, access to improved health and education facilities, strengthening of the economy by easy transportation of the different materials of daily use, etc. It also resolves the traffic congestion in Mumbai and to enable the creation of the much needed recreational open spaces.

MCGM awarded a project to CSIR-National Institute of Oceanography (NIO), to provide extreme water levels, waves and morphology changes due to proposed coastal road, especially due to the reclamation areas. The extreme water levels are required to fix the top level of the coastal road. The morphological impacts of the reclamations are required so that there is minimal impact on the near shore coastal dynamics.

1.2 Objectives

The scope of work for the study is as follows:

a) to undertake extreme wave analysis studies to establish the extreme wave climate at select points along proposed coastal road

b) to provide storm surge and associated extreme water levels, information on probable tsunami heights considering earlier events at select points along proposed coastal road

c) to model the hydrodynamics and morphology changes along the proposed coastal road

d) to provide advisories on the proposed coastal road interaction with the coast

1.3 Activities carried out related to this project

a. Numerical model simulations of cyclonic storms to obtain extreme waves and surge levels.
b. Estimation of design wave heights from hindcast wave data.
c. Numerical simulation of tsunami heights.
d. Numerical modelling of hydrodynamics and morphology changes.
e. Expert advisories on the location/orientation of bund structures, erosion mitigation measures, etc.

Chapter 2

2 EXTREME WAVES

2.1 Introduction

Assessment of wave climate in the region is essential for a range of coastal works, of which the design of coastal structures is of primary importance. The wave climate also influences the morphology of the near shore regions along with the near shore currents. Extreme waves generally occur during cyclonic storms and wave measurements during storms along the west coast of India are scarcely available. In order to obtain storm waves numerical modelling is carried out. In this study, 21 cyclonic storms that have passed within 500 km radius of Mumbai over a period of 35 years is considered. The tracks of the 21 storms are presented in Fig. 2.1 to Fig. 2.4.

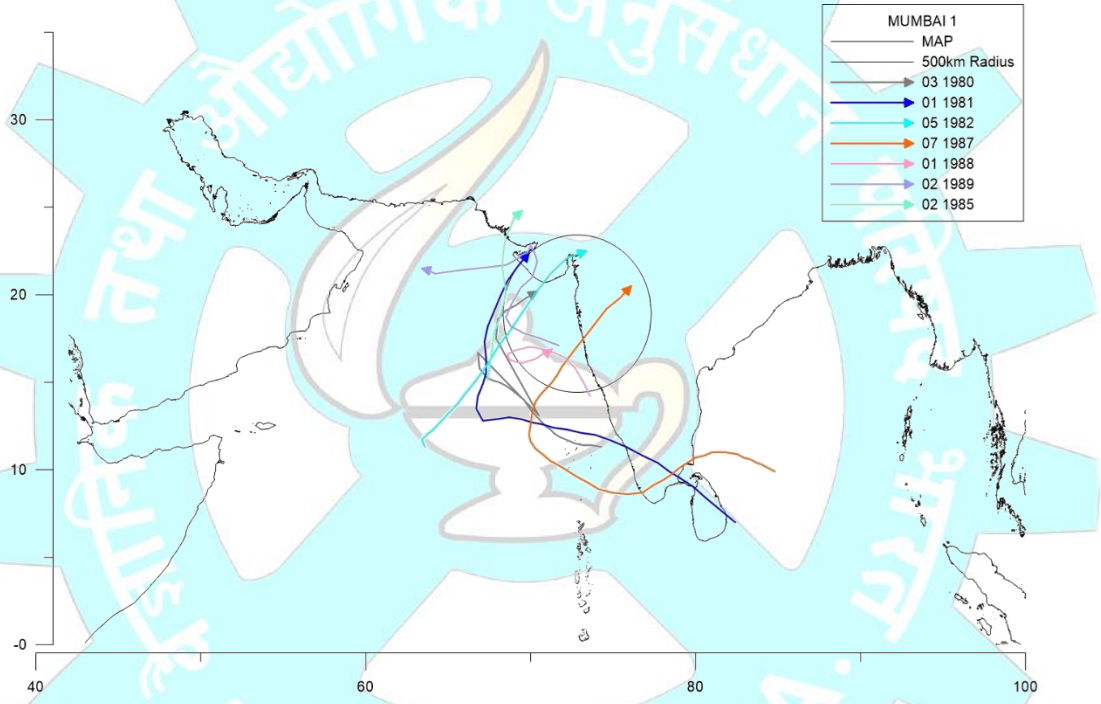

Fig. 2.1. Cyclones that passed near Mumbai coast between 1980 and 1990

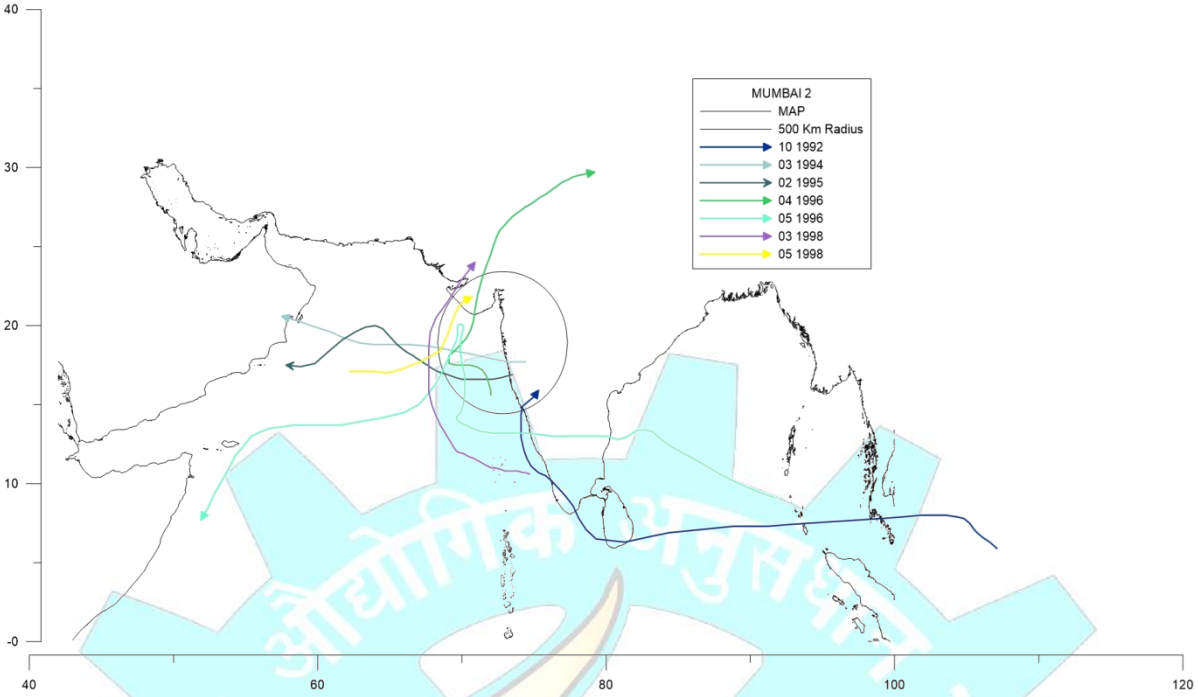

Fig. 2.2. Cyclones that passed near Mumbai coast between 1991 and 2000

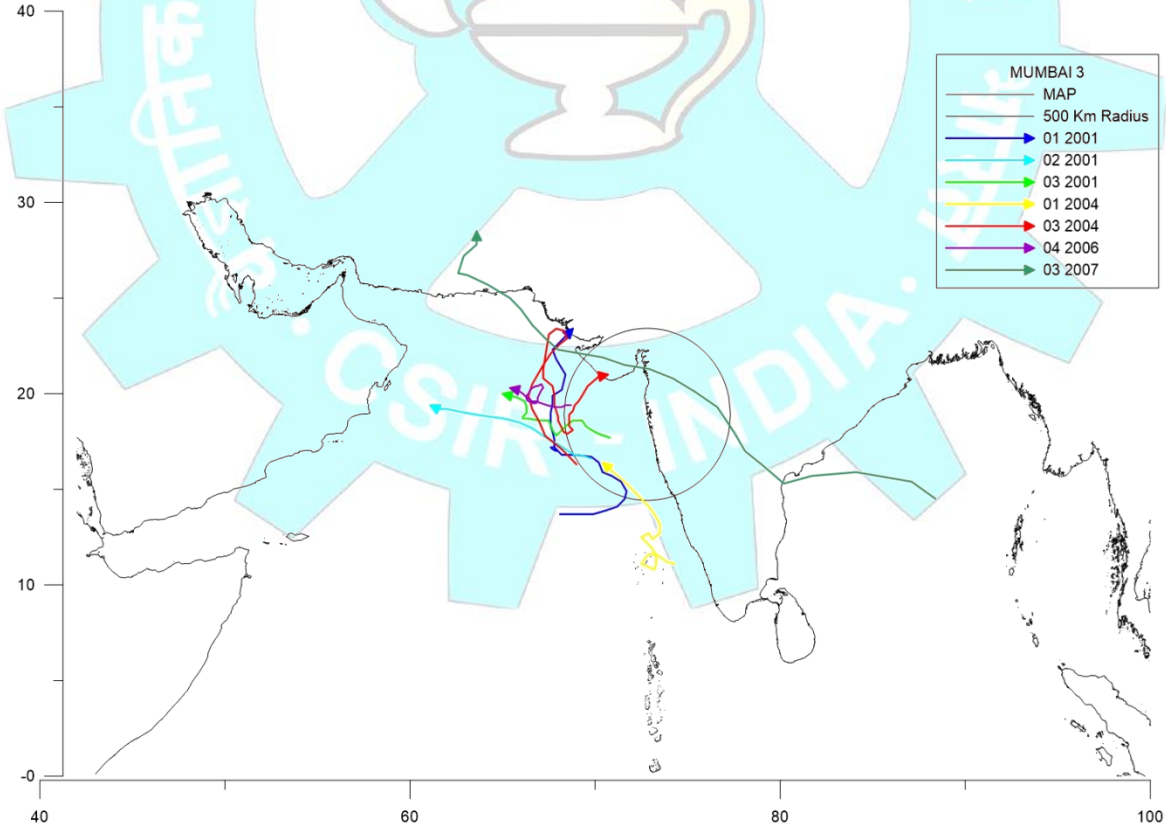

Fig. 2.3. Cyclones that passed near Mumbai coast between 2001 and 2010

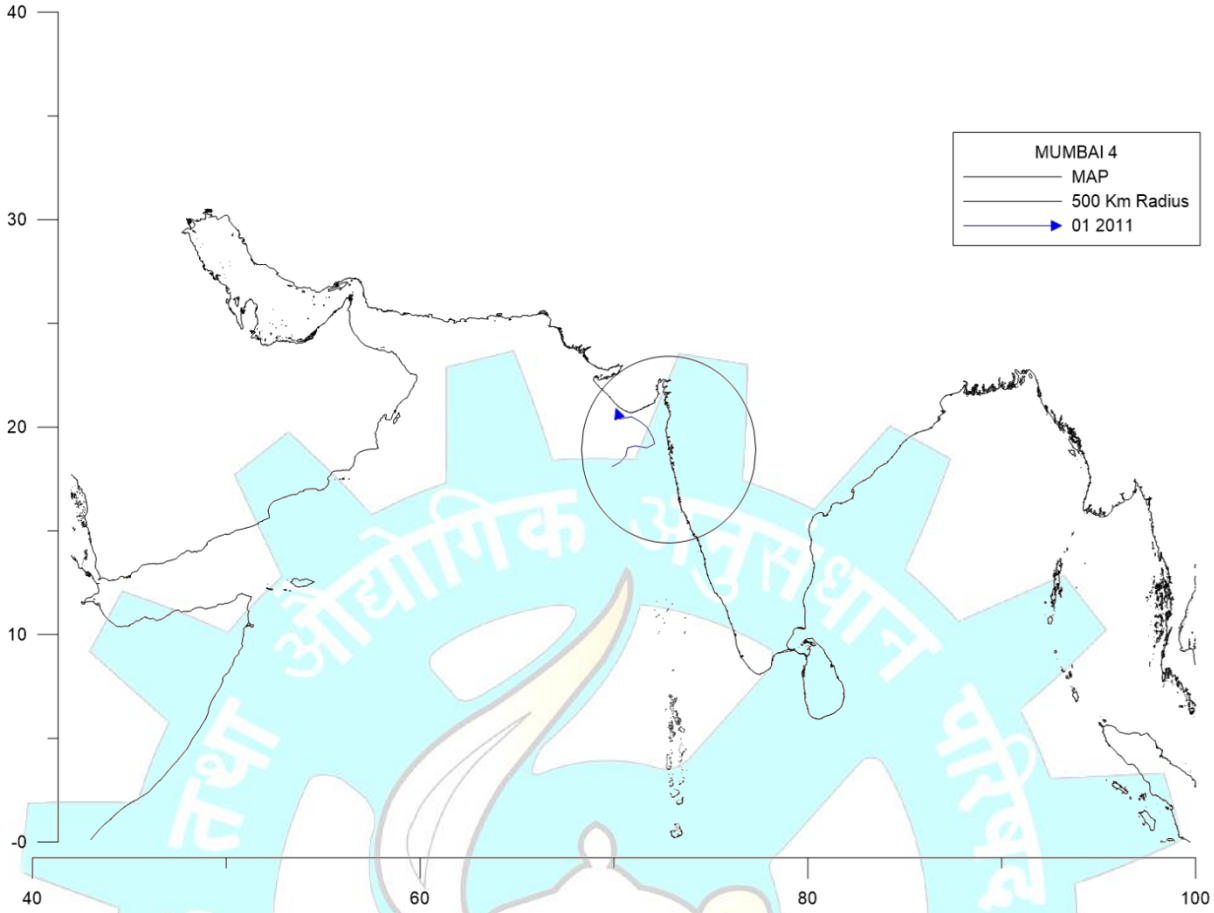

Fig. 2.4. Cyclones that passed near Mumbai coast between 2011 and 2014

2.1.1 Storm winds

Storm winds are generated over the study region using parametric storm wind models. The MIKE21-cyclone wind generation tool was used with parametric inputs obtained from the Joint Typhoon Warning Centre (JTWC) site (http://metoc.ndbc.noaa.gov/jtwc/best_tracks). The Rankine parametric model was used for generating wind field for each of the 21 cyclones between 1980 and 2014. The wind field output consists of space and time varying wind speed, wind direction and pressure fields. The modified Rankine vortex model uses the following velocity distribution:

$$V_g(r) = \begin{cases} V_{max} \cdot \left(\frac{r}{R_{mw}}\right) & for\ 0 \le r < R_{mw} \\ V_{max} \cdot \left(\frac{r}{R_{mw}}\right)^X & for\ r > R_{mw} \end{cases}$$

where:

R_{mw} is the radius to maximum wind

V_{max} is the maximum wind speed

r is radius from centre to the desired point in the domain

X is shape parameter

The shape parameter X is used to adjust the wind speed distribution in the radial direction. Typical values of X are in the range of 0.4 to 0.6

The input data used to this parametric wind model includes bathymetry of model area (Fig. 2.5), radius to maximum winds (R_m), maximum wind speed (V_{max}), forward speed (V_f), central pressure (P_c) and neutral pressure.

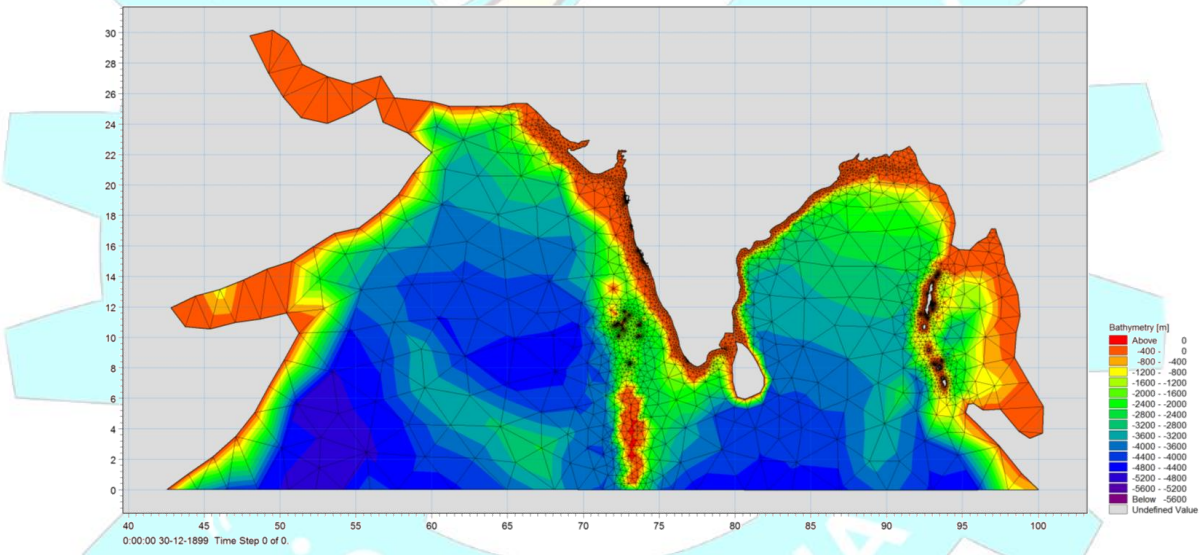

Fig. 2.5. Bathymetry and mesh adopted for model area

The maximum wind speed among the storms passing through Mumbai is 24.73m/s was generated by the storm developed during May 2001. The maximum wind speeds that have occurred for the 21 storms off Mumbai are presented in Table 2.1. The wind speeds shown in the table are extracted at location 18.92ºN; 72.82ºE located in the Back Bay region.

Table 2.1. Maximum wind speeds of storms off Mumbai coast

Sl. No.	STORM NO.	DURATION		MAX. WIND SPEED (m/s)
		FROM	TO	
1	bio198003	12-11-1980	19-11-1980	20.46
2	bio198101	25-10-1981	02-11-1981	14.54
3	bio198205	04-11-1982	09-11-1982	18.08
4	bio198502	28-05-1985	01-06-1985	12.65
5	bio198707	02-12-1987	13-12-1987	13.28
6	bio198801	08-06-1988	12-06-1988	11.33
7	bio198902	07-06-1989	13-06-1989	7.62
8	bio199210	06-11-1992	17-11-1992	8.96
9	bio199502	11-10-1995	18-10-1995	12.58
10	bio199604	15-06-1996	25-06-1996	13.93
11	bio199605	14-10-1996	02-11-1996	17.58
12	bio199803	01-06-1998	09-06-1998	20.75
13	bio199805	15-10-1998	18-10-1998	9.63
14	bio200101	21-05-2001	29-05-2001	24.73
15	bio200102	24-09-2001	28-09-2001	9.02
16	bio200103	08-10-2001	13-10-2001	10.56
17	bio200401	04-05-2004	09-05-2004	10.30
18	bio200403	30-09-2004	10-10-2004	8.68
19	bio200604	19-09-2006	26-09-2006	9.58
20	bio200703	20-06-2007	27-06-2007	8.36
21	bio201101	09-06-2011	12-06-2011	3.18

2.1.2 Storm waves

The storm winds generated are used as input in the MIKE21-spectral wind wave model to generate storm induced waves. Simulations were carried out in order to generate different wave parameters such as significant wave height, wave period, and wave direction. The maximum significant wave height for each cyclone and corresponding location was obtained by analysing the model outputs. The values of maximum significant wave height at 20m water depth (19° 4'14.74"N; 72°35'21.65"E) for the 21 cyclones are given in Table 2.2.

Table 2.1. Maximum storm induced significant wave heights at 20m water depth

Sl. No.	STORM NO.	DURATION		MAX SIGNIFICANT WAVE HEIGHT (m)
		FROM	TO	
1	bio198003	12-11-1980	19-11-1980	2.63
2	bio198101	25-10-1981	02-11-1981	2.48
3	bio198205	04-11-1982	09-11-1982	4.89
4	bio198502	28-05-1985	01-06-1985	1.65
5	bio198707	02-12-1987	13-12-1987	1.66
6	bio198801	08-06-1988	12-06-1988	1.31
7	bio198902	07-06-1989	13-06-1989	0.69
8	bio199210	06-11-1992	17-11-1992	0.41
9	bio199502	11-10-1995	18-10-1995	1.51
10	bio199604	15-06-1996	25-06-1996	2.87
11	bio199605	14-10-1996	02-11-1996	3.52
12	bio199803	01-06-1998	09-06-1998	3.94
13	bio199805	15-10-1998	18-10-1998	1.45
14	bio200101	21-05-2001	29-05-2001	4.23
15	bio200102	24-09-2001	28-09-2001	0.92
16	bio200103	08-10-2001	13-10-2001	1.32
17	bio200401	04-05-2004	09-05-2004	1.10
18	bio200403	30-09-2004	10-10-2004	1.01
19	bio200604	19-09-2006	26-09-2006	1.31
20	bio200703	20-06-2007	27-06-2007	0.28
21	bio201101	09-06-2011	12-06-2011	0.31

2.1.3 Design waves

Design wave heights are obtained by statistical extreme value analysis of the significant wave heights over a period of time. Wave data for a period of 46 years at 20m water depth off Mumbai available at CSIR-NIO is used in this analysis. This historic hindcast data is obtained from a validated regional wave model available at CSIR-NIO and does not contain storm waves. Therefore the storm wave data obtained from model simulations is included in the hindcast wave data at 20m depth and is subjected to extreme value analysis. Weibull-3 parameter statistical distribution method is used to arrive at the design waves for return periods of 1, 50 and 100 years at 20m water depth. These design wave heights for different return

periods are shown in Table 2.3. These design wave heights are further transformed close to coast. Two different wave periods (8s and 10s) and two wave directions (225° and 247.5°) are considered for each of the design wave height. The transformed design wave heights at 19 points (Fig. 2.6. and Table 2.4) along the proposed coastal road are extracted. The design wave heights for different return periods are provided in Table 2.5.

Table 2.3. Design wave heights at 20m water depth off Mumbai

Return Period	Wave height (m)
1 in 1 year	5.68
1 in 50 year	6.98
1 in 100 year	7.20

Fig. 2.6. Figure showing 19 locations for extraction of wave, surge and tsunami data

Table 2.4. Positions of 19 points considered

Location	Longitude (°N)	Latitude (°E)	Water Depth w.r.t MSL (m)
L1	72.81865	19.11973	5.00
L2	72.81679	19.07294	3.80
L3	72.81628	19.0628	3.50
L4	72.81918	19.05485	4.60
L5	72.81645	19.04815	6.60
L6	72.81506	19.042	5.70
L7	72.81114	19.00915	4.10
L8	72.80907	19.00201	5.00
L9	72.80953	18.99531	3.50
L10	72.80851	18.98877	3.70
L11	72.81159	18.98385	2.60
L12	72.80503	18.9792	2.70
L13	72.80052	18.97249	3.50
L14	72.79864	18.96762	3.50
L15	72.79831	18.96297	2.90
L16	72.80687	18.94932	2.51
L17	72.81563	18.92323	3.50
L18	72.82242	18.94352	2.60
L19	72.79873	18.96019	2.51

Table 2.5. Design wave heights

Return Period	1 in 1 Year				1 in 50 Year				1 in 100 Year			
Wave period (s)	8	8	10	10	8	8	10	10	8	8	10	10
Wave direction (°)	225	247.5	225	247.5	225	247.5	225	247.5	225	247.5	225	247.5
L1	0.77	0.82	0.90	0.94	0.80	0.85	0.93	0.95	0.80	0.85	0.94	**0.95**
L2	0.99	1.07	1.11	1.17	1.03	1.10	1.14	1.18	1.03	1.11	1.15	**1.18**
L3	1.27	1.33	1.45	1.47	1.32	1.37	1.48	1.49	1.32	1.38	1.48	**1.49**
L4	1.19	1.31	1.41	1.55	1.25	1.38	1.51	1.62	1.25	1.39	1.52	**1.62**
L5	1.23	1.40	1.44	1.65	1.30	1.47	1.55	1.71	1.30	1.48	1.56	**1.72**
L6	1.28	1.46	1.50	1.72	1.35	1.53	1.62	1.78	1.36	1.54	1.63	**1.79**
L7	1.27	1.35	1.37	1.42	1.31	1.36	1.40	1.45	1.32	1.36	1.40	**1.46**
L8	1.43	1.66	1.63	1.85	1.51	1.71	1.74	1.89	1.52	1.72	1.75	**1.89**
L9	1.33	1.39	1.41	1.42	1.36	1.40	1.43	1.43	1.36	1.40	1.43	**1.43**
L10	1.31	1.42	1.43	1.48	1.36	1.44	1.48	1.49	1.37	1.45	1.48	**1.49**
L11	0.70	0.74	0.72	0.74	0.72	0.74	0.73	0.74	0.72	0.74	0.73	**0.74**
L12	1.16	1.16	1.19	1.19	1.17	1.16	1.19	1.19	1.17	1.16	1.19	**1.19**
L13	1.41	1.46	1.49	1.49	1.45	1.47	1.51	1.50	1.45	1.47	**1.51**	1.50
L14	1.42	1.46	1.49	1.50	1.45	1.47	1.50	1.50	1.45	1.47	**1.51**	1.50
L15	1.23	1.24	1.27	1.28	1.24	1.25	1.28	1.28	1.24	1.25	1.28	**1.28**
L16	0.53	0.55	0.60	0.63	0.55	0.56	0.63	0.64	0.55	0.56	0.63	**0.65**
L17	0.48	0.50	0.52	0.53	0.49	0.52	0.53	0.54	0.49	0.52	0.53	**0.55**
L18	0.39	0.42	0.44	0.48	0.40	0.43	0.45	0.49	0.41	0.44	0.47	**0.49**
L19	1.02	1.02	1.04	1.05	1.02	1.02	1.04	1.05	1.02	1.02	1.05	**1.05**

Chapter 3

3 EXTREME WATER LEVELS

3.1 Introduction

Extreme water levels considered in this study are due to a) tidal elevation, b) storm surge and c) tsunami height. The storm surge is obtained from numerical simulations of cyclonic storms that passed within 500 km radius of Mumbai over the past 35 years. The tsunami heights are obtained from numerical modelling of Tsunami for three different earthquake magnitudes.

3.1.1 Tidal elevations

The tidal elevations for Mumbai as provided by the Naval Hydrographic Office Chart Number 2016 are shown in Table 3.1.

Table 3.1. Tidal elevations for Mumbai

Place	Latitude (°N)	Longitude (°E)	Heights in meters above Chart Datum				
			MHWS	MHWN	MLWN	MLWS	MSL
Mumbai (Apollo Bandar)	18° 55’	72° 50’	4.4	3.3	1.9	0.8	2.5

From the tidal elevation data, the tidal range for Mumbai is 3.6m and the maximum elevation from the tides can be considered as 4.4m above Chart Datum. However, based on the information available from literature in public domain, the recorded maximum water level is 5.1m and maximum tidal range was 5.24m.

3.1.2 Storm surge

The increase in water levels due to a cyclonic storm is termed as storm surge. MIKE21 Flexible Mesh flow model (MIKE21-FM), a state-of-the-art flexible mesh flow model developed by DHI, was used to study the storm induced water levels in the study region. The passage of storms along the west coast of India is considerably less compared to that on the east coast. The cyclonic storm wind data generated for the 21 cyclones is used as input. Tide data is not considered in the model so as to obtain the surge alone. The model simulations are carried out for each of the storm duration to estimate the surge levels. The surge elevations at each of the 19 points are extracted and the maximum surge values are obtained. Storms that generated

surge levels of at least 0.1m are considered and presented in Table 3.2. From the storm surge estimations, it is observed that the cyclonic storm of 2001 produced the maximum surge of about 1.5m off Mumbai coast.

Table 3.2. Storm surge (m) values off Mumbai for various storms

Cyclone	L1	L2	L3	L4	L5	L6	L7	L8	L9	L10	L11	L12	L13	L14	L15	L16	L17	L18	L19
bio198003	0.15	0.14	0.14	0.14	0.13	0.13	0.13	0.13	0.13	0.13	0.13	0.13	0.13	0.12	0.12	0.13	0.13	0.13	0.13
bio198101	0.19	0.18	0.17	0.16	0.16	0.16	0.15	0.15	0.15	0.15	0.15	0.15	0.14	0.14	0.14	0.16	0.17	0.17	0.14
bio198205	0.72	0.65	0.62	0.60	0.58	0.57	0.53	0.52	0.51	0.52	0.53	0.53	0.52	0.51	0.51	0.55	0.56	0.59	0.51
bio198502	0.12	0.10	0.10	0.10	0.10	0.09	0.09	0.09	0.09	0.09	0.09	0.09	0.08	0.08	0.08	0.09	0.10	0.10	0.08
bio198902	0.14	0.14	0.14	0.14	0.14	0.14	0.14	0.14	0.14	0.14	0.14	0.14	0.14	0.14	0.14	0.14	0.14	0.14	0.14
bio199210	0.19	0.19	0.19	0.19	0.19	0.19	0.19	0.19	0.19	0.19	0.19	0.19	0.19	0.19	0.19	0.19	0.20	0.19	0.19
bio199502	0.19	0.19	0.19	0.19	0.19	0.19	0.19	0.19	0.19	0.19	0.19	0.19	0.19	0.19	0.19	0.19	0.19	0.19	0.19
bio199604	0.31	0.26	0.25	0.24	0.23	0.23	0.20	0.20	0.20	0.20	0.20	0.20	0.19	0.19	0.19	0.22	0.22	0.24	0.19
bio199605	0.37	0.34	0.33	0.33	0.32	0.32	0.31	0.31	0.30	0.30	0.30	0.30	0.30	0.30	0.30	0.33	0.30	0.32	0.30
bio199803	0.52	0.48	0.46	0.44	0.43	0.42	0.39	0.39	0.38	0.39	0.40	0.40	0.39	0.38	0.38	0.42	0.43	0.45	0.39
bio199805	0.09	0.08	0.08	0.08	0.08	0.08	0.07	0.07	0.07	0.07	0.07	0.07	0.07	0.07	0.07	0.08	0.08	0.08	0.07
bio200101	0.50	0.48	0.48	0.47	0.47	0.47	0.46	0.46	0.45	0.46	0.46	0.46	0.46	0.46	0.46	0.49	0.46	0.47	0.46
bio200102	**1.51**	**1.49**	**1.49**	**1.48**	**1.48**	**1.48**	**1.45**	**1.44**	**1.44**	**1.43**	**1.43**	**1.43**	**1.42**	**1.41**	**1.41**	**1.41**	**1.40**	**1.41**	**1.41**
bio200103	0.19	0.19	0.19	0.19	0.19	0.19	0.19	0.19	0.19	0.19	0.19	0.19	0.19	0.19	0.19	0.19	0.19	0.19	0.19
bio200403	0.12	0.11	0.11	0.11	0.11	0.11	0.11	0.11	0.11	0.11	0.11	0.11	0.11	0.11	0.11	0.11	0.11	0.11	0.11

3.1.3 Tsunami heights

Tsunamis are mostly generated by earthquakes that occur on the seabed. The vertical movement of the seafloor due to the earthquake displaces the seawater above generating waves of a large magnitude at the earthquake source. These large waves radially propagate from the source to distant places. Often the tsunami waves away from the source will have smaller amplitude and a large wave period. As these waves approach the coast, due to shoaling, the amplitude increases and owing to their longer wave periods, these waves inundate the coast and hinterland.

In order to assess the tsunami amplitudes off the Mumbai coast, earthquake sources at the Makaran subduction region are considered. The recent tsunamigenic earthquake on the west coast being the 1947 Makaran earthquake having a moment magnitude of 8.2Mw. The mega tsunami on the east coast during 2004 was due to an earthquake magnitude of about 9.0Mw.

Therefore, these two earthquake magnitudes of 8.2Mw, and 9.0Mw were considered as tsunami sources in this study.

The Community Model Interface for Tsunami developed by the United States National Oceanic and Atmospheric Administration (NOAA) was used in this study. This model interface utilises the Method of Splitting Tsunamis (MOST) tsunami model and the initial tsunami source elevation database. This model is being used worldwide for tsunami inundation modelling. The model outputs tsunami heights, inundation depths on land, maximum current speeds. In this study the maximum tsunami heights are considered.

The Indian Ocean in its entirety was considered for the initial elevation and the Arabian Sea region shown in Fig. 3.1 is considered as outer model domain and the region shown in Fig. 3.2 is considered for the coastal region off Mumbai. The unit sources considered for the earthquake magnitude 8.2Mw simulation case is shown in Fig. 3.3 and the earthquake magnitude 9.0Mw the unit sources considered is shown in Fig. 3.4.

The tsunami amplitude values at the 19 locations along the coastal road were extracted and the maximum tsunami amplitude at each of the location for both the tsunami simulations is presented in Table 3.3. The maximum amplitude over the inner domain for the simulations are shown in Fig. 3.5 and Fig. 3.6 respectively for 8.2Mw and 9.0Mw earthquake magnitudes.

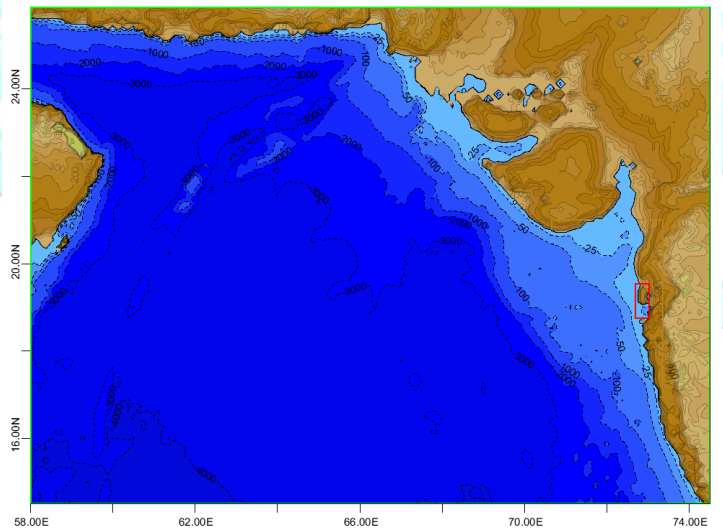

Fig. 3.1. Bathymetry grid considered for tsunami propagation - outer domain. The rectangle in red is the inner domain close to coast

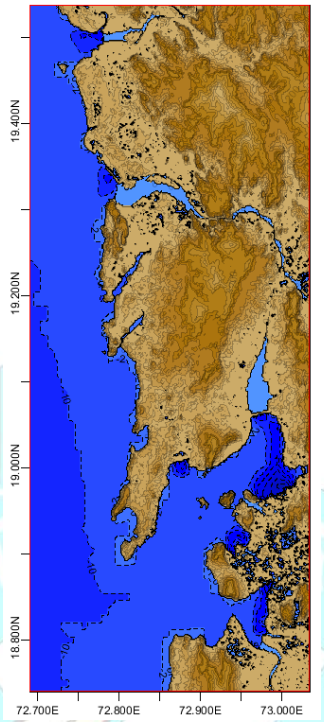

Fig. 3.2. Bathymetry region considered for tsunami propagation - inner domain

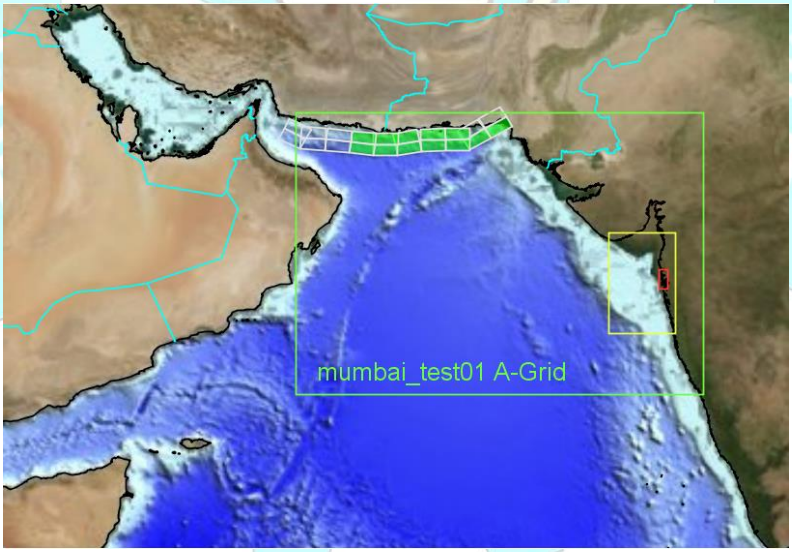

Fig. 3.3. Figure showing the unit sources considered for earthquake magnitude 8.2Mw

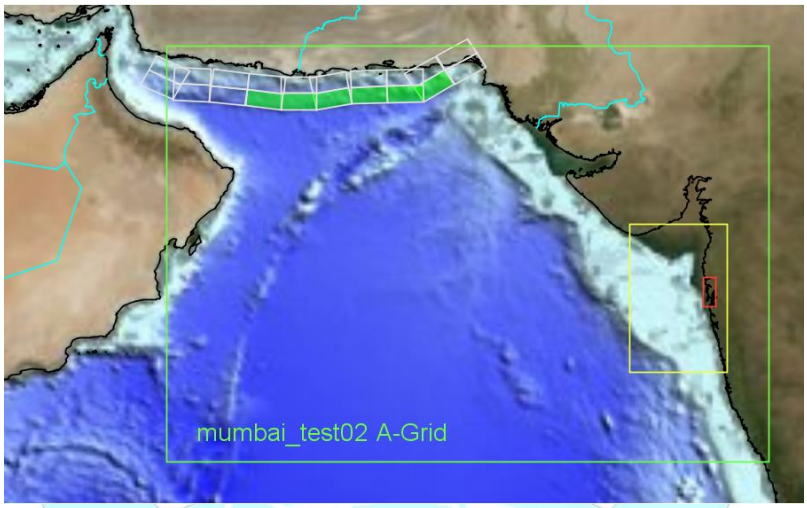

Fig. 3.4. Figure showing the unit sources considered for earthquake magnitude 9.0Mw

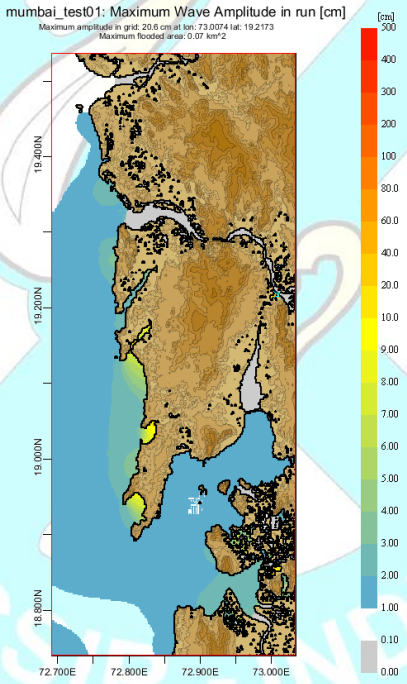

Fig. 3.5. Maximum tsunami amplitude for earthquake magnitude 8.2Mw

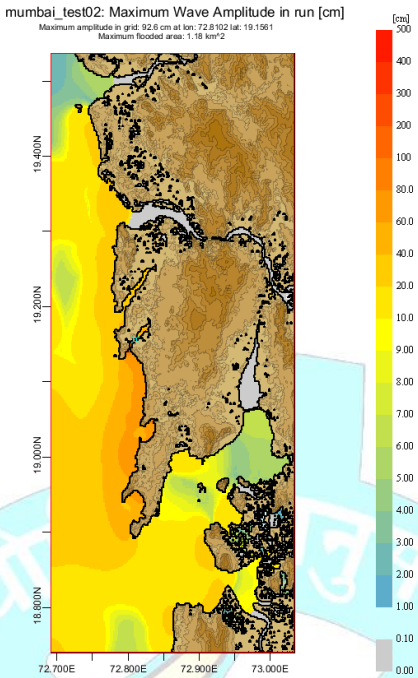

Fig. 3.6. Maximum tsunami amplitude for earthquake magnitude 8.2Mw

Table 3.3. Maximum tsunami amplitude at 19 points along Mumbai coastal road

Locations	Tsunami Amplitude (m)	
Tsunami magnitude →	Mw=8.2	**Mw=9.0**
L1	0.06	**0.71**
L2	0.03	**0.65**
L3	0.03	**0.66**
L4	0.03	**0.71**
L5	0.03	**0.69**
L6	0.03	**0.66**
L7	0.03	**0.72**
L8	0.03	**0.71**
L9	0.03	**0.72**
L10	0.04	**0.71**
L11	0.04	**0.73**
L12	0.04	**0.68**
L13	0.03	**0.59**
L14	0.03	**0.56**
L15	0.03	**0.53**
L16	0.08	**0.67**
L17	0.05	**0.48**
L18	0.07	**0.66**
L19	0.06	**0.53**

Chapter 4

4 HYDRODYNAMICS AND MORPHOLOGY CHANGES

4.1 Introduction

State of the art numerical modelling software suite (MIKE by DHI) is used to simulate the coupled hydrodynamics and morphology of the region. The coupled model consists of modules for hydrodynamics, waves, mud transport and sediment transport. All these modules take feedback from each other as well as provide inputs to each other. For example, the hydrodynamic model or flow model provides flow conditions to the wave model which uses it to include the wave current interaction and provides the modified wave condition to the flow model. The modified wave conditions taken into the flow model then provides the modified flow conditions which are used in the morphology model and the mud transport model. The sediment and mud transport models also utilise the wave parameters from the wave model. In this manner, the coupled model provides output of modified flow, wave and changes in the bed morphology in the study region.

4.2 Brief description of models

The numerical models used in this study are described in this section. The coupled modelling comprising of flow model, wave model, mud transport model and sediment transport model is used to study the hydrodynamics and morphology impact in the region due to different scenarios.

4.2.1 Coupled modelling

The MIKE 21 coupled model FM is used in this study which dynamically couples the flow, sediment transport and wave calculations. Full feedback of bed level changes on flow and wave calculations is included in this formulation. The coupled model FM is mostly used for investigating the morphological evolution of the near shore bathymetry due to the impact of engineering works (coastal structures, dredging works etc.) and also to study the morphological evolution of tidal inlets. It is most suitable for medium-term morphological investigations (several weeks to months) over a limited coastal area. The computational effort can become quite large for long-term simulations, or for larger areas. The different models used in the coupled model are briefly described below.

4.2.2 Hydrodynamic model

The Hydrodynamic Module is the basic computational component of the entire MIKE21 Flow Model FM modelling system. The MIKE 21 Flow Model FM is a modelling system based on a flexible mesh approach providing the hydrodynamic basis for the Mud Transport Module and Sand Transport Module as well as providing input for water level changes for the spectral wave model.

The modelling system is based on the numerical solution of the two-dimensional shallow water equations i.e., depth-integrated incompressible Reynolds Averaged Navier-Stokes equations. Thus, the model consists of continuity, momentum, temperature, salinity and density equations. In the horizontal domain both Cartesian and spherical coordinates can be used. The spatial discretization of the basic equations is performed using a cell-centred finite volume method wherein the spatial domain is discretized by subdivision of the continuum into non-overlapping element/cells. An unstructured grid comprising of triangles or quadrilateral element is used in the horizontal plane. An approximate Riemann solver is used for computation of the convective fluxes, which makes it possible for MIKE21 FM model to handle discontinuous solutions. For the time integration an explicit scheme is used. Coriolis term, eddy viscosity using Smagoransky formulation and bed friction are included in the model. For more details of the MIKE21 FM module the scientific manual can be referred.

In this study, the model domain considered has Mumbai coastline at its centre and the model extends to about 100km north, about 90km to the south and about 220 km offshore direction reaching up to water depths of 100m (Fig. 4.1). This model domain was further used for all simulations.

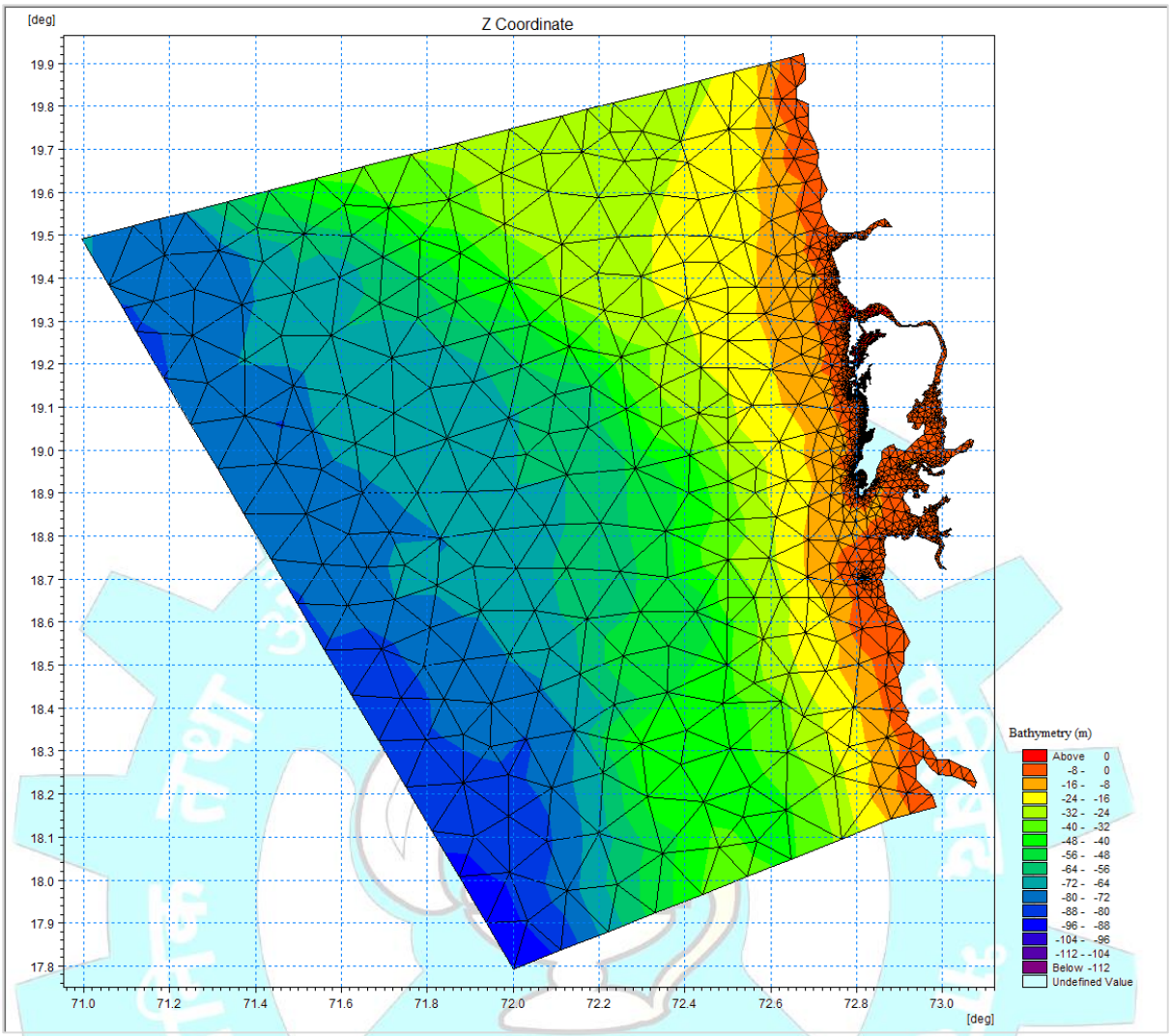

Fig. 4.1. Bathymetry of the coastal and offshore region off Mumbai.

The region showing the northern portion of the coastal road is shown in Fig. 4.2 and the region showing the southern portion of the coastal road is shown in Fig. 4.3.

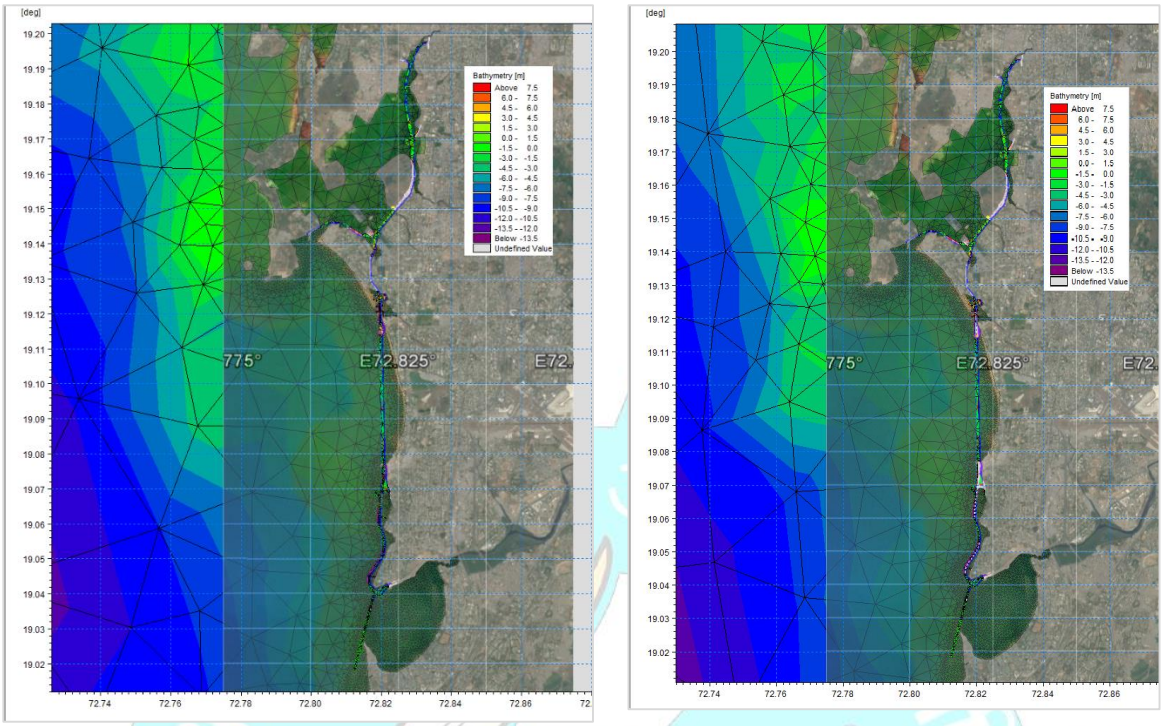

Fig. 4.2. Bathymetry of the coastal region along the northern portion of coastal road (a) without coastal road (b) with coastal road.

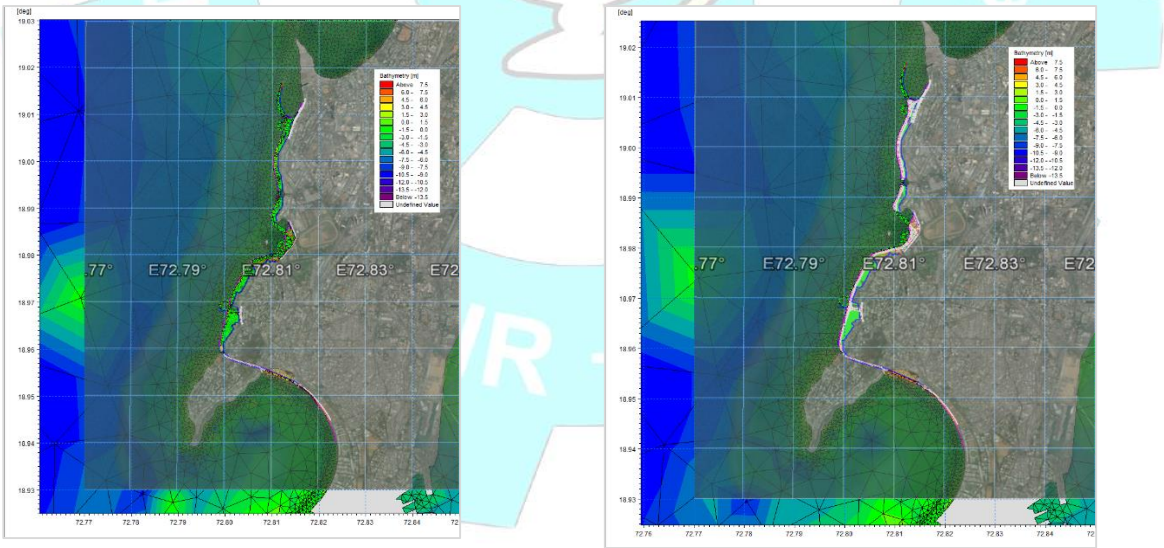

Fig. 4.3. Bathymetry of the coastal region along the southern portion of coastal road (a) without coastal road (b) with coastal road.

4.2.3 Wave model

MIKE 21 SW, a state-of-the-art numerical tool for prediction and analysis of wave climates in offshore and coastal areas is used for simulating the waves in the study region. MIKE 21 SW includes a new 3rd generation spectral wind-wave model based on unstructured meshes. The model simulates the growth, decay and transformation of wind-generated waves in offshore and coastal areas. MIKE 21 SW includes two different formulations viz., Directional decoupled parametric formulation and fully spectral formulation. In this study the fully spectral formulation has been used. The fully spectral formulation is based on the wave action conservation equation, where the directional-frequency wave action spectrum is the dependent variable.

MIKE 21 SW includes the following physical phenomena: (i) wave growth by action of wind, (ii) non-linear wave-wave interaction, (iii) dissipation due to white-capping, (iv) dissipation due to bottom friction, (v) dissipation due to depth-induced wave breaking, (vi) refraction and shoaling due to depth variations, (vii) wave-current interaction, (viii) effect of time-varying water depth and flooding and drying.

The discretization of the governing equation in geographical and spectral space is performed using cell-centred finite volume method similar to the hydrodynamic model. In the geographical domain, an unstructured mesh technique is used. The time integration is performed using a fractional step approach where a multi-sequence explicit method is applied for the propagation of wave action. MIKE 21 SW is also used in connection with the calculation of the sediment transport, which for a large part is determined by wave conditions and associated wave-induced currents. MIKE 21 SW can be used to calculate the wave conditions and associated radiation stresses. Subsequently the wave-induced flow is calculated using MIKE 21 Flow Model FM.

The input parameters used in wave model in the present study are the winds measured off Mahim bay as well as the global wind parameters available in the literature. The global winds obtained from NCEP/NCAR re-analysis data base is used to generate the long distant waves (swells) and the local winds are used to generate the local wind waves (seas). Influence of cyclonic winds is not considered in this study. The output parameters from the wave model are significant wave height, maximum wave height, peak wave period, mean wave period, mean

wave direction, wave velocity components, wave radiation stresses, etc., amongst other parameters.

The wave model simulations are carried out for the study region and for the period of measurements. The statistical maximum and mean significant waves are obtained from the model results and are presented in this report. The changes in the wave climate for different scenarios of coastal changes are further reported by comparing the waves for existing situation and the modified scenarios.

4.2.4 Mud transport model

The mud transport module calculates the resulting transport of cohesive materials based on the flow conditions found in the hydrodynamic calculations. The transport is dominated by the advection of the water column. MIKE 21 MT can simulate suspended transport of fine grained non-cohesive sediment into account. This is done by calculating an equilibrium concentration profile based on the sediment properties and the hydrodynamics. The bed is assumed to erode as flakes which mean that the distribution of sediment fractions within the bed is also the distribution when eroded. This means that the erosion formula used in the MT section controls the maximum erosion of all fractions. After the flakes are eroded it is assumed that they are destroyed or regrouped by turbulence. Since the sand fractions has no cohesive properties it will be freed by this and behave independently. The model does this by calculating the maximum possible equilibrium concentration for the given sand under the given hydrodynamic properties. If this is above the concentration of the sand fraction, the extra sand will be deposited so that the concentration is the equilibrium concentration.

In the MT model the bed is considered to be consisting of number of layers. In this study three layers were considered, the top layer being 0.3m of soft mud (clay sized particles), a second layer of 0.5m consisting of medium hard mud (silty clay sediments) and the third or bottom layer of 3m consisting of hard mud (stiff clay). This assumption is made considering the local sediments observed in the field off Mahim and Colaba. The MT model output consists of sediment transport rates, bed level changes, sediment concentrations amongst other parameters.

4.2.5 Non-cohesive Sediment transport model

The Sand Transport module calculates the resulting transport of non-cohesive materials based on the flow conditions found in the hydrodynamic calculations and, if included, wave

conditions from wave calculations. A mean sediment grain size can be given as input to the model over the entire domain or varying in the domain. The model output consists of sediment transport rates, bed level changes, amongst other parameters. In this study the wave and current formulation of sediment transport is considered with the flow model providing the currents and the wave information obtained from the wave model.

4.3 Methodology

The inputs considered to the numerical model are bathymetry, coastline, tides, winds and waves. In order to obtain reliable results from the model, reliable input data is required. The coastline from the available Google® imageries was considered as input to the numerical model. The shoreline was digitized and used in preparation of the bathymetry of the study region. The modified coastline considering the reclamation regions, as provided by MCGM, is used further in the numerical models. The bathymetry used in the model is taken from the NHO charts primarily meant for navigational purposes which cover specific areas of interest to shipping routes. Even though the NHO chart data is a good data to start with as input to a numerical model, it is observed that the data required for a specific site are sparsely available and also these charts are not frequently updated, therefore for critical projects it is always recommended to obtain fresh/recent bathymetry survey carried out. In the present study sufficient information on the bathymetry data exists from NHO charts, as well as bathymetry survey chart obtained from Maharashtra Maritime Board (MMB) which is used in the model studies.

The coupled numerical model described in the following sections is setup for various scenarios initially to ascertain the validity of the model for the study region and then for different coastal configurations. In order to test the validity of the model, purely tidal forcing is given to the model and the model results are compared with the tidal components of the measured data. The tidal model is included with the local winds and waves from offshore as driving forces. A detailed hydrodynamics modelling study for the base case is carried out in a previous study carried out through Mumbai Transformation Support Unit of the All India Institute of Local Self Government. The validation of the hydrodynamics model is not presented in this report.

The base case scenario (Case-1) is the case with existing or present coastline condition. The second scenario (Case-2) used is the modified coast scenario wherein the proposed coastal road elements that affect the coastal waters, viz., the reclamation regions and major pile structures that would encroach the coastal waters, are included. The region of the road which passes

beyond the coastal waters in the hinterland is not considered in this study. In this study the effects of the coastal road on the hydrodynamics and morphology are studied by comparing with the base case scenario. This base case scenario model therefore provides a basis for comparison with the modified coast model runs. All the model simulations were carried out for a period of 4 weeks similar to that of the measurement period as in previous report submitted to MTSU. The model results of each scenario are presented in different sections.

4.4 Assessment of reclamation impact

Based on the modelling of the hydrodynamics of the region, and considering the components involved in general reclamation projects, possible impacts due to the proposed developments are reported in terms of (i) hydrodynamics impact and (ii) morphological impact. The difference between the base case and modified coastline case are studied to ascertain the changes in flow patterns and the bed morphology changes. The flow pattern changes are studied by comparing the tidal elevations and flow speeds at 21 points in the study region. The flow patterns for each of the scenarios are also presented at low tide, mid tide and high tide times. The bed morphology changes give the expected change in bed levels in the study region.

4.4.1 Hydrodynamic impact

Any change to the prevailing hydrodynamics, considered being in equilibrium, in terms of changes to bathymetry or adjoining coastline results in changes in the local hydrodynamics till such a time a new equilibrium is attained. Till then the local hydrodynamics would be in dynamic mode adjusting to the new and changing conditions. The extent of change in the hydrodynamics can be ascertained through comparison field data obtained before and after the completion of the reclamation, as in this case. In this study, the impact assessment is carried out through numerical modelling. The impact on the tidal levels (or sea level changes), waves and currents in the study region is ascertained by studying the differences between the validated model results for pre- and post- project conditions of the coastline and bathymetry.

The hydrodynamic impacts in terms of changes would be reported qualitatively for the Waves, Currents and Water levels. The new shoreline derived from the proposed coastal road project is studied without changing the nearby bathymetry so as to ascertain the changes in the hydrodynamics due to new coastal configuration. The flow pattern changes are also assessed by comparing the flow speeds at 21 points in the study region.

4.4.2 Morphological impact

The morphological impacts in terms of changes in the bathymetry is reported. The impact of changed coastline due to reclamation and formation of roads would change the local bottom topography due to changes in the local hydrodynamics. Numerical modelling studies on the sediment transport and bed level changes are carried out and the changes in the bed morphology for base case as well as the proposed coastal road scenario. Mud transport numerical model is used to assess the bed morphology changes. The bed morphology studies assume that the seabed consists of different layers of sediment with the top layer of 0.3m being soft mud (clay sized particles), next layer of 0.5m consisting of medium hard mud (silty clay sediments) and the bottom layer consisting of hard mud (stiff clay).

4.5 Results

The results of the numerical modelling study are presented in this section. Flow and wave model validations are not presented here since this is carried out and detailed in the report submitted to MTSU (Report No. NIO/SP-26/2015). The wave, flow and morphology results are presented at five sections, three sections for the north coastal road region and two sections for the south coastal road region. The Section-I along the north portion of coastal road starts from north of Juhu beach till the midway of proposed tunnel as shown in Fig. 4.4. The Section-II is between the middle of tunnel to Joggers Park (Fig. 4.5) and the section-III is from Joggers Park till south end of the Bandra-Worli sea link (Fig. 4.6). The first section of the southern portion of coastal road referred as section-IV (Fig. 4.7) is between the mouth end of Bandra-Worli sea link and Priya Darshini Park. And the second south road section, referred as Section-V (Fig. 4.8) comprises of the Back Bay region including Girgaon Chowpatty beach and marine drive. Please note that the sections mentioned in the results are not same as the sections defined by MCGM. The results of the study are presented in these five section comparing with and without coastal road.

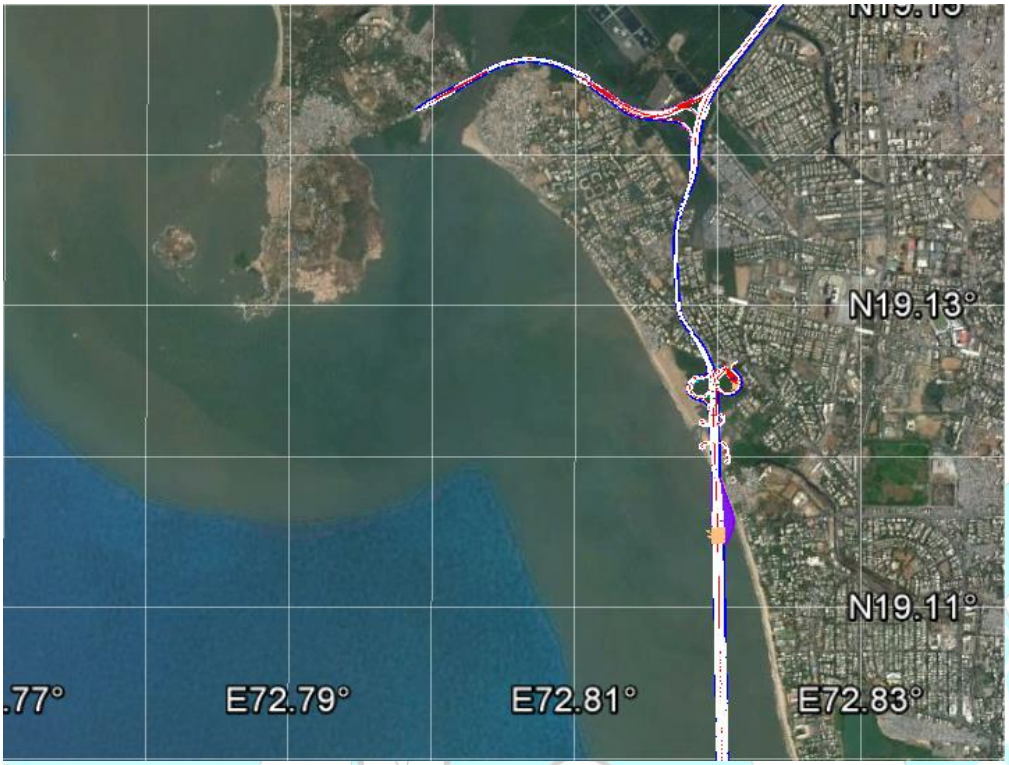

Fig. 4.4. The north Coastal Road – Section I

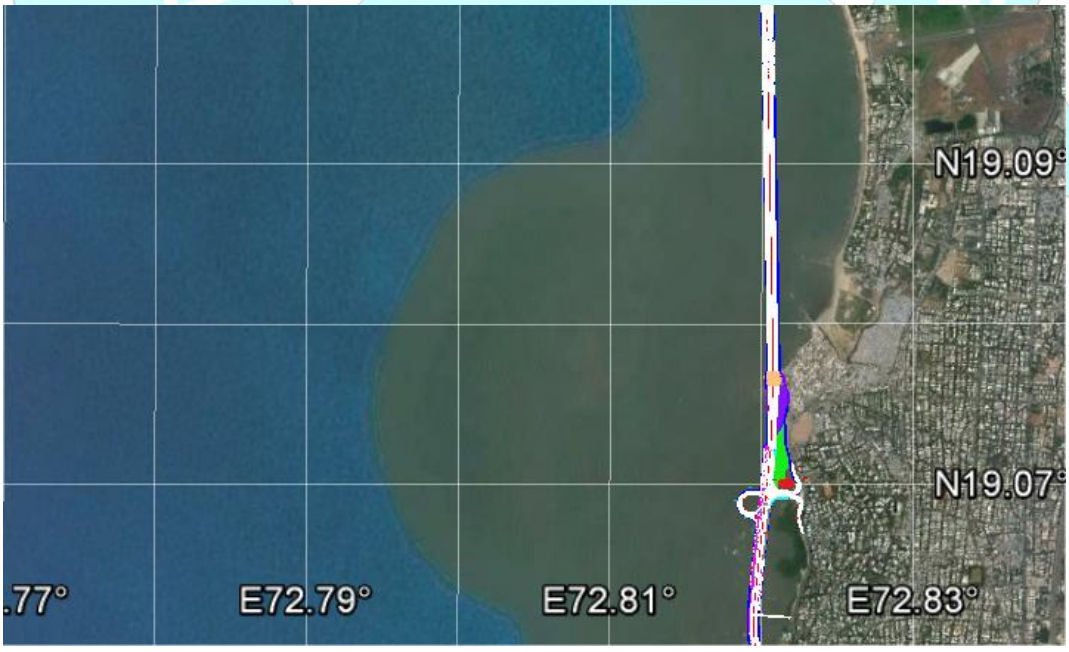

Fig. 4.5. The north Coastal Road – Section II

Fig. 4.6. The north Coastal Road – Section III

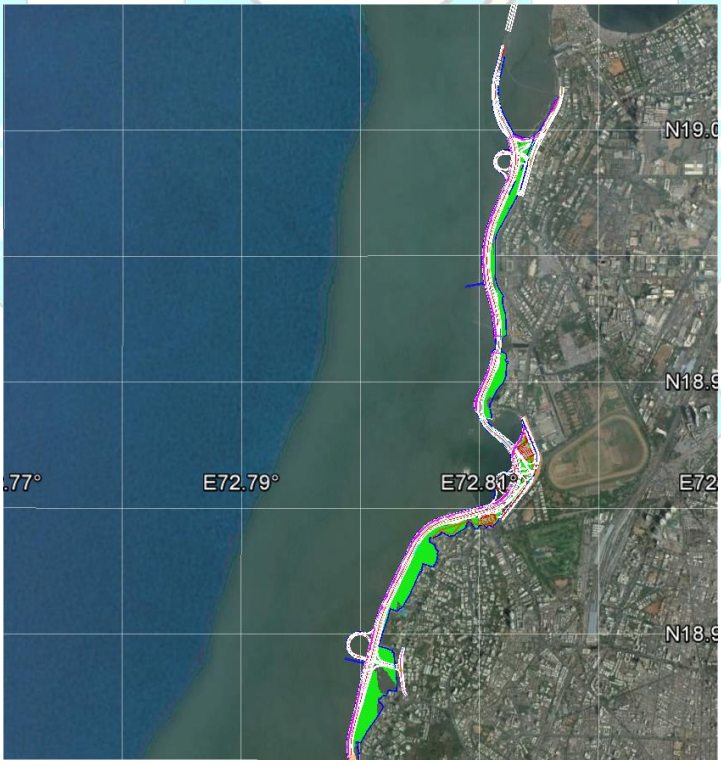

Fig. 4.7. The south Coastal Road – Section IV

Fig. 4.8. The south Coastal Road – Section V

4.5.1 Wave model

The wave model results for the base case (Case I) and the coastal road case (Case-2) are shown in this section. The wave rose plots for the five sections are shown in Figs 4.9 to 4.13. In the Section-I, Section-II and Section-IV, no significant variation in the wave characteristics due to proposed coastal road is observed. The wave heights are observed to be unchanged at these sections. At Section-III, increase in waves from southwest is observed for the coastal road scenario (case-2) compared to the base case (case-1), while the waves from west were observed to reduce. And at section-V the direction of waves from southwest observed to increase while the waves from WNW were found to reduce. While the wave heights are found to be unchanged, the directions are observed to be slightly modified in the coastal road scenario. These changes in wave directions in these sections could be attributed to the overall reworking of waves to adjust to the new coastline configuration. However, in order to ascertain any major changes in the wave climate, continuous monitoring of the waves are essential prior to commencement of the project.

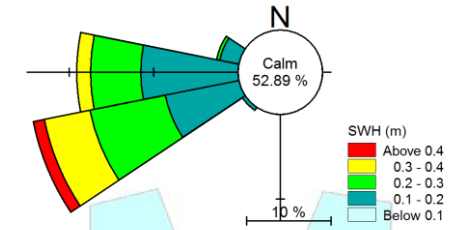

(a)

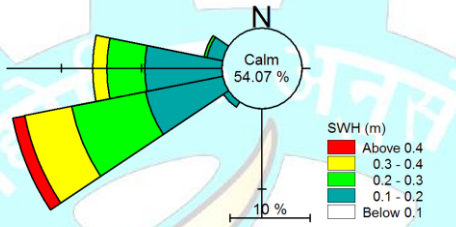

(b)

Fig. 4.9. Wave rose plot for section-I (a) Case I (b) Case 2

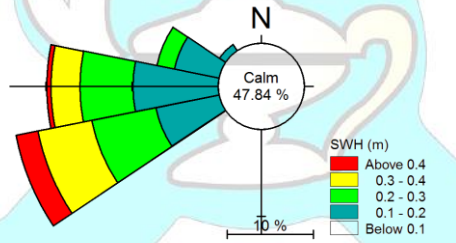

(a)

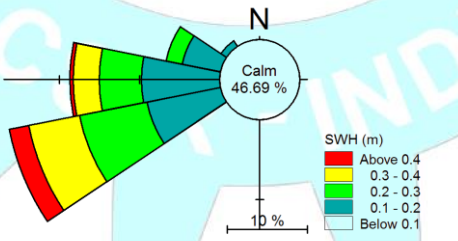

(b)

Fig. 4.10. Wave rose plot for section-II (a) Case I (b) Case 2

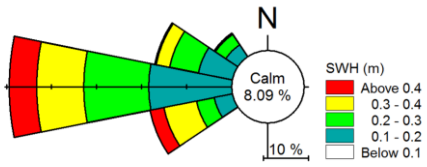

(a)

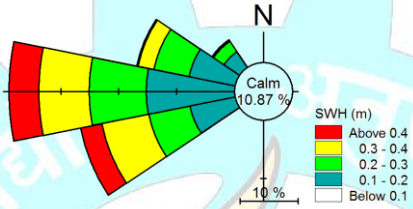

(b)

Fig. 4.11. Wave rose plot for section-III(a) Case I (b) Case 2

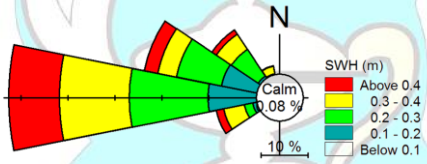

(a)

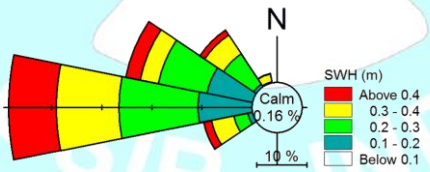

(b)

Fig. 4.12. Wave rose plot for section-IV (a) Case I (b) Case 2

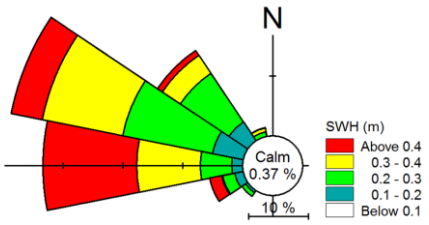

(a)

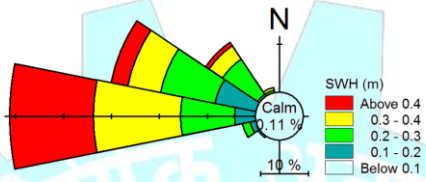

(b)

Fig. 4.13. Wave rose plot for section-V (a) Case I (b) Case 2

4.5.2 Flow model

The flow model results for the two cases are presented in this section. The flow vectors for various phases of the tide during spring and neap tide viz., during low tide, mid tide and high tide are presented respectively in Fig. 4.14 to Fig. 4.49.

Comparison between the flow vectors for different phases of tide for the case without and with coastal road configuration model results, did not shown any significant differences in the coastal and offshore region. There is no significant change in the current speeds or direction along the coastline.

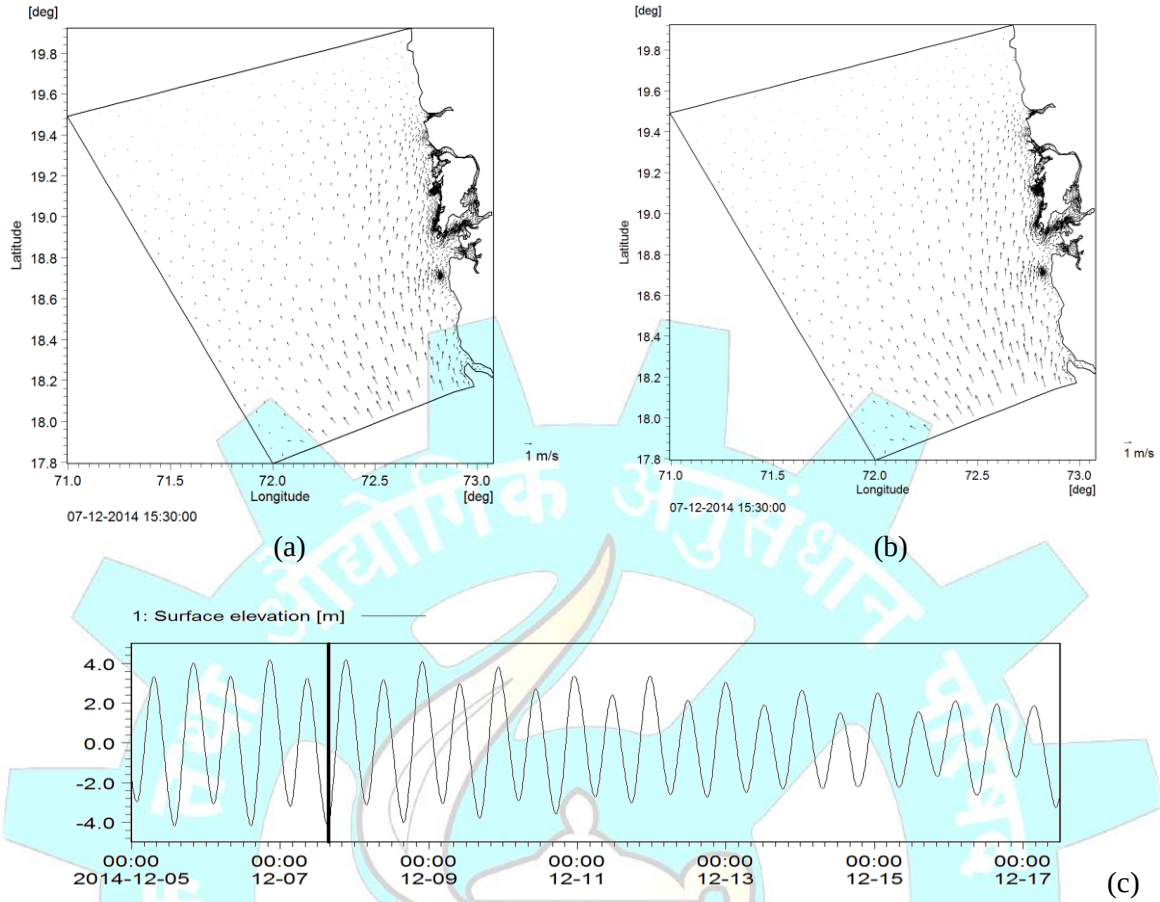

Fig. 4.14. Vector plot at low tide during spring tide (a)Without Coastal Road (b) With Coastal Road (c) phase of tide

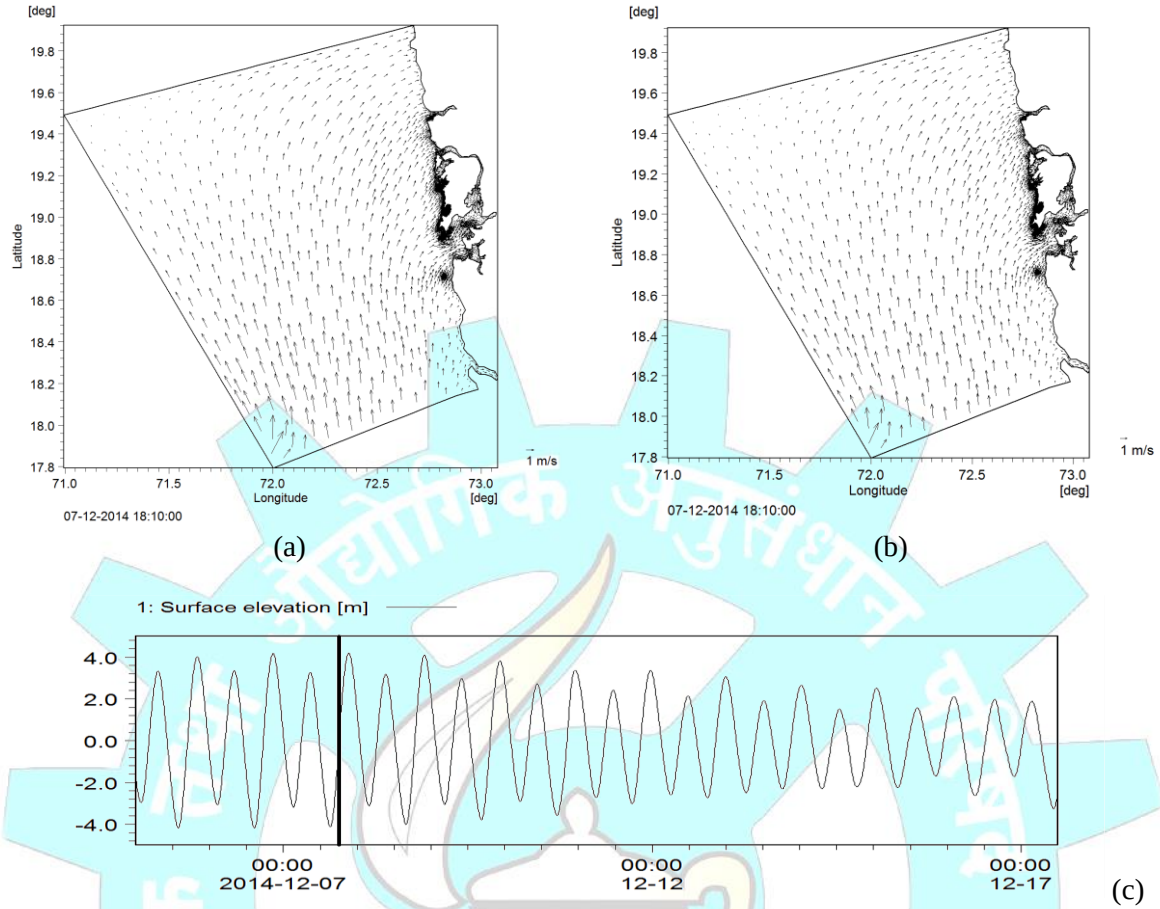

Fig. 4.15. Vector plot at mid tide during spring tide (a)Without Coastal Road (b) With Coastal Road (c) phase of tide

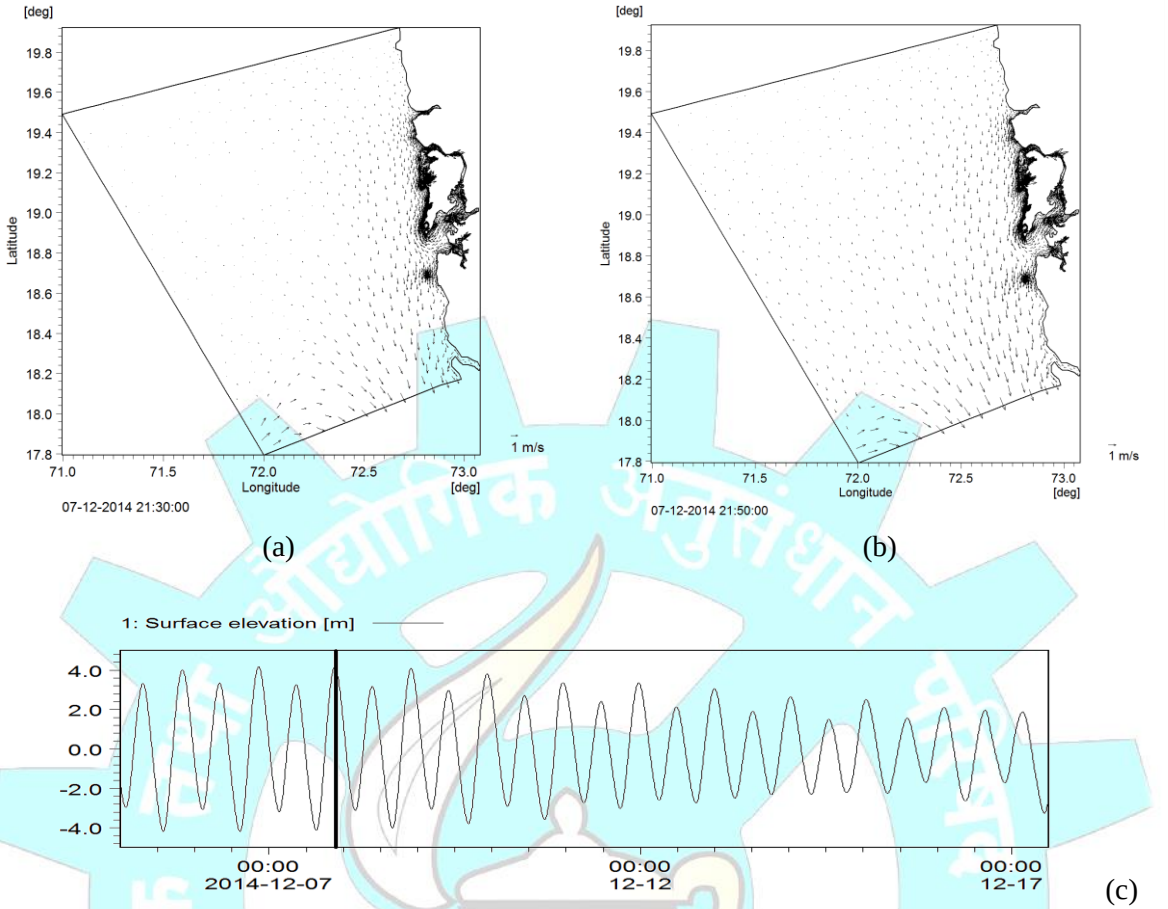

Fig. 4.16. Vector plot at high tide during spring tide (a)Without Coastal Road (b) With Coastal Road (c) phase of tide

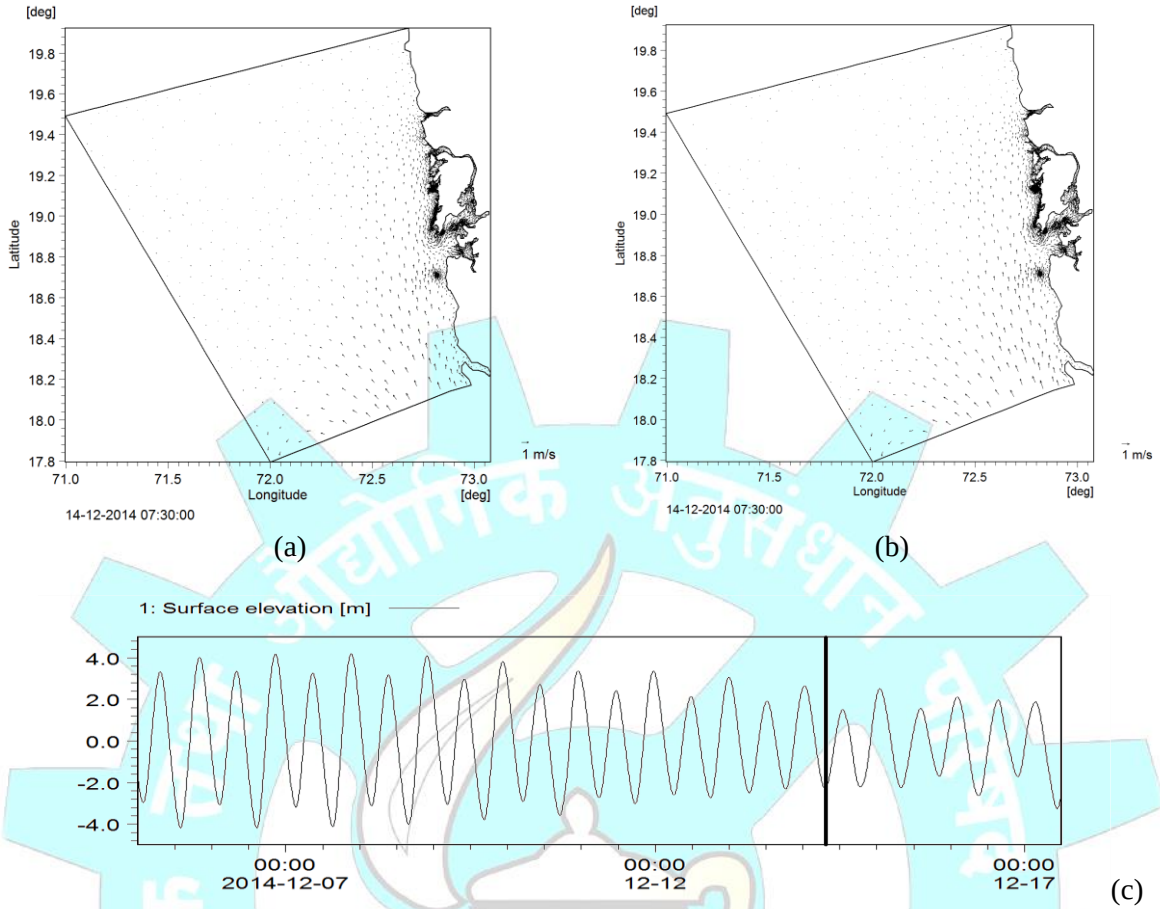

Fig. 4.17. Vector plot at low tide during neap tide (a)Without Coastal Road (b) With Coastal Road (c) phase of tide

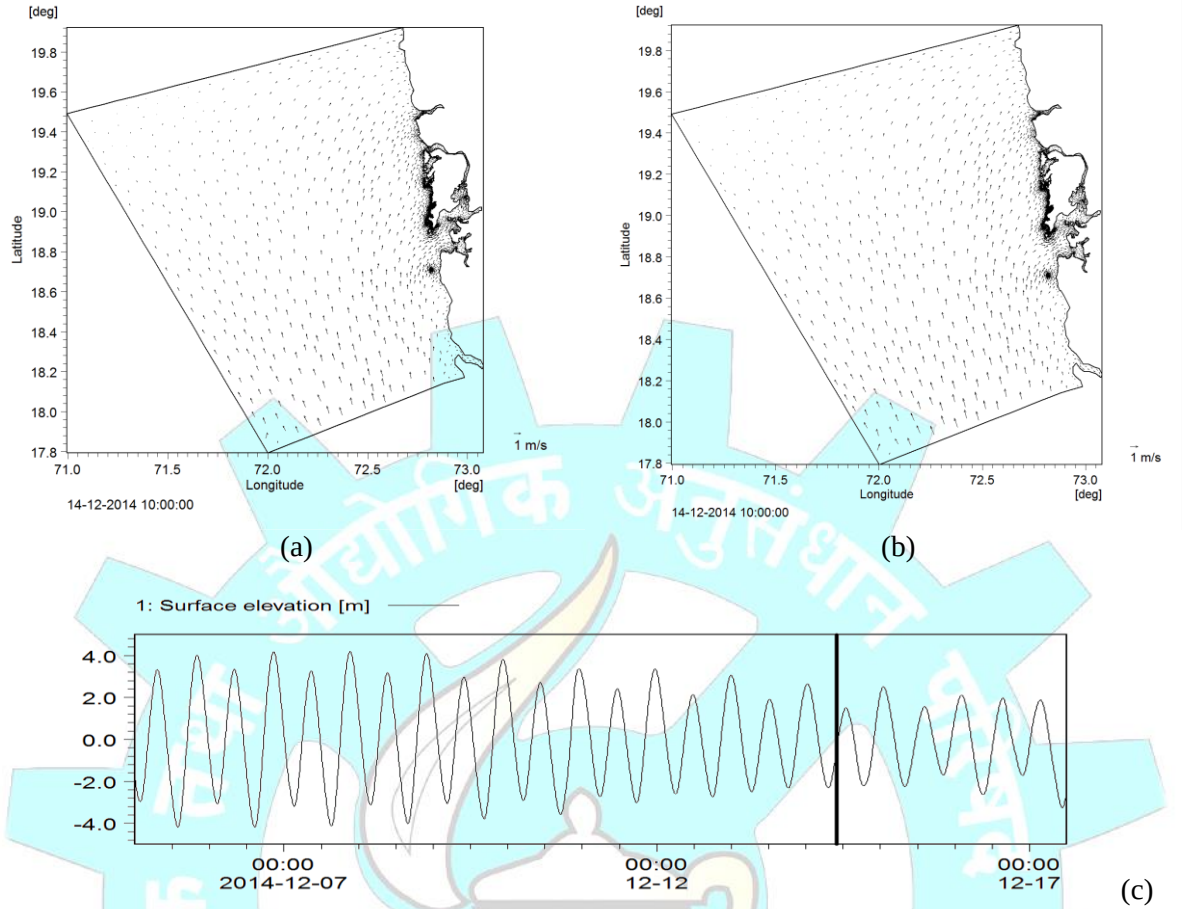

Fig. 4.18. Vector plot at mid tide during neap tide (a)Without Coastal Road (b) With Coastal Road (c) phase of tide

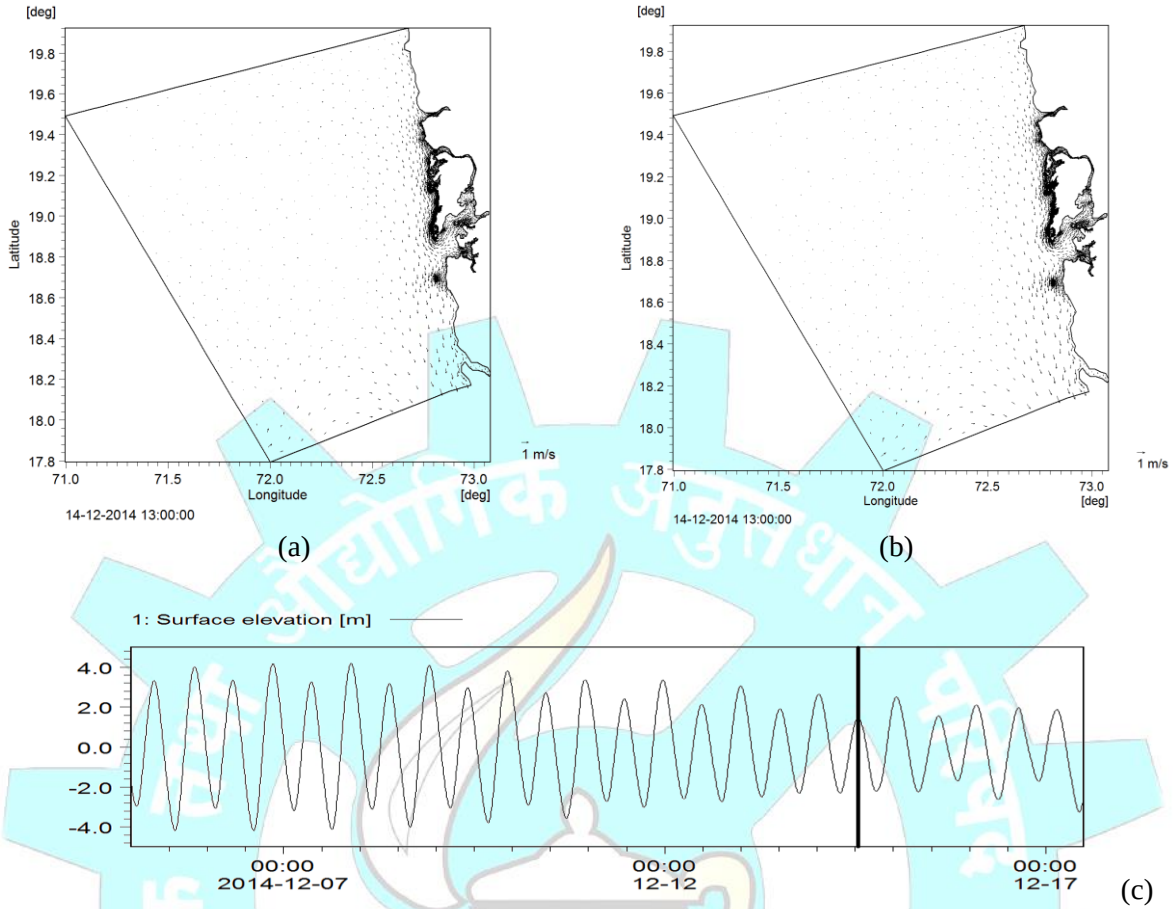

Fig. 4.19. Vector plot at high tide during neap tide (a)Without Coastal Road (b) With Coastal Road (c) phase of tide

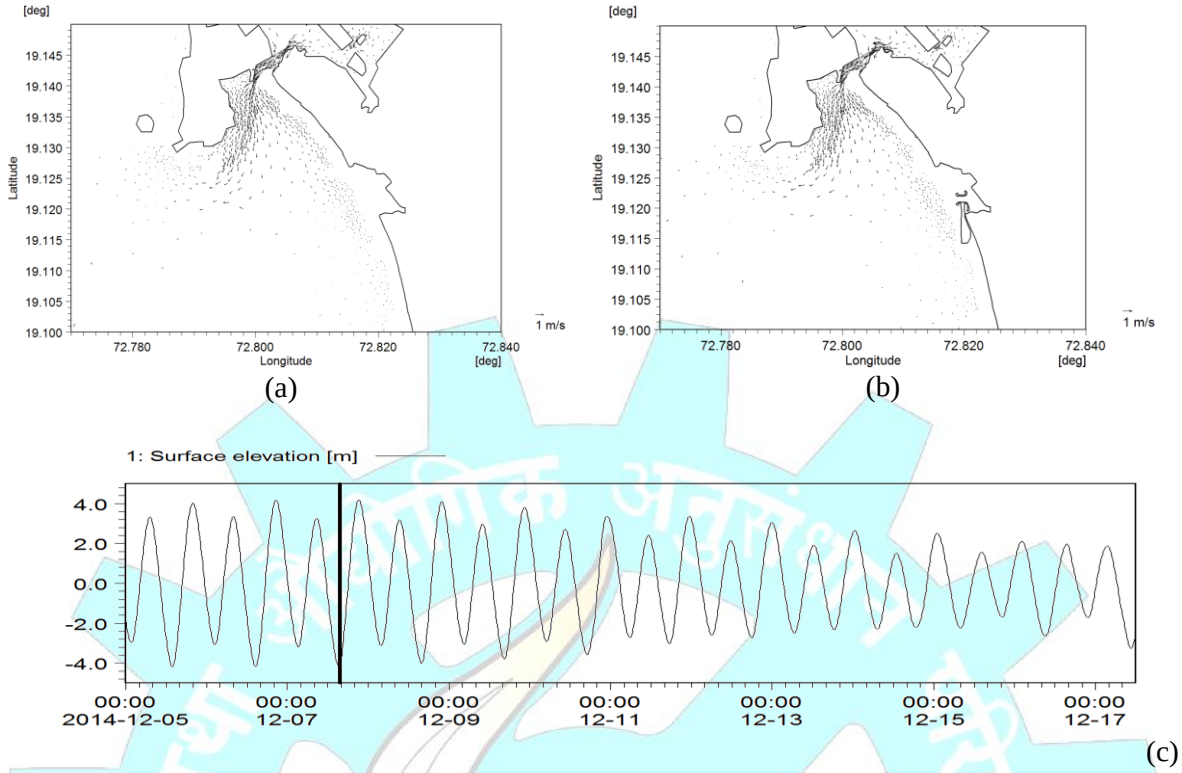

Fig. 4.20. Vector plot at low tide during spring tide for section-I (a)Without Coastal Road (b) With Coastal Road (c) phase of tide

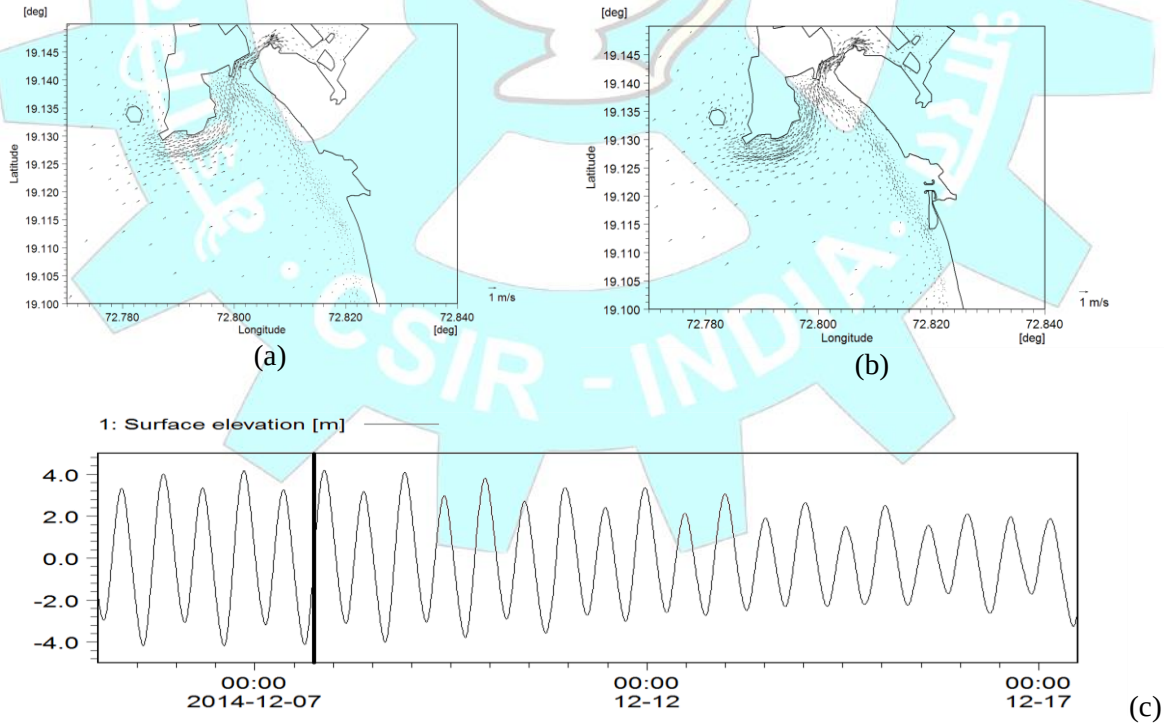

Fig. 4.21. Vector plot at mid tide during spring tide for section-I (a)Without Coastal Road (b) With Coastal Road (c) phase of tide

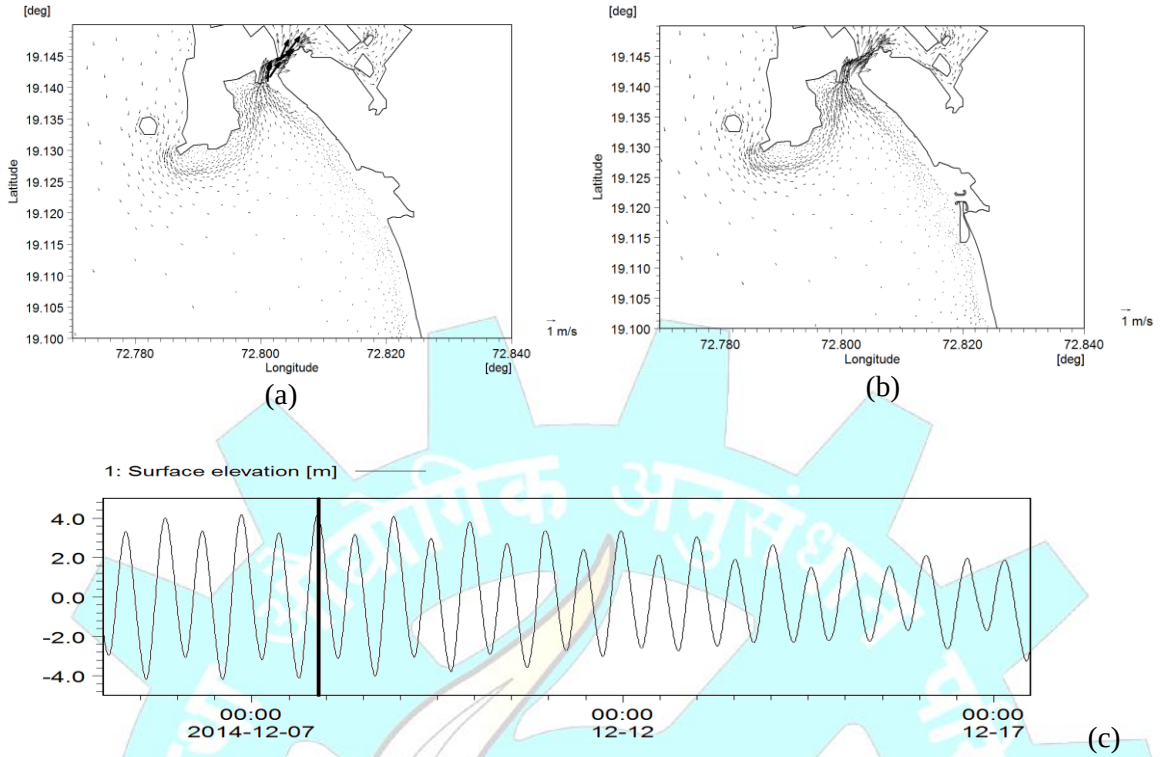

Fig. 4.22. Vector plot at high tide during spring tide for section-I (a)Without Coastal Road (b) With Coastal Road (c) phase of tide

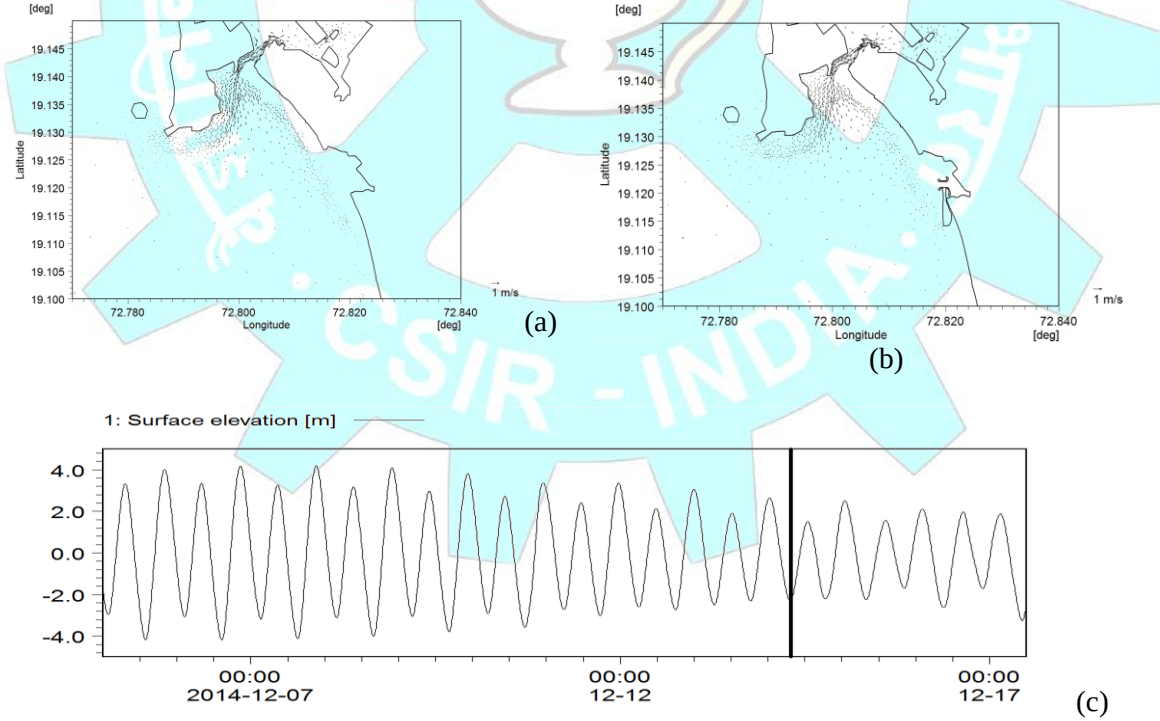

Fig. 4.23. Vector plot at low tide during neap tide for section-I (a)Without Coastal Road (b) With Coastal Road (c) phase of tide

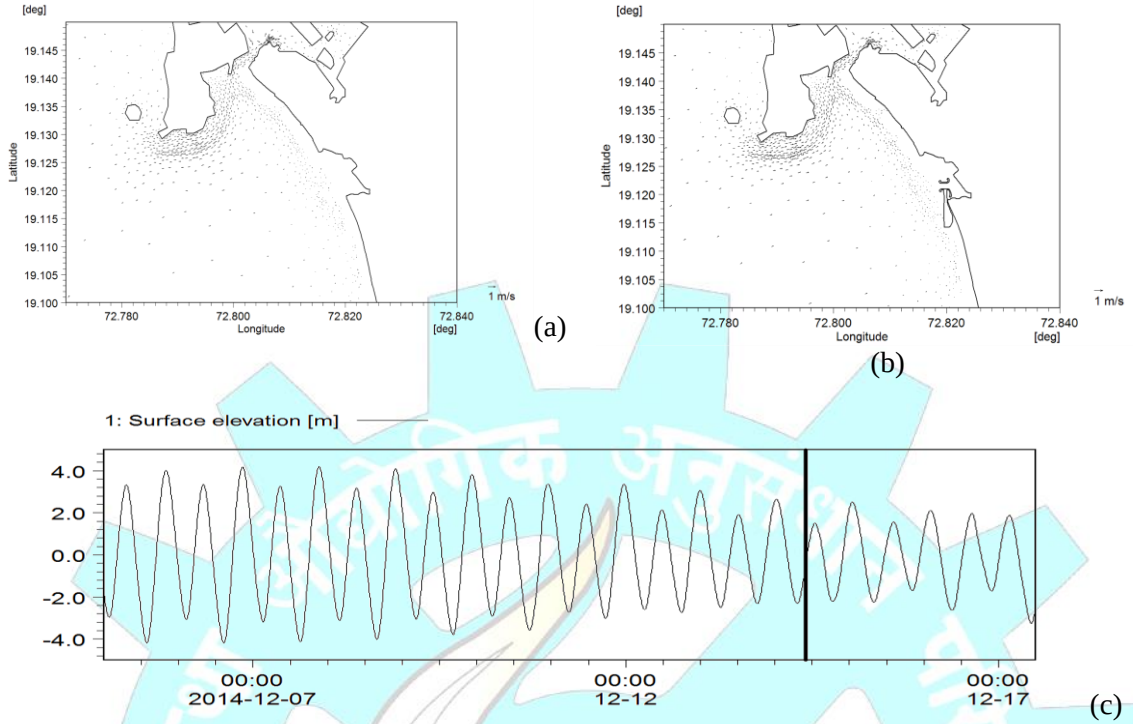

Fig. 4.24. Vector plot at mid tide during neap tide for section-I (a)Without Coastal Road (b) With Coastal Road (c) phase of tide

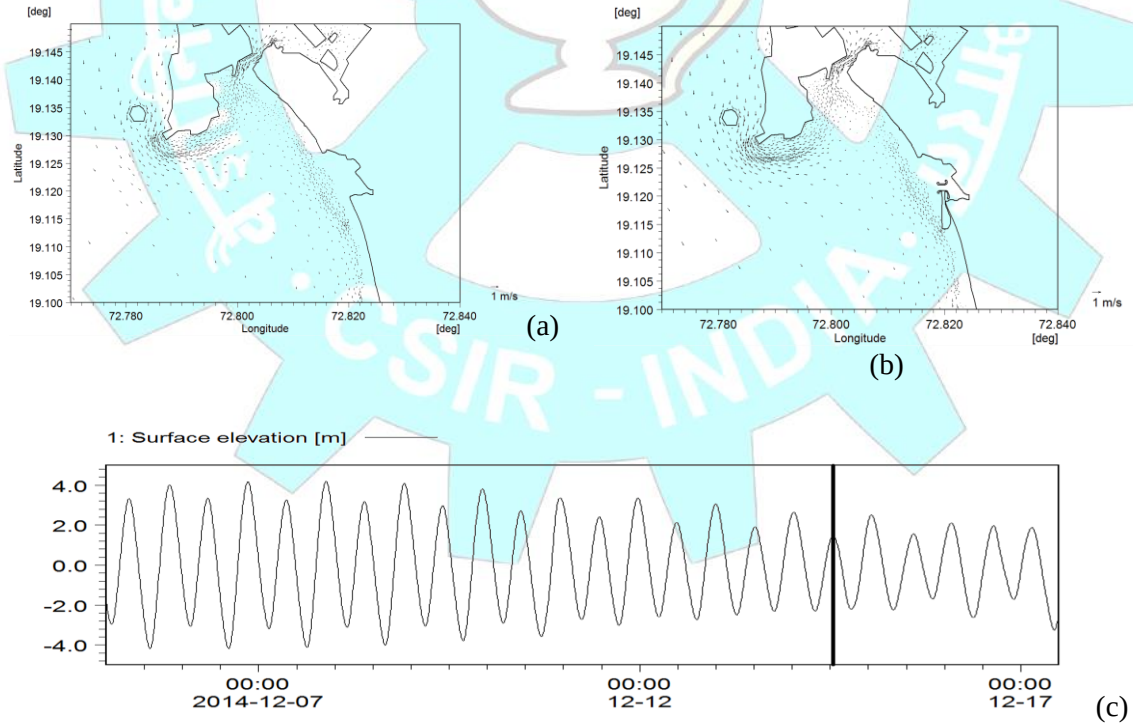

Fig. 4.25. Vector plot at high tide during neap tide for section-I (a)Without Coastal Road (b) With Coastal Road (c) phase of tide

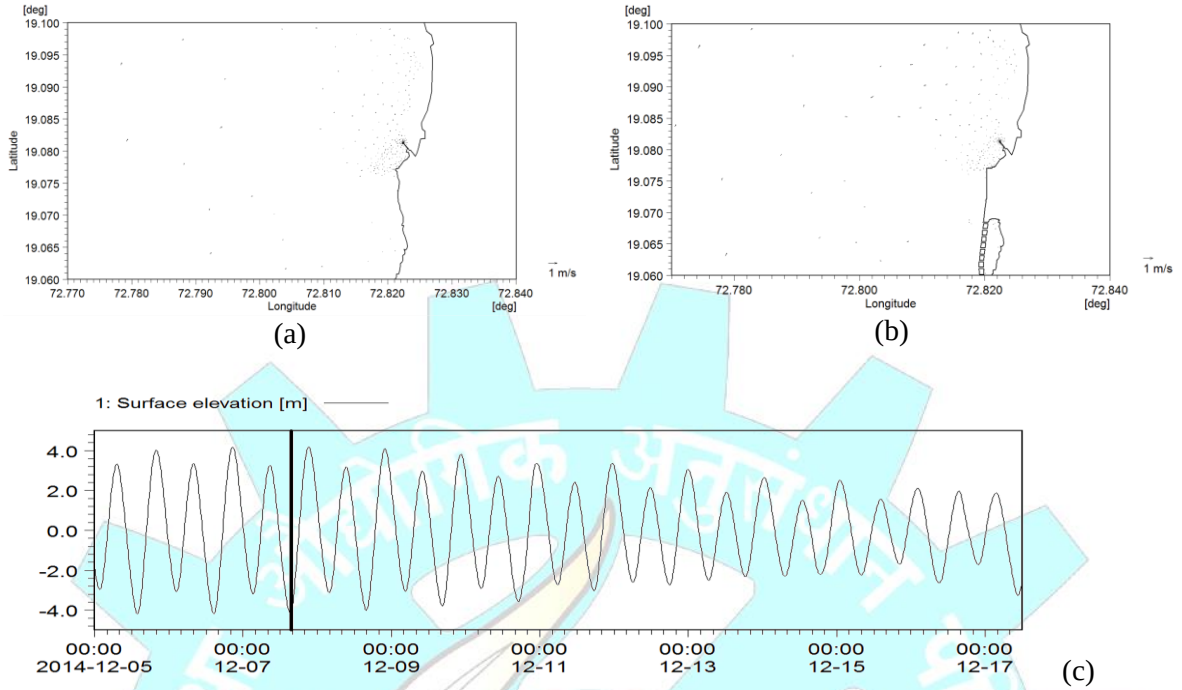

Fig. 4.26. Vector plot at low tide during spring tide for section-II (a)Without Coastal Road (b) With Coastal Road (c) phase of tide

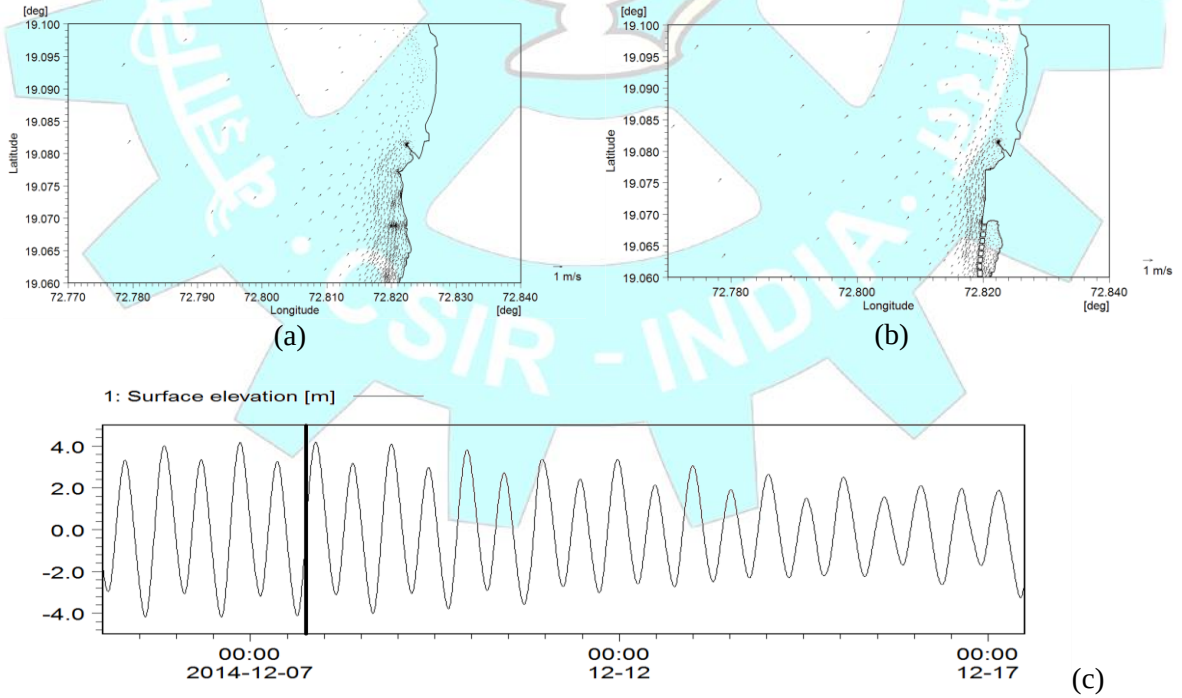

Fig. 4.27. Vector plot at mid tide during spring tide for section-II (a)Without Coastal Road (b) With Coastal Road (c) phase of tide

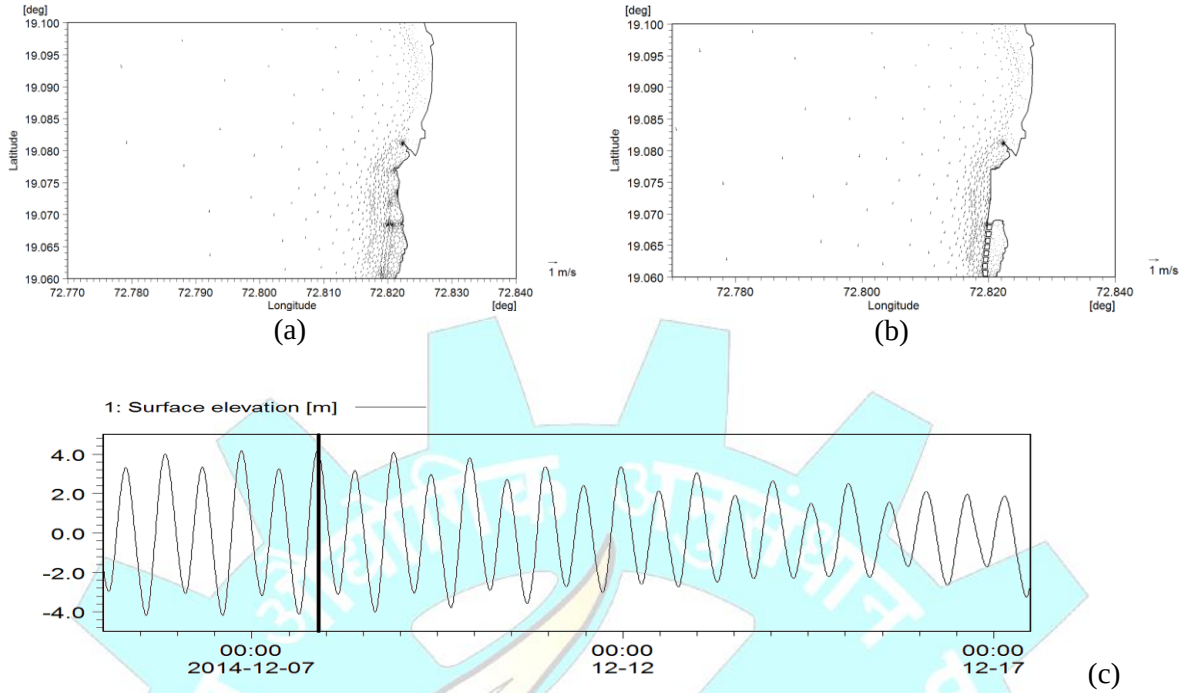

Fig. 4.28. Vector plot at high tide during spring tide for section-II (a)Without Coastal Road (b) With Coastal Road (c) phase of tide

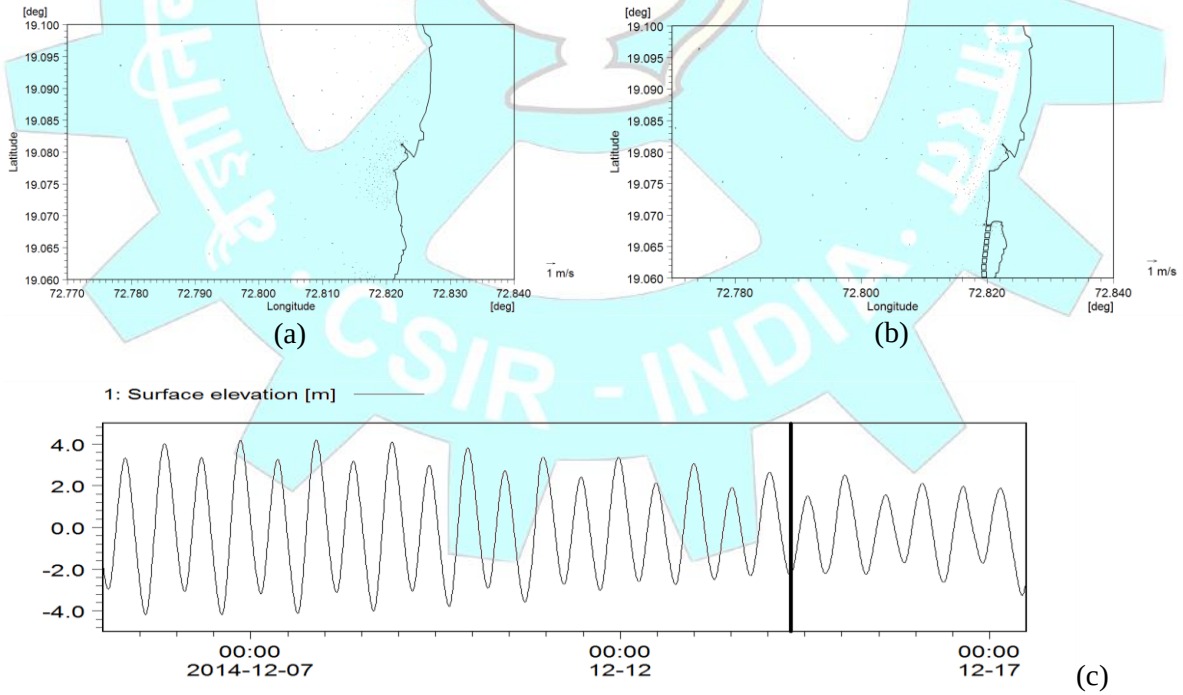

Fig. 4.29. Vector plot at low tide during neap tide for section-II (a)Without Coastal Road (b) With Coastal Road (c) phase of tide

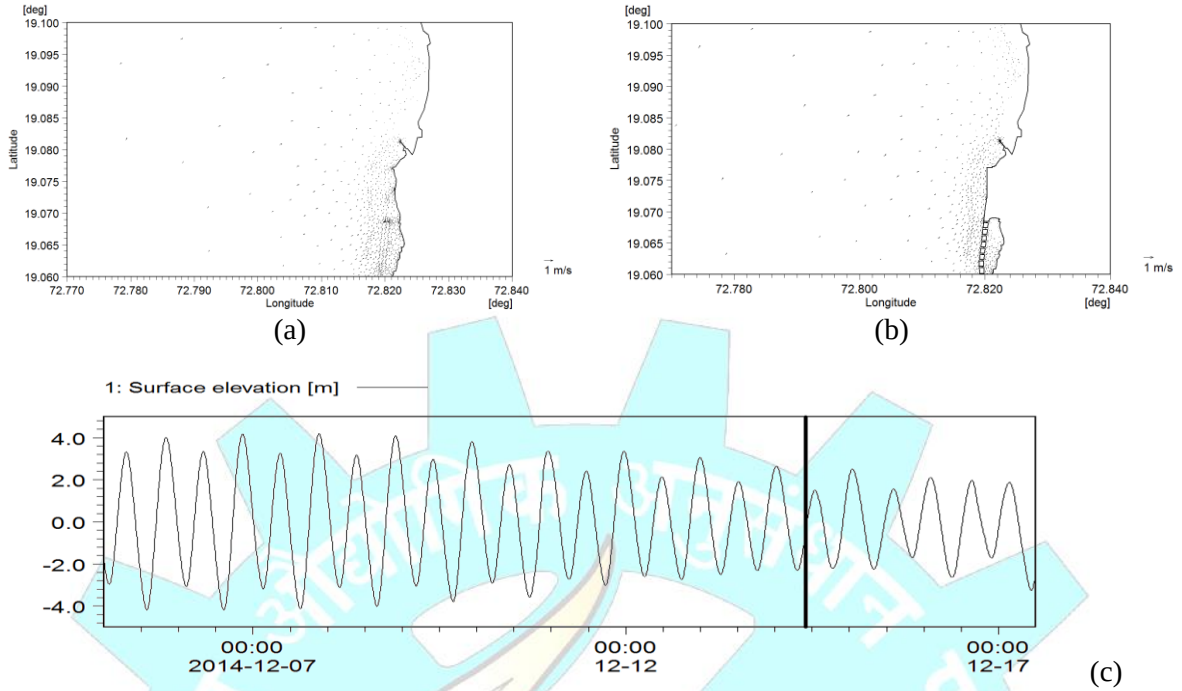

Fig. 4.30. Vector plot at mid tide during neap tide for section-II (a)Without Coastal Road (b) With Coastal Road (c) phase of tide

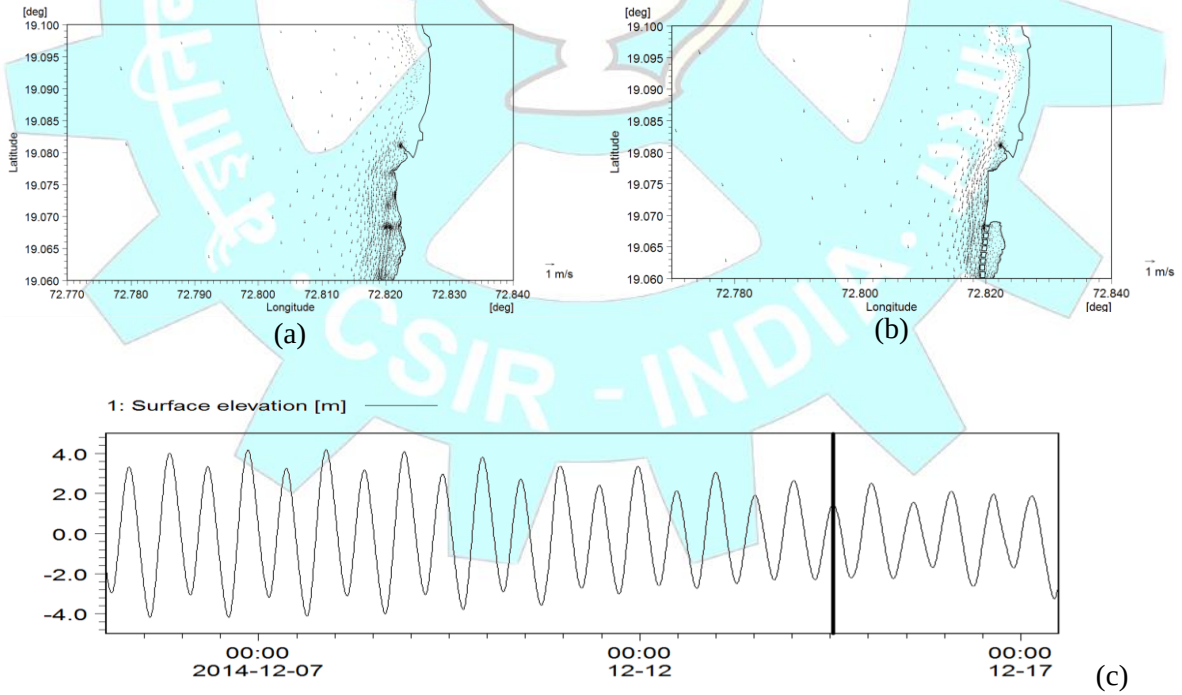

Fig. 4.31. Vector plot at high tide during neap tide for section-II (a)Without Coastal Road (b) With Coastal Road (c) phase of tide

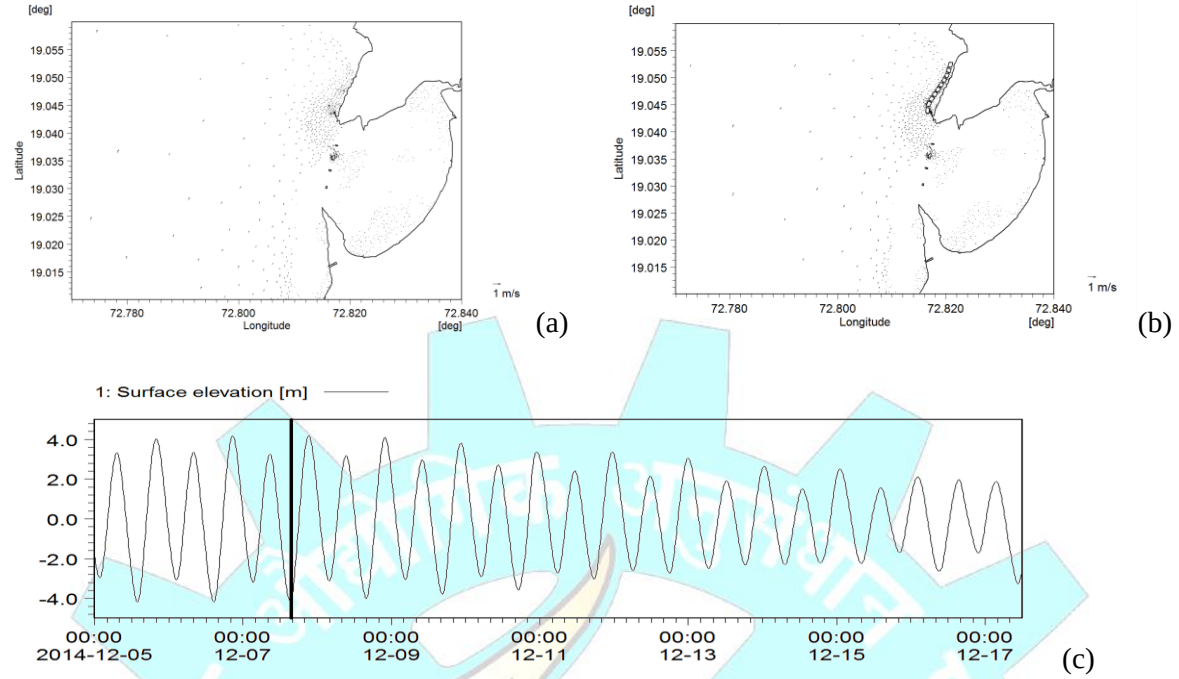

Fig. 4.32. Vector plot at low tide during spring tide for section-III (a)Without Coastal Road (b) With Coastal Road (c) phase of tide

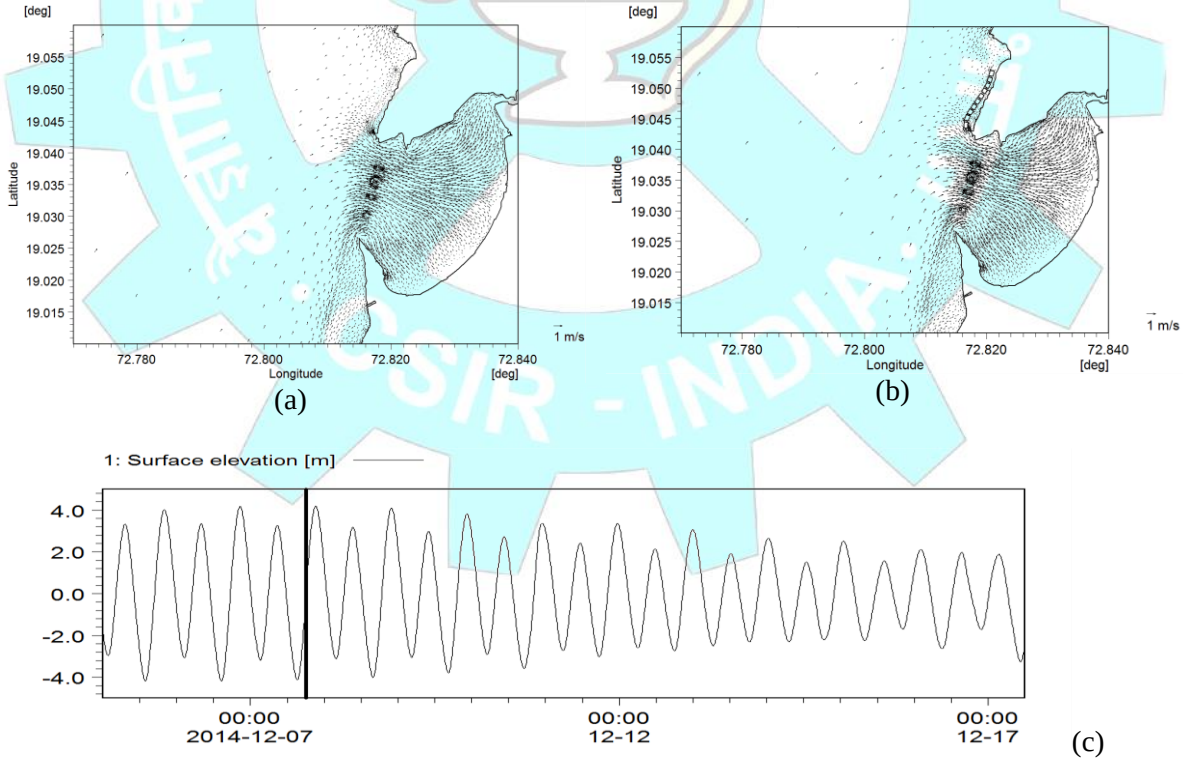

Fig. 4.33. Vector plot at mid tide during spring tide for section-III (a)Without Coastal Road (b) With Coastal Road (c) phase of tide

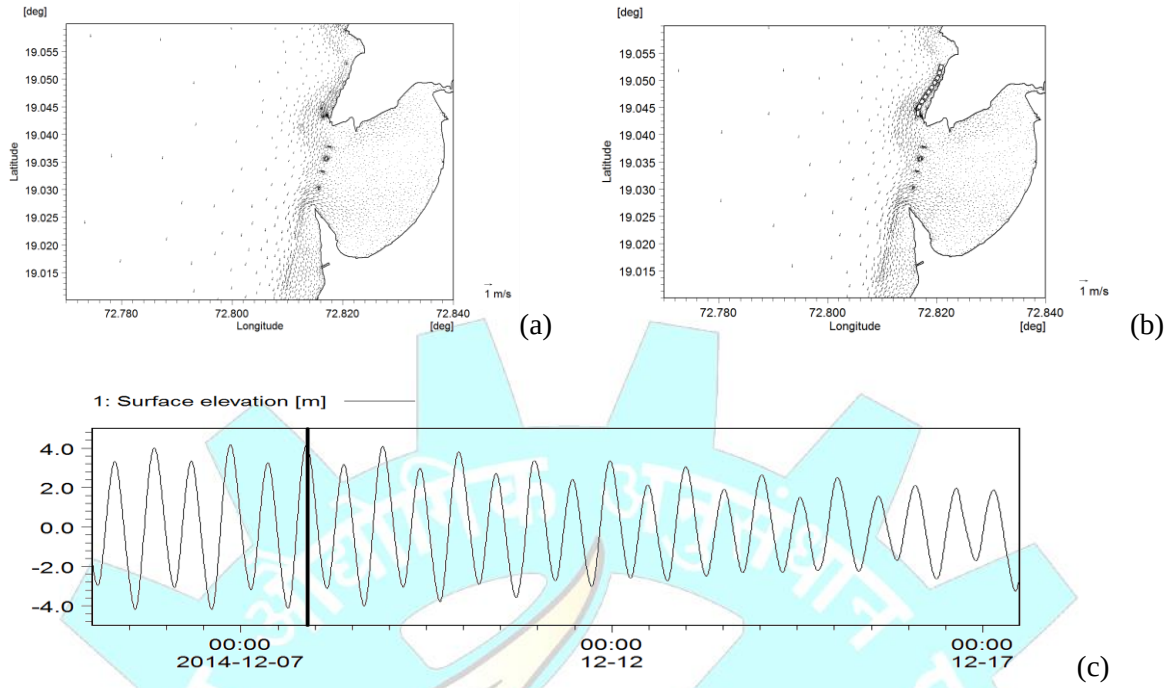

Fig. 4.34. Vector plot at high tide during spring tide for section-III (a)Without Coastal Road (b) With Coastal Road (c) phase of tide

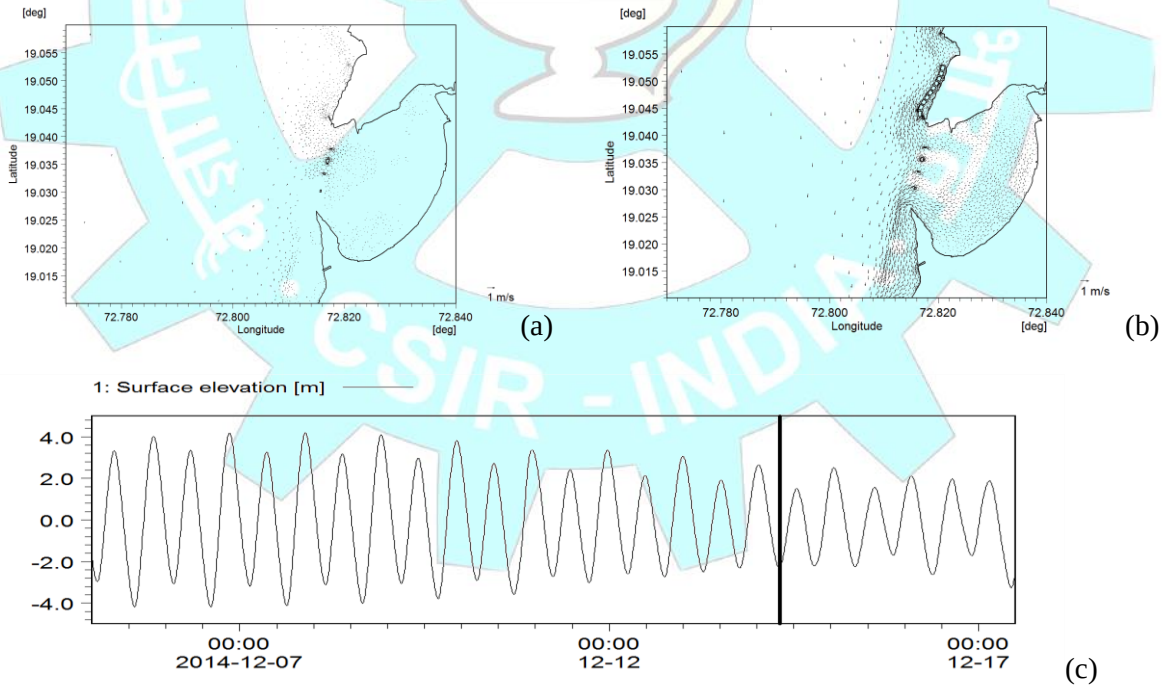

Fig. 4.35. Vector plot at low tide during neap tide for section-III (a)Without Coastal Road (b) With Coastal Road (c) phase of tide

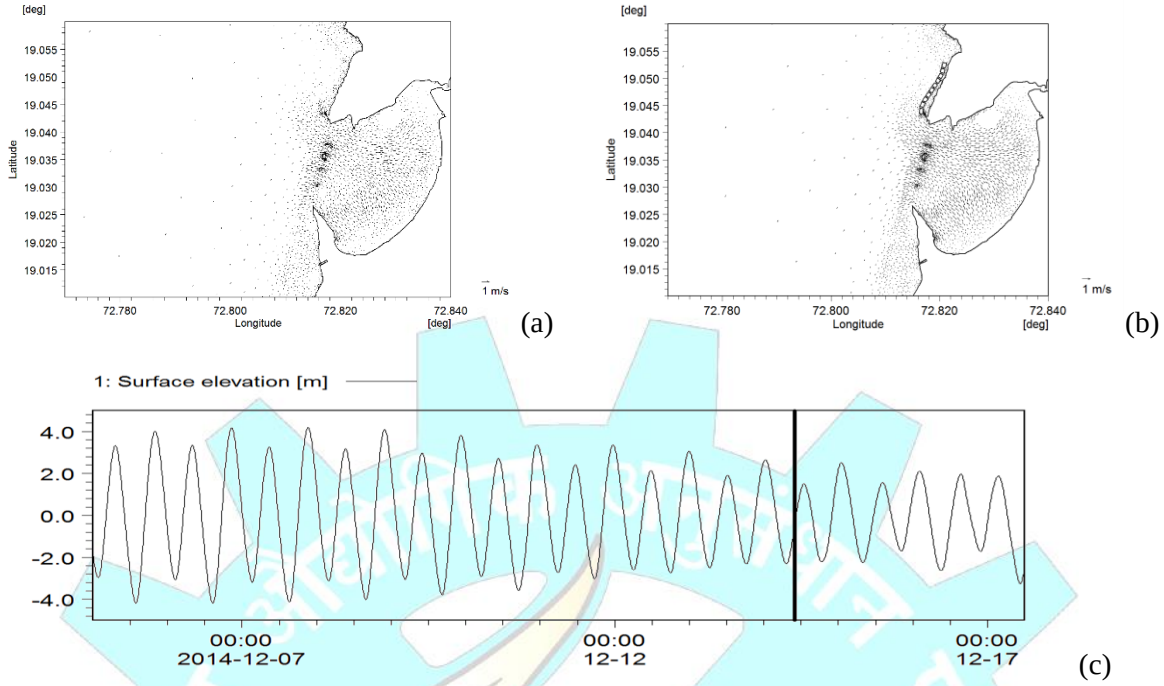

Fig. 4.36. Vector plot at mid tide during neap tide for section-III (a)Without Coastal Road (b) With Coastal Road (c) phase of tide

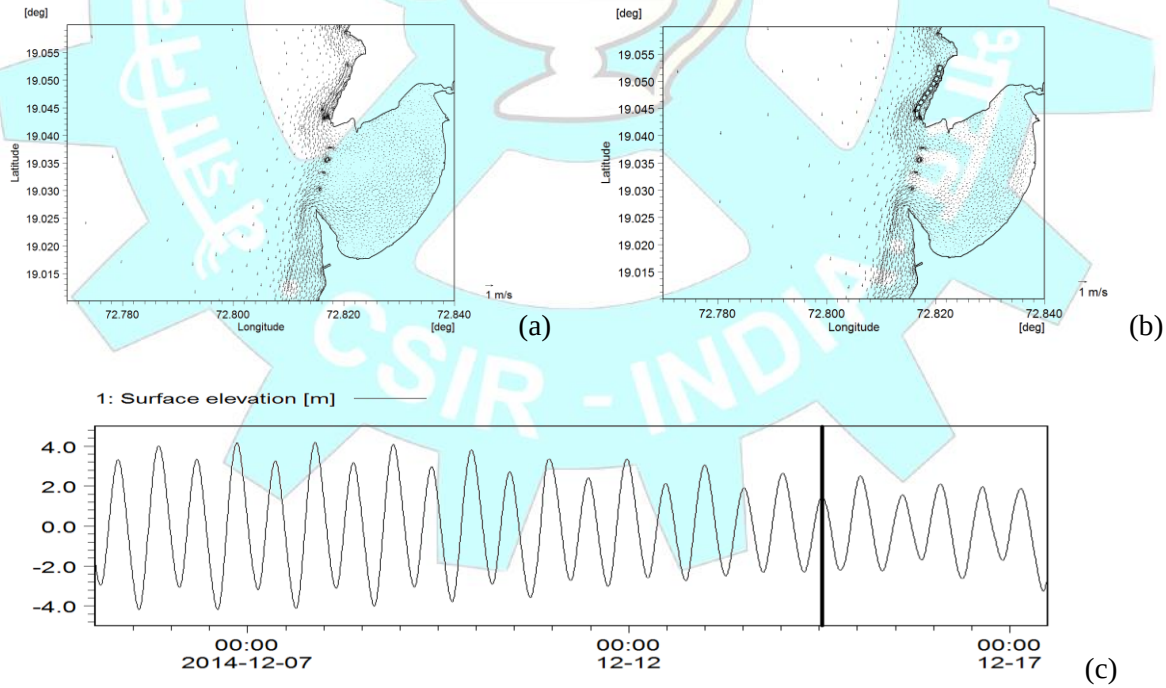

Fig. 4.37. Vector plot at high tide during neap tide for section-III (a)Without Coastal Road (b) With Coastal Road (c) phase of tide

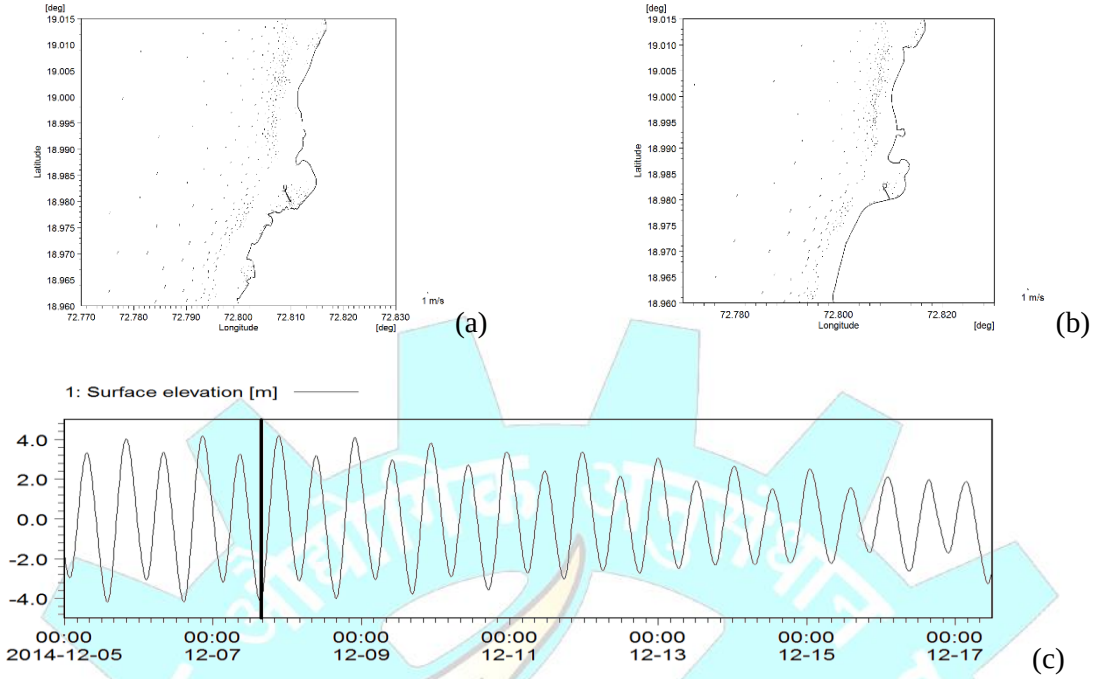

Fig. 4.38. Vector plot at low tide during spring tide for section-IV (a)Without Coastal Road (b) With Coastal Road (c) phase of tide

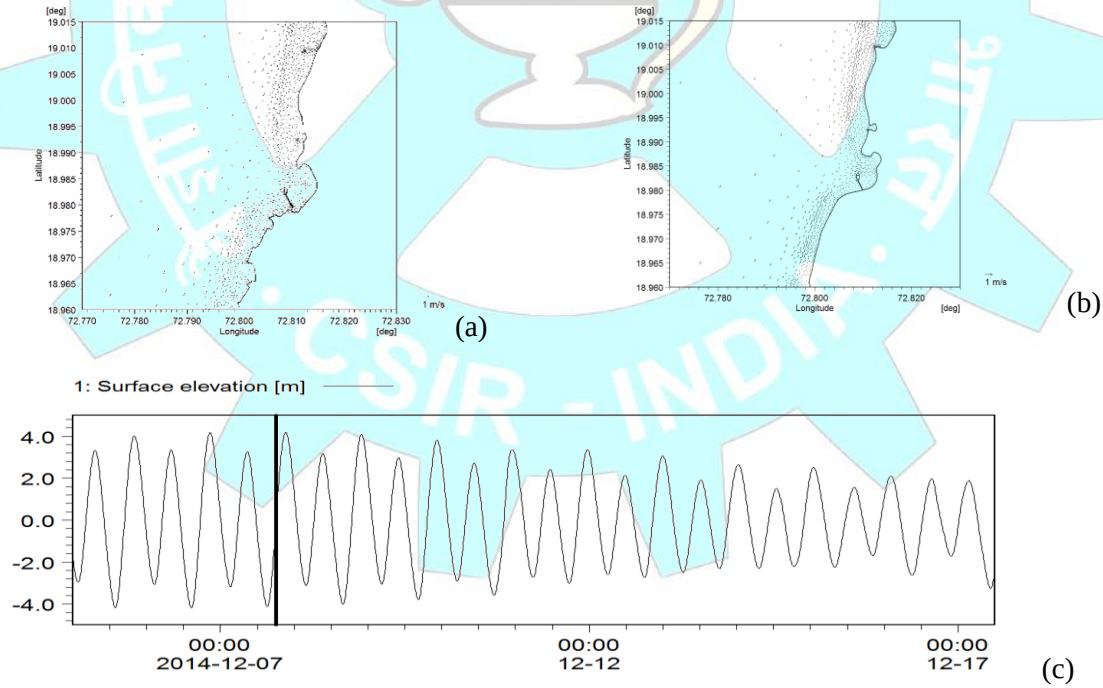

Fig. 4.39. Vector plot at mid tide during spring tide for section-IV (a)Without Coastal Road (b) With Coastal Road (c) phase of tide

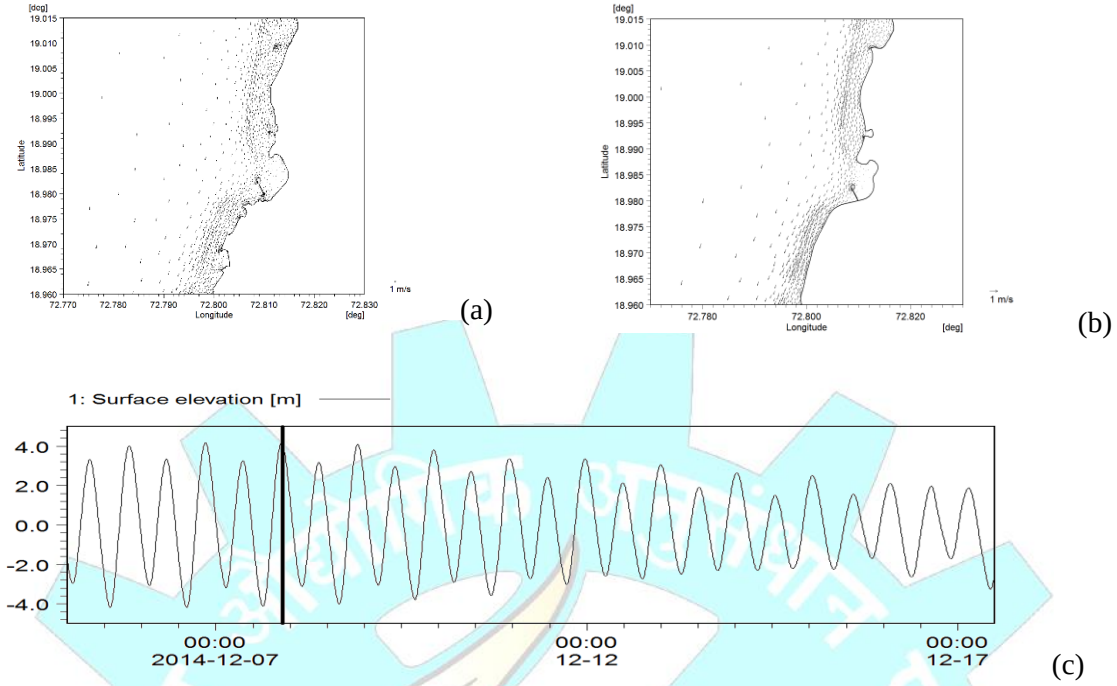

Fig. 4.40. Vector plot at high tide during spring tide for section-IV (a)Without Coastal Road (b) With Coastal Road (c) phase of tide

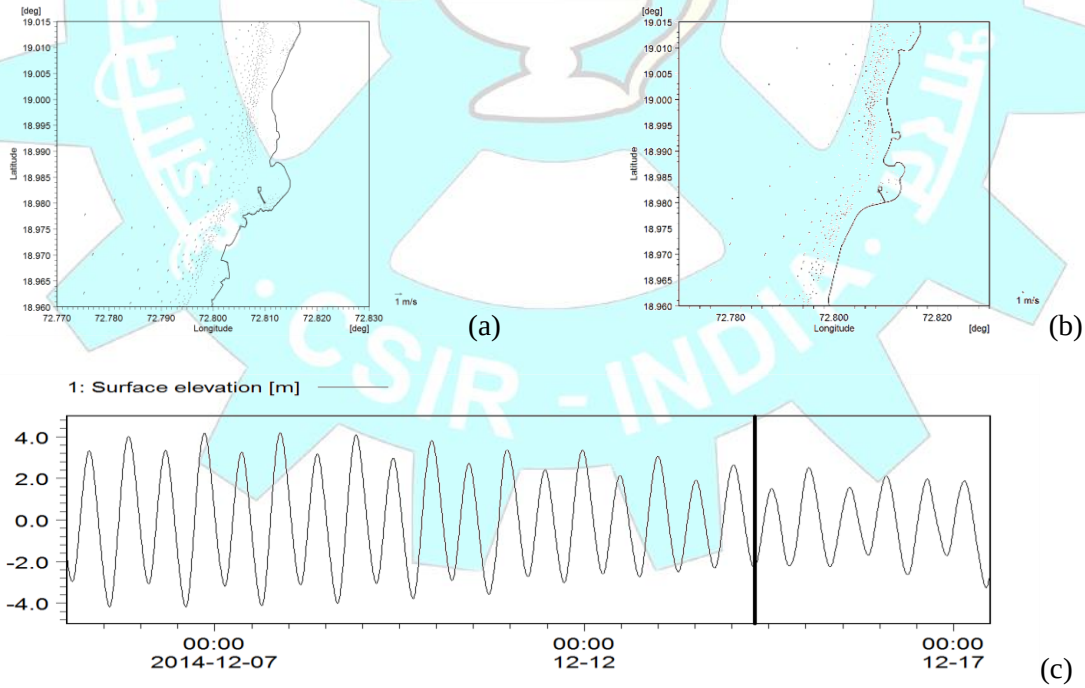

Fig. 4.41. Vector plot at low tide during neap tide for section-IV (a)Without Coastal Road (b) With Coastal Road (c) phase of tide

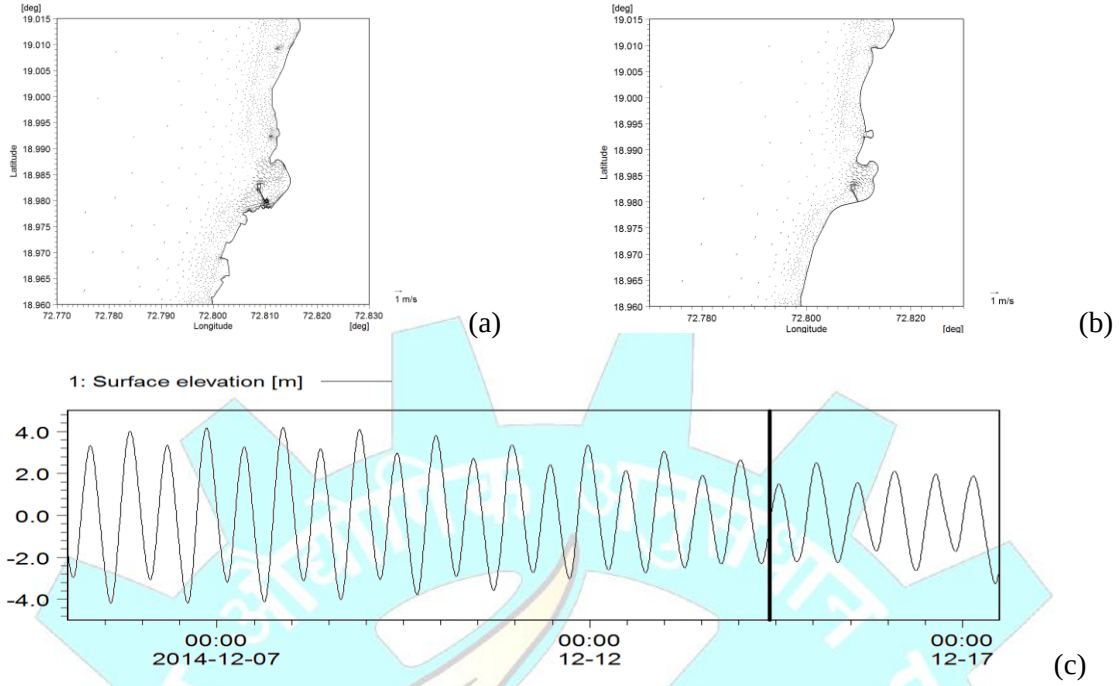

Fig. 4.42. Vector plot at mid tide during neap tide for section-IV (a)Without Coastal Road (b) With Coastal Road (c) phase of tide

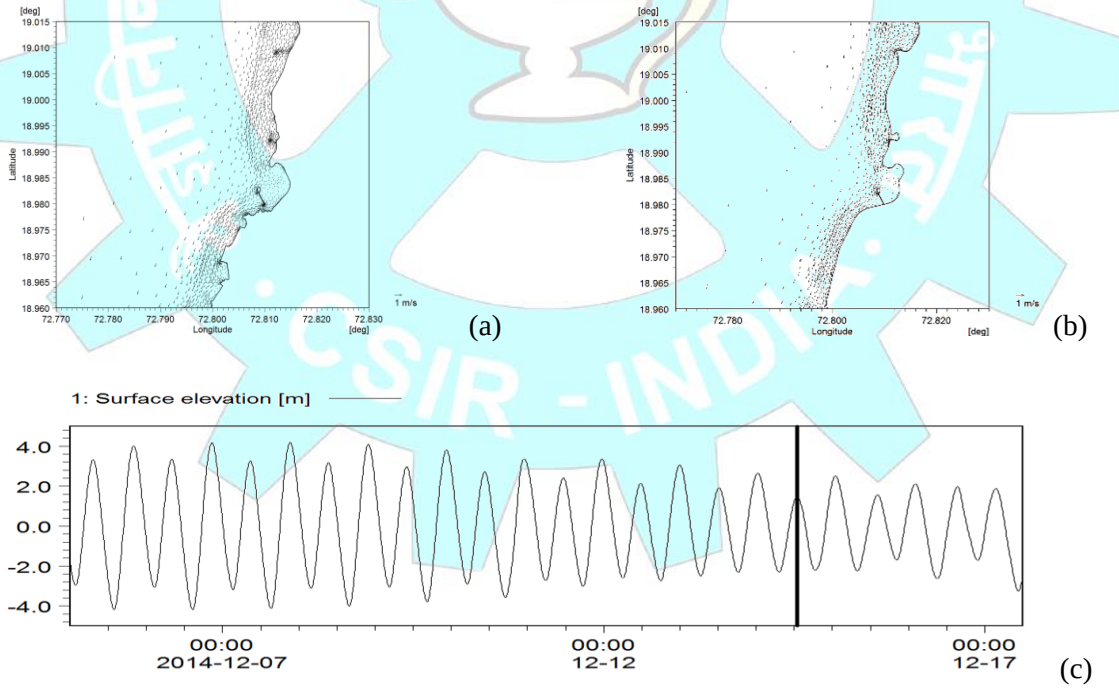

Fig. 4.43. Vector plot at high tide during neap tide for section-IV (a)Without Coastal Road (b) With Coastal Road (c) phase of tide

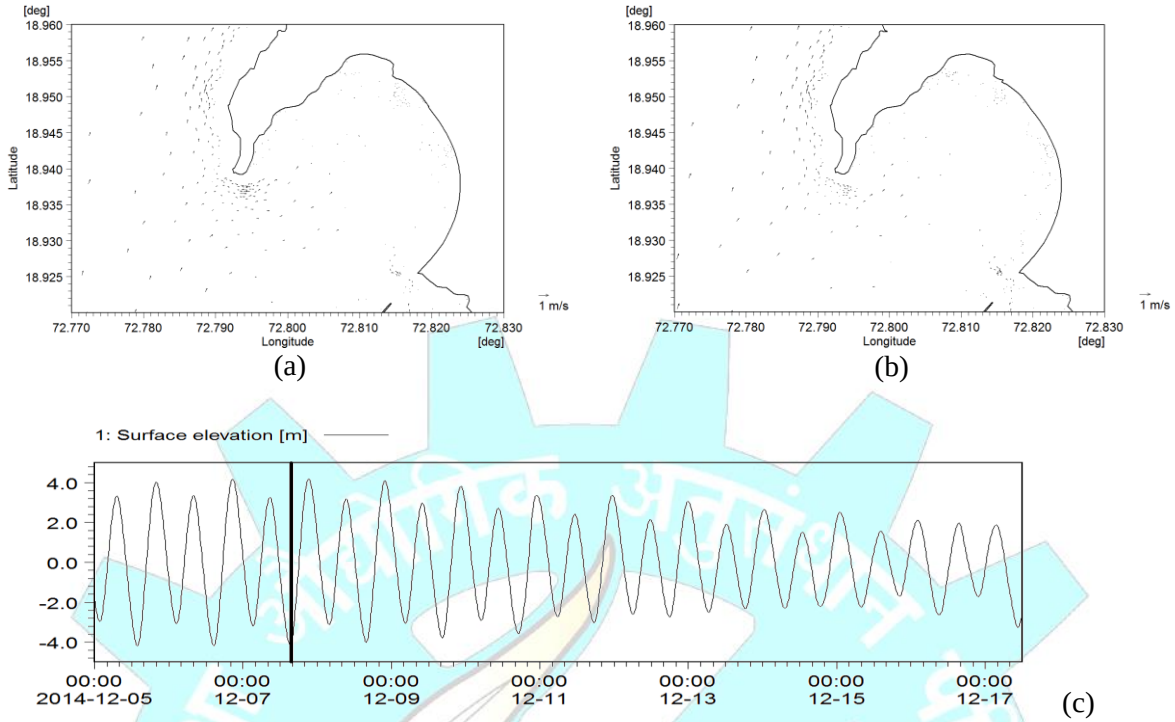

Fig. 4.44. Vector plot at low tide during spring tide for section-V (a)Without Coastal Road (b) With Coastal Road (c) phase of tide

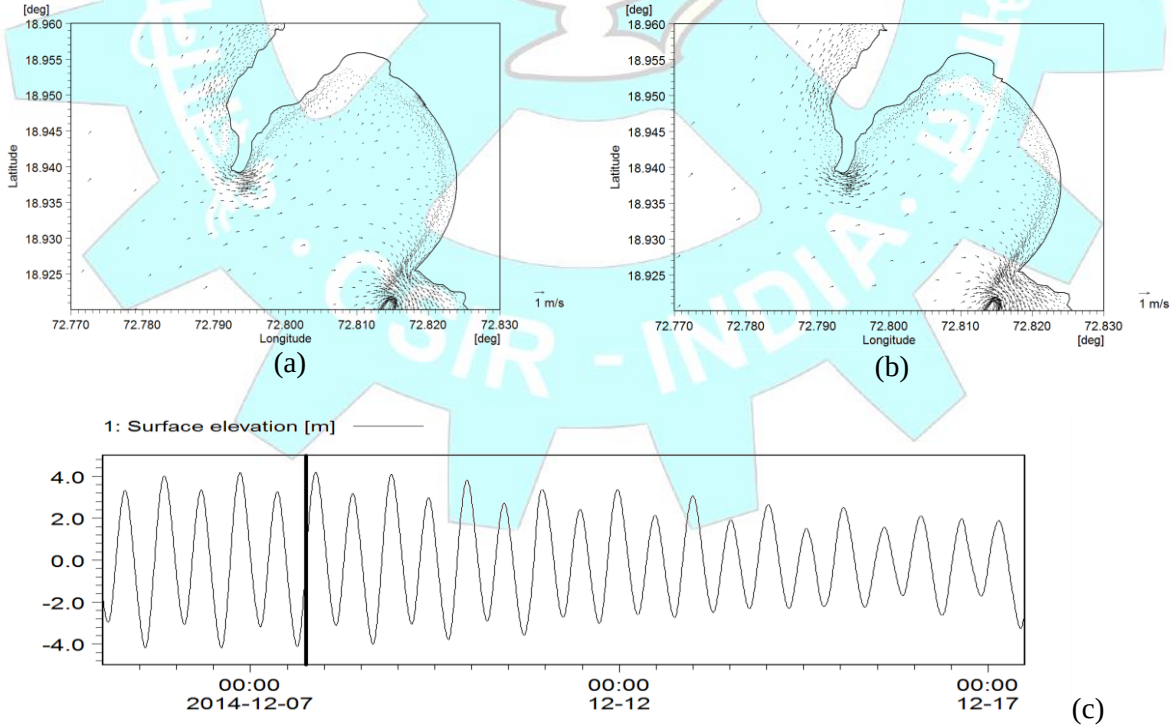

Fig. 4.45. Vector plot at mid tide during spring tide for section-V (a)Without Coastal Road (b) With Coastal Road (c) phase of tide

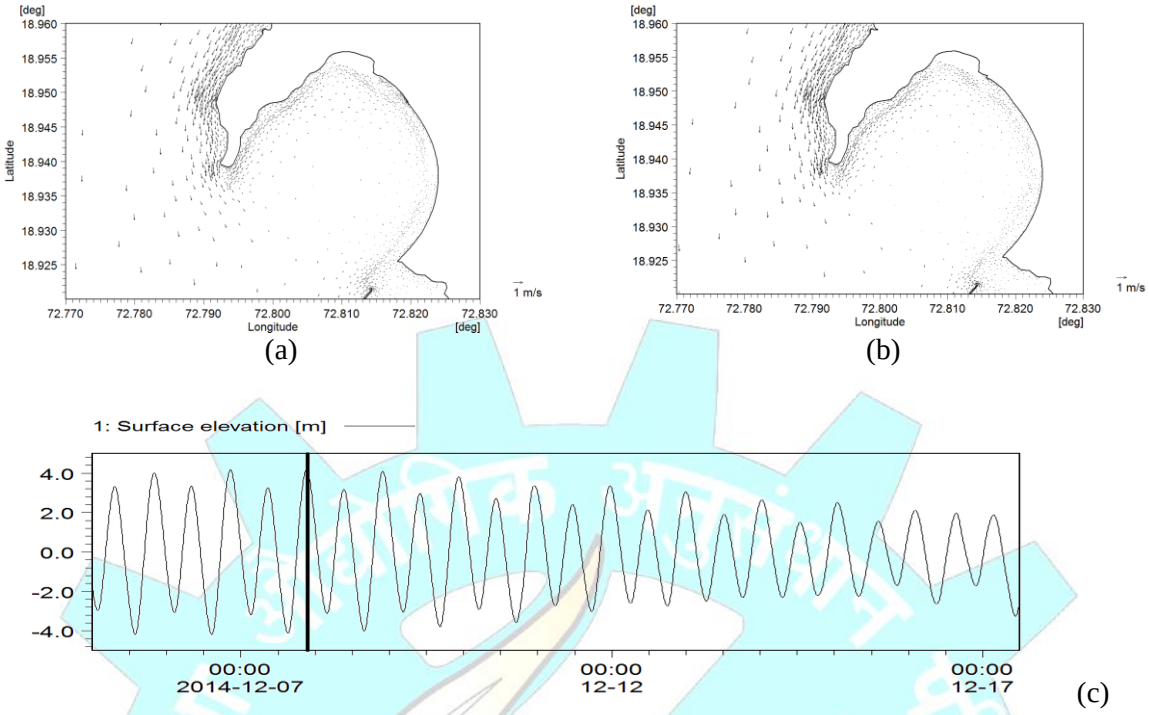

Fig. 4.46. Vector plot at high tide during spring tide for section-V (a)Without Coastal Road (b) With Coastal Road (c) phase of tide

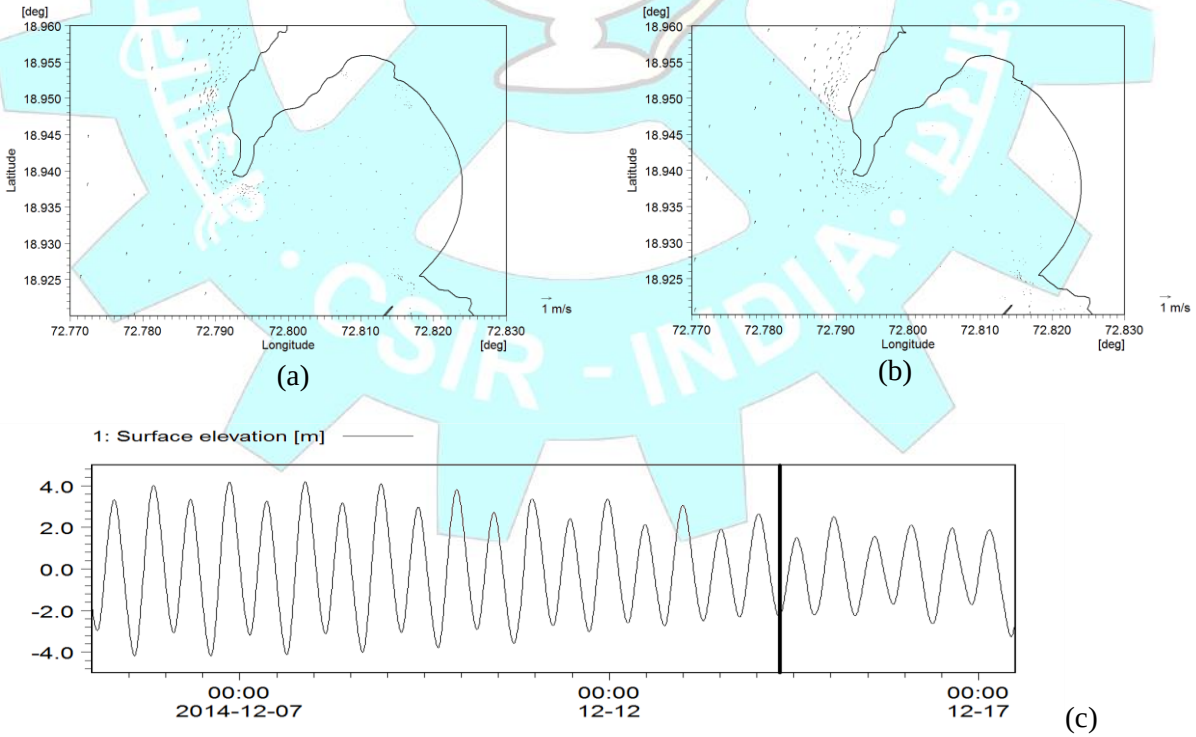

Fig. 4.47. Vector plot at low tide during neap tide for section-V (a)Without Coastal Road (b) With Coastal Road (c) phase of tide

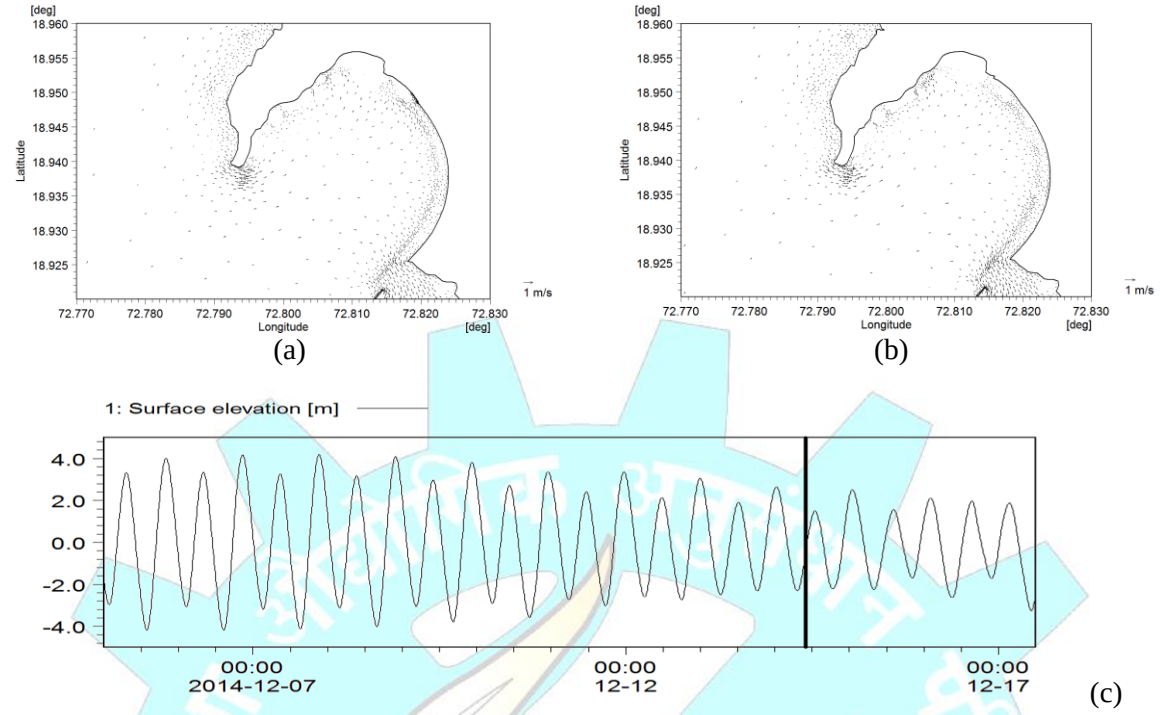

Fig. 4.48. Vector plot at mid tide during neap tide for section-V (a)Without Coastal Road (b) With Coastal Road (c) phase of tide

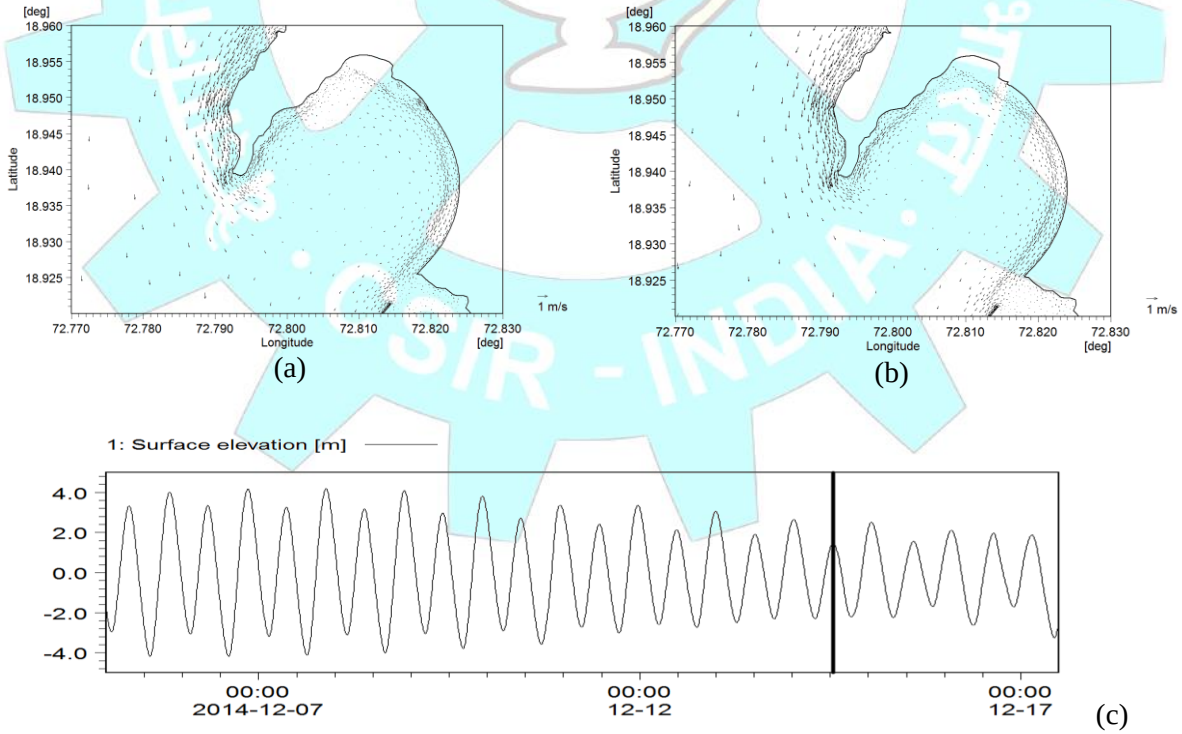

Fig. 4.49. Vector plot at high tide during neap tide for section-V (a)Without Coastal Road (b) With Coastal Road (c) phase of tide

4.5.3 Bed morphology change

The bed morphology changes after the end of 4 weeks simulation is presented in Fig. 4.50 to Fig. 4.54. Owing to the flow conditions, the morphology changes in the study region did not show any significant change. Overall changes in the bed morphology due to the proposed coastal road is less than 0.2m which is not significant in the near shore region. However, during the construction phase due to activities like trenching, placement of armour stones or driving of sheet pile walls, etc., there could be temporary changes in the near shore morphology. Such changes due to temporary construction activities would eventually be stabilized once these activities are complete.

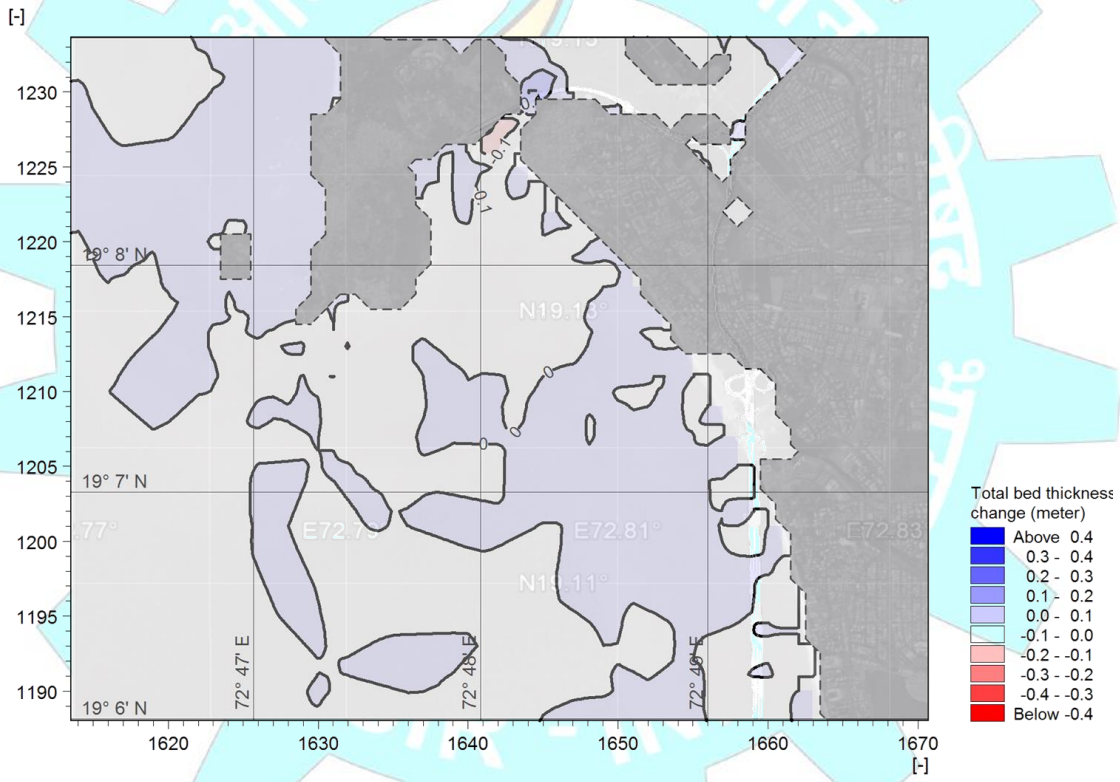

Fig. 4.50. Bed Level Change for Section-I

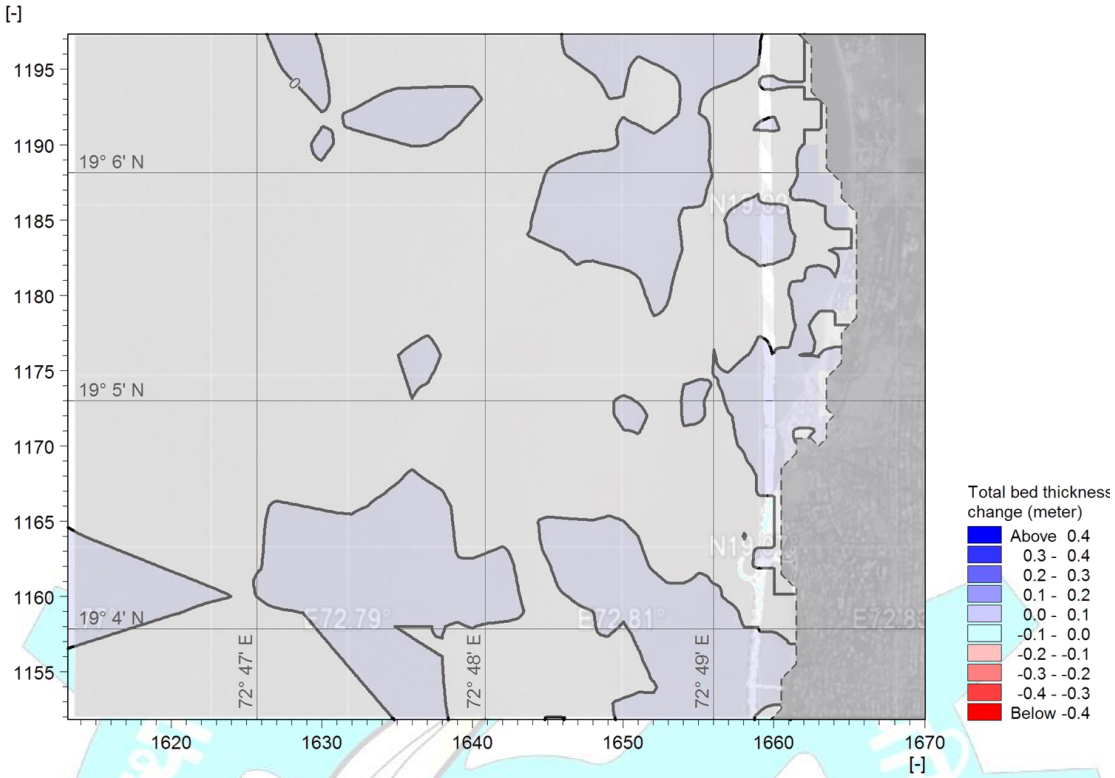

Fig. 4.51. Bed Level Change for Section-II

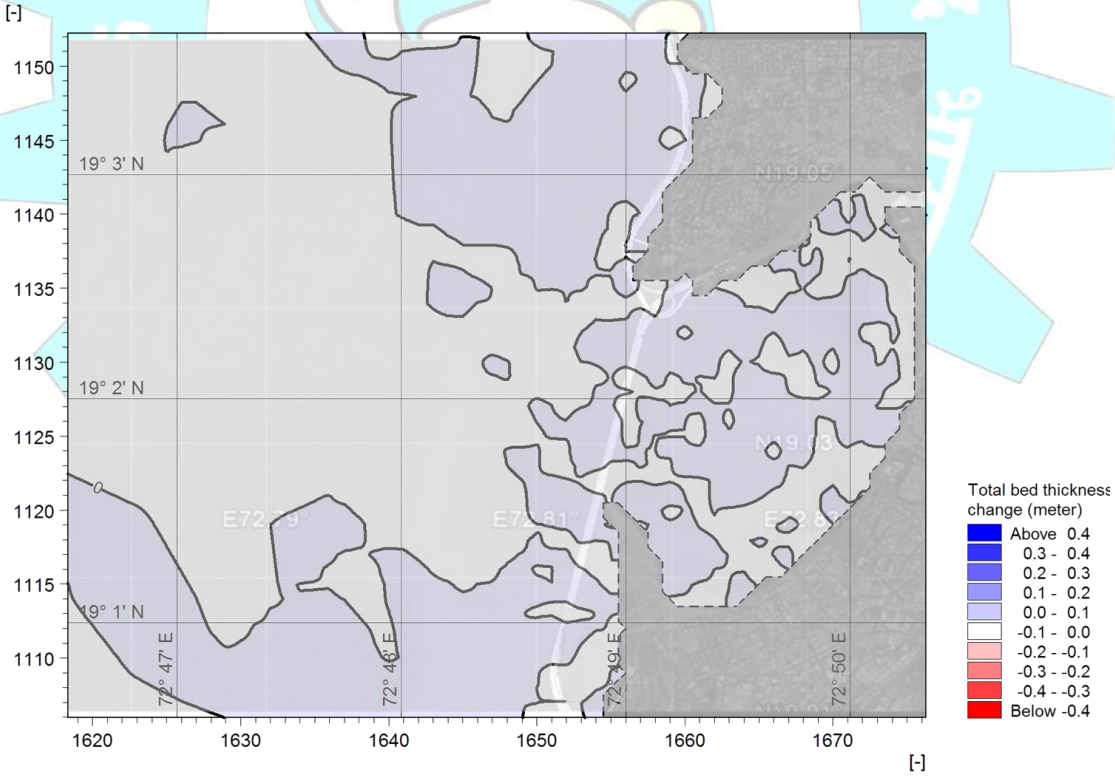

Fig. 4.52. Bed Level Change for Section-III

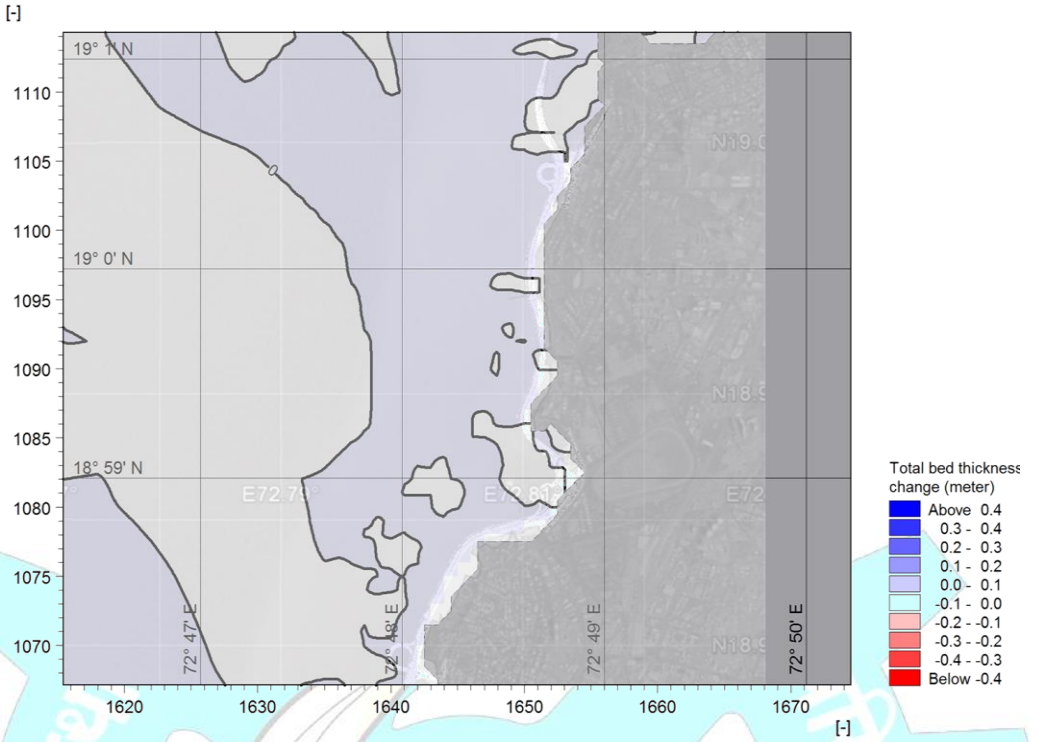

Fig. 4.53. Bed Level Change for Section-IV

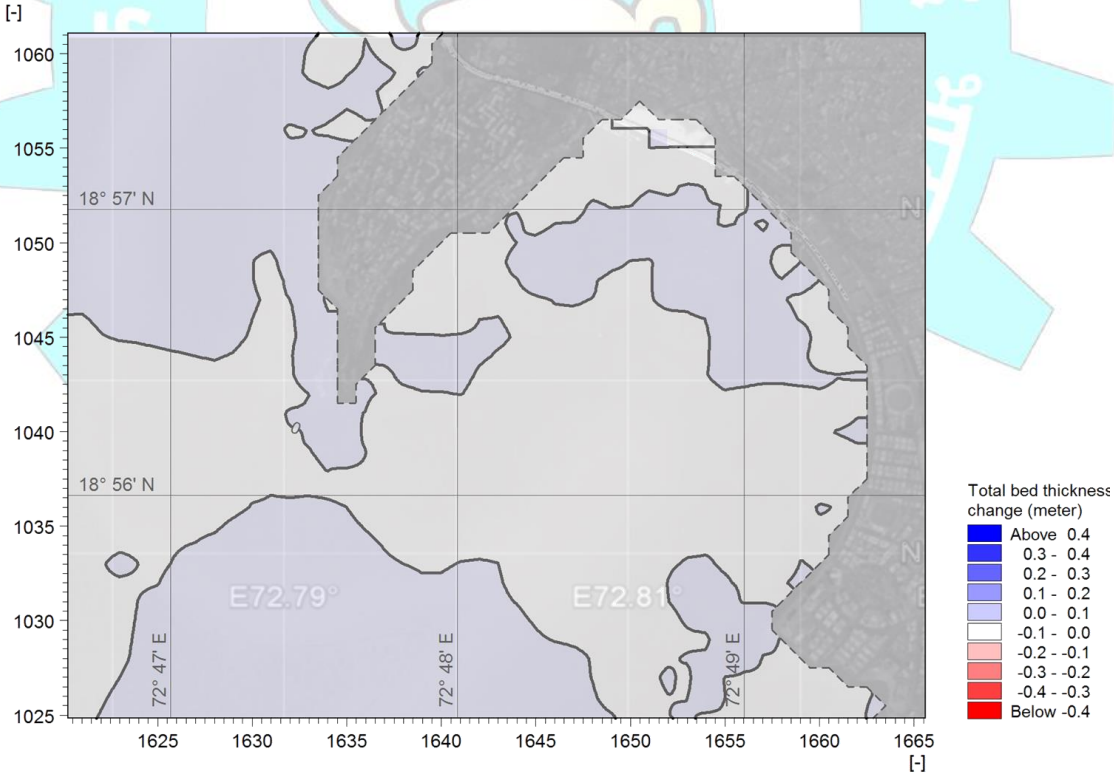

Fig. 4.54. Bed Level Change for Section-V

4.6 Impact assessment

The impacts on the hydrodynamics and morphology due to proposed changes in the coastal alignment are studied by comparing the model simulated flow conditions and morphology changes for modified scenario with the base case scenario. Twenty one points of which 9 points along the 10m contour (D1 to D9) and 12 points along 4 transects (Transect-1: T11,T12,T13; Transect-2: T21 to T23; Transect-3: T31 to T33 and Transect-4: T41 to T44) from shore to 70m depth (Fig. 4.55) are considered for comparing the changes in flow speeds and water levels.

The variation of flow speeds at these transect points for a period of 4 weeks is shown in Fig. 4.56 to Fig. 4.61. The change in flow speed at each of the transect point is estimated with reference to the base case. Similarly the variation of water level variation at each of the transect points for a same period is shown Fig. 4.62 to Fig. 4.67.

No significant changes in flow velocities are observed at all the control transect points considered in the study region. No significant changes in the water levels is observed in the study region due to the coastal road.

The bed morphology changes in the base case simulation are observed to be of the order 0.2m in the whole domain, which is insignificant.

The model study indicated that the influence of coastal road on the overall hydrodynamics and morphology of the region is negligible.

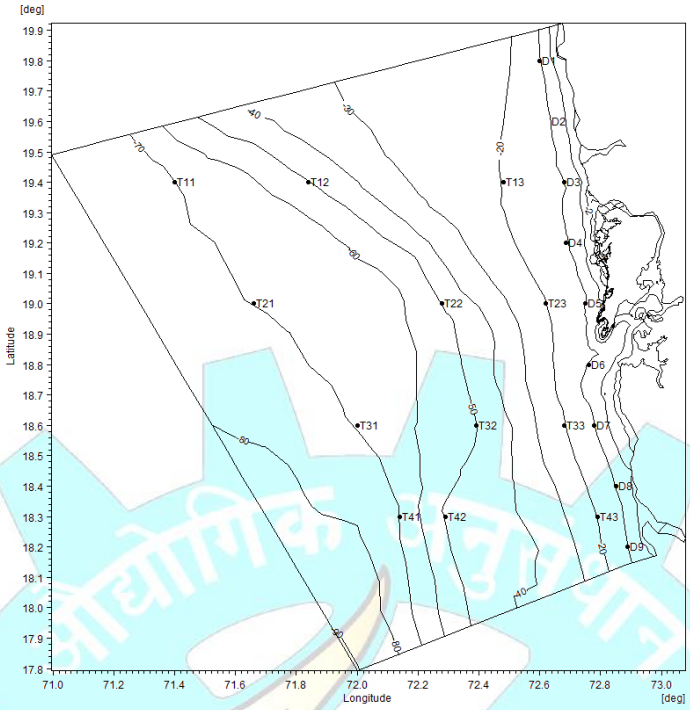

Fig. 4.55. Plot showing the locations considered for comparing time series of tides and flow speeds for the two cases

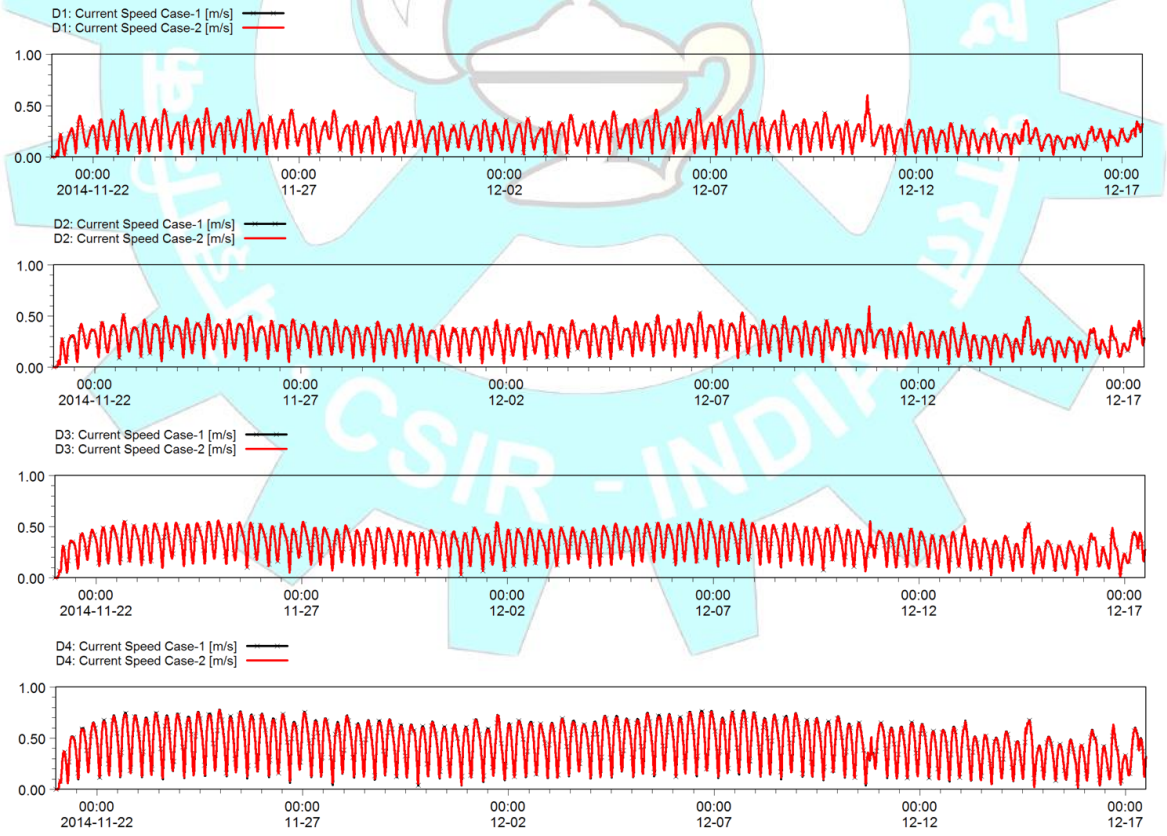

Fig. 4.56. Plot showing variation of current speed at points D1 to D4 along 10m contour for Case-1(Base), Case-2(with coastal road)

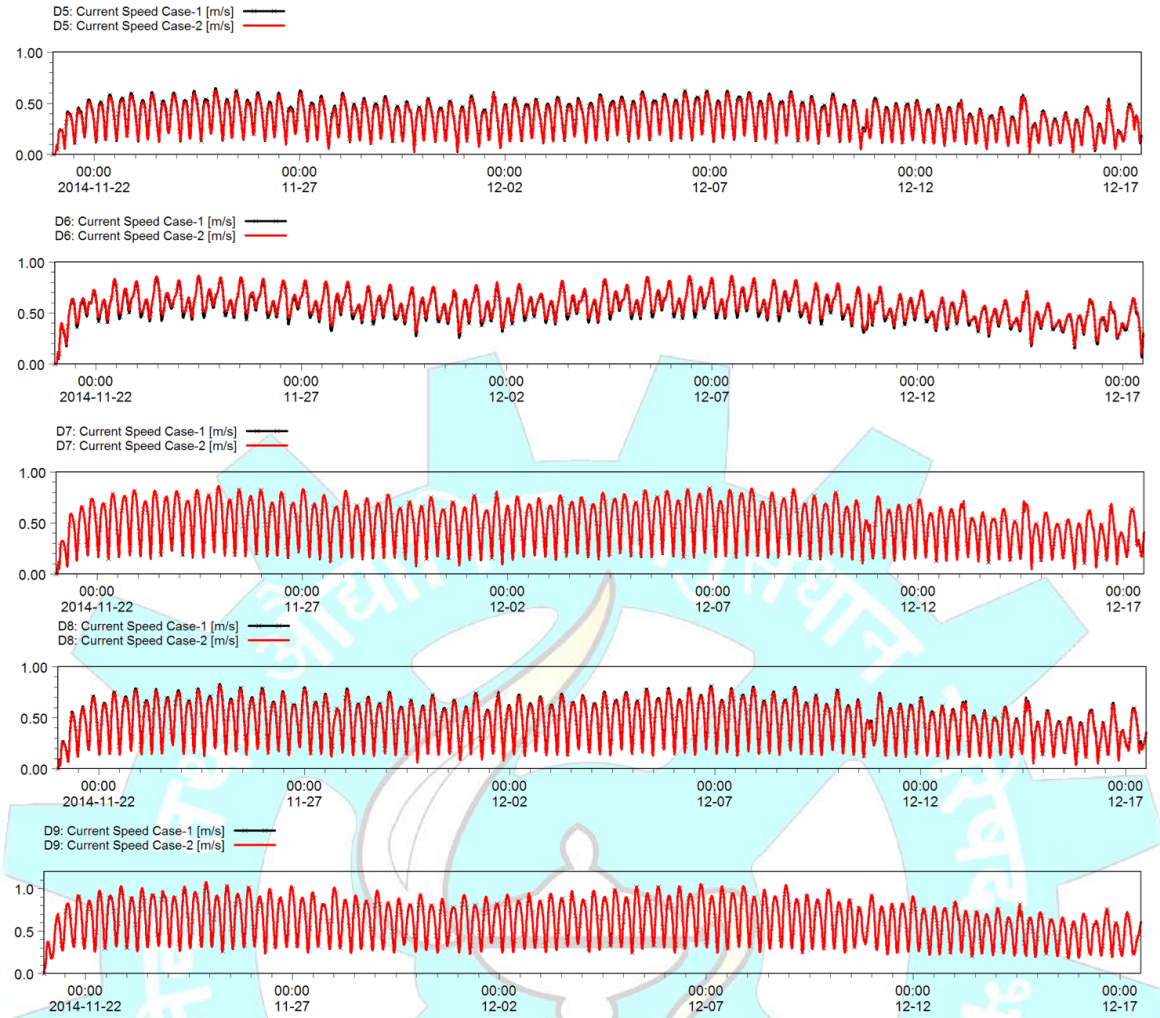

Fig. 4.57. Plot showing variation of current speed at points D5 to D9 along 10m contour for Case-1(Base), Case-2(with coastal road)

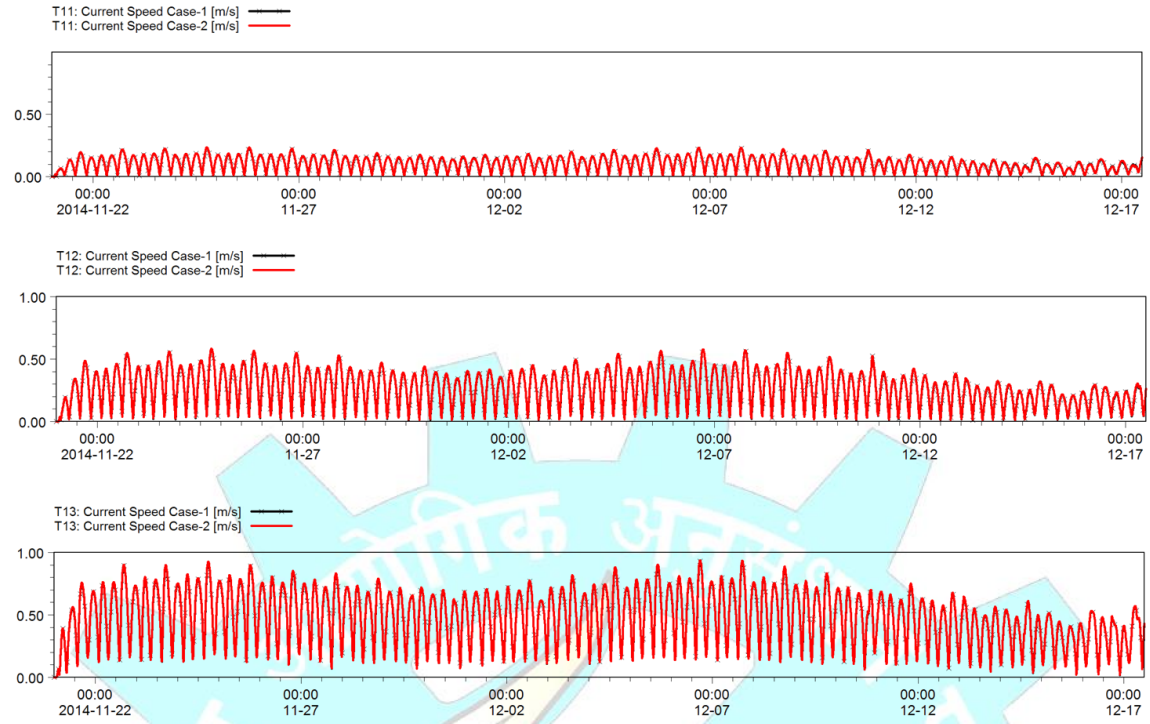

Fig. 4.58. Plot showing variation of current speed at points T11 to T13 along transect T1 for Case-1(Base), Case-2(with coastal road)

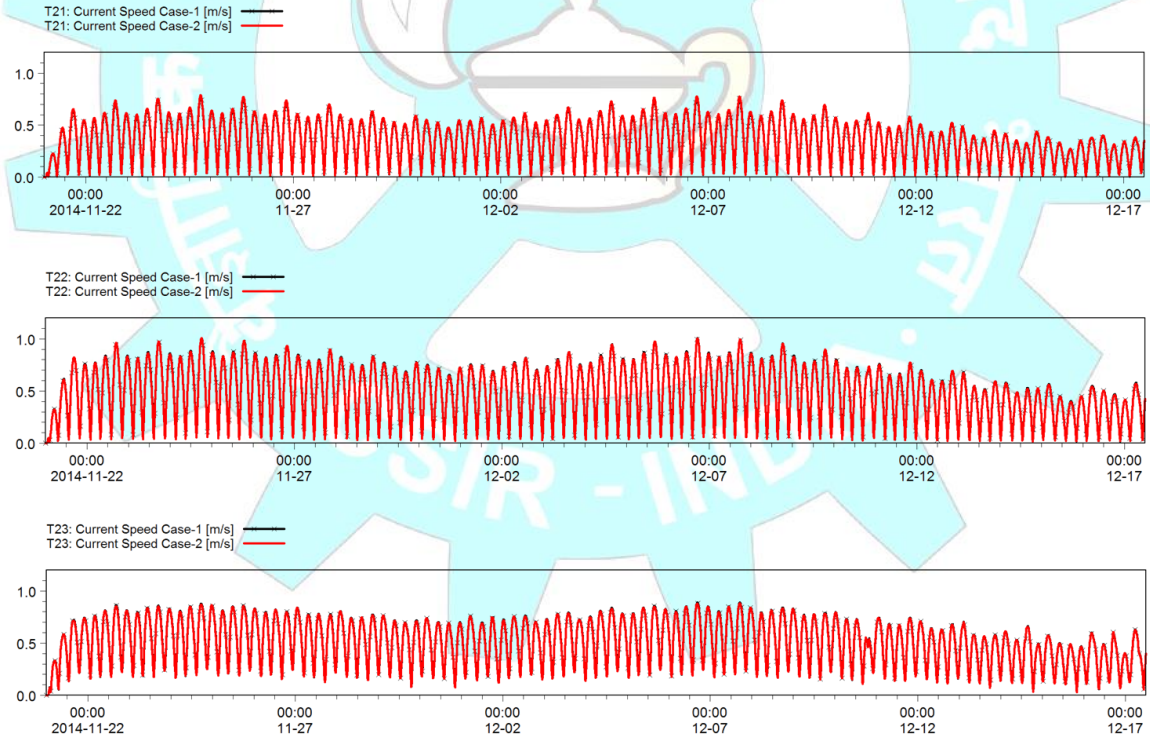

Fig. 4.59. Plot showing variation of current speed at points T21 to T23 along transect T2 for Case-1(Base), Case-2(with coastal road)

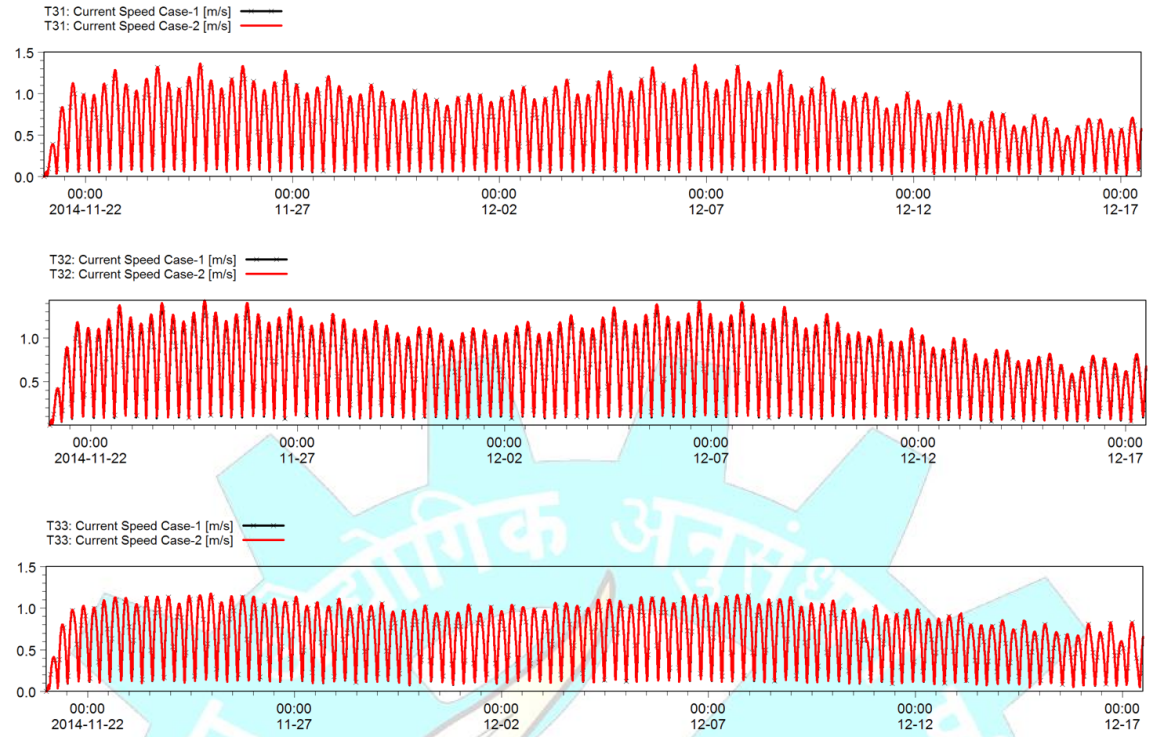

Fig. 4.60. Plot showing variation of current speed at points T31 to T33 along transect T3 for Case-1(Base), Case-2(with coastal road)

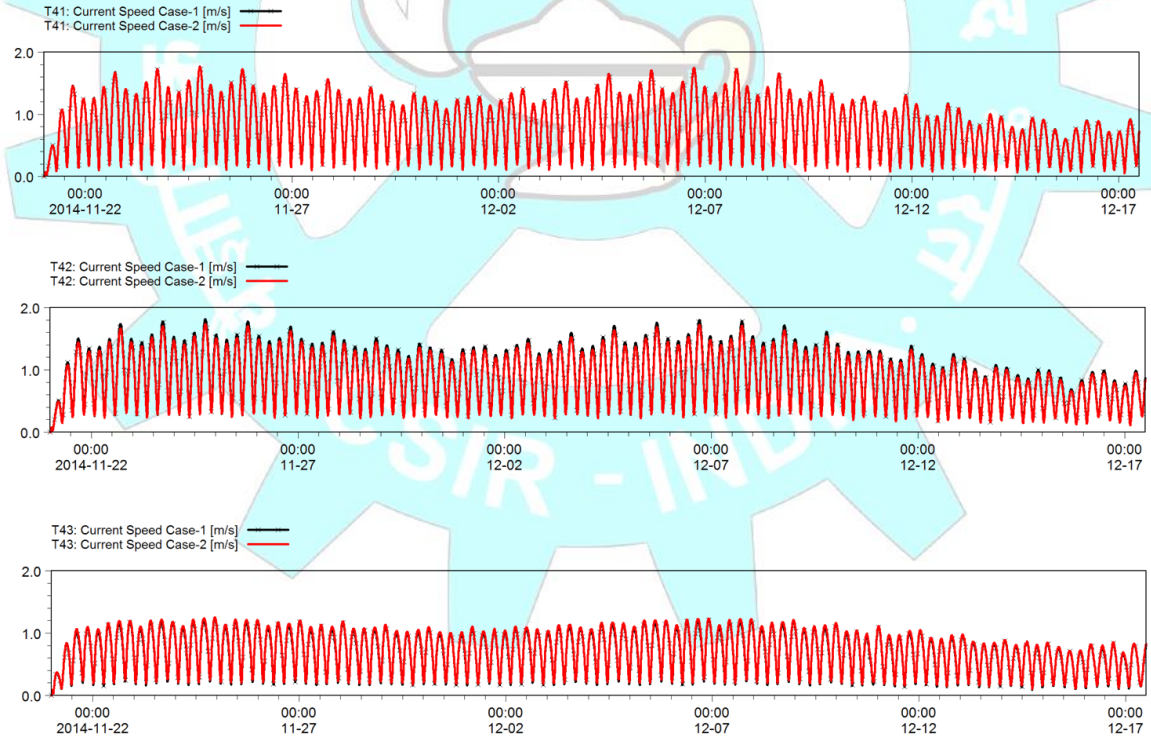

Fig. 4.61. Plot showing variation of current speed at points T41 to T43 along transect T4 for Case-1(Base), Case-2(with coastal road)

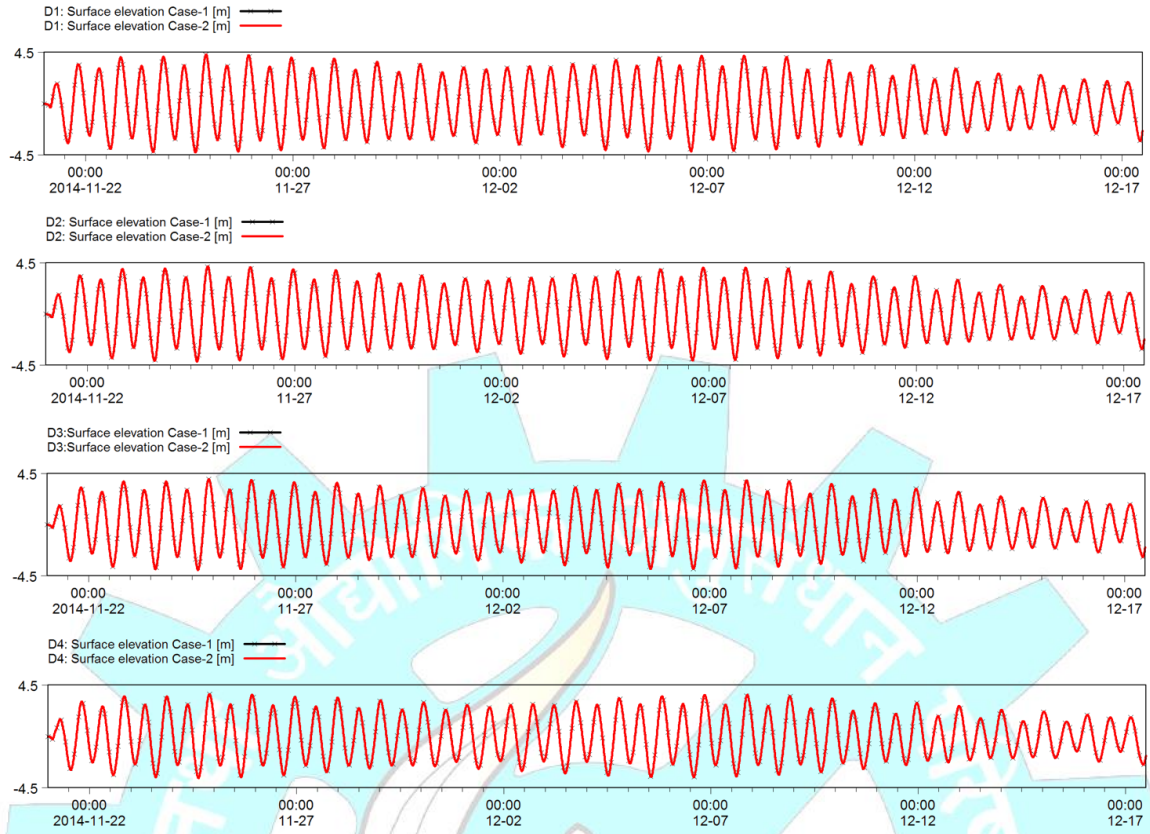

Fig. 4.62. Plot showing variation of surface elevation at points D1 to D4 along 10m contour for Case-1(Base), Case-2(with coastal road)

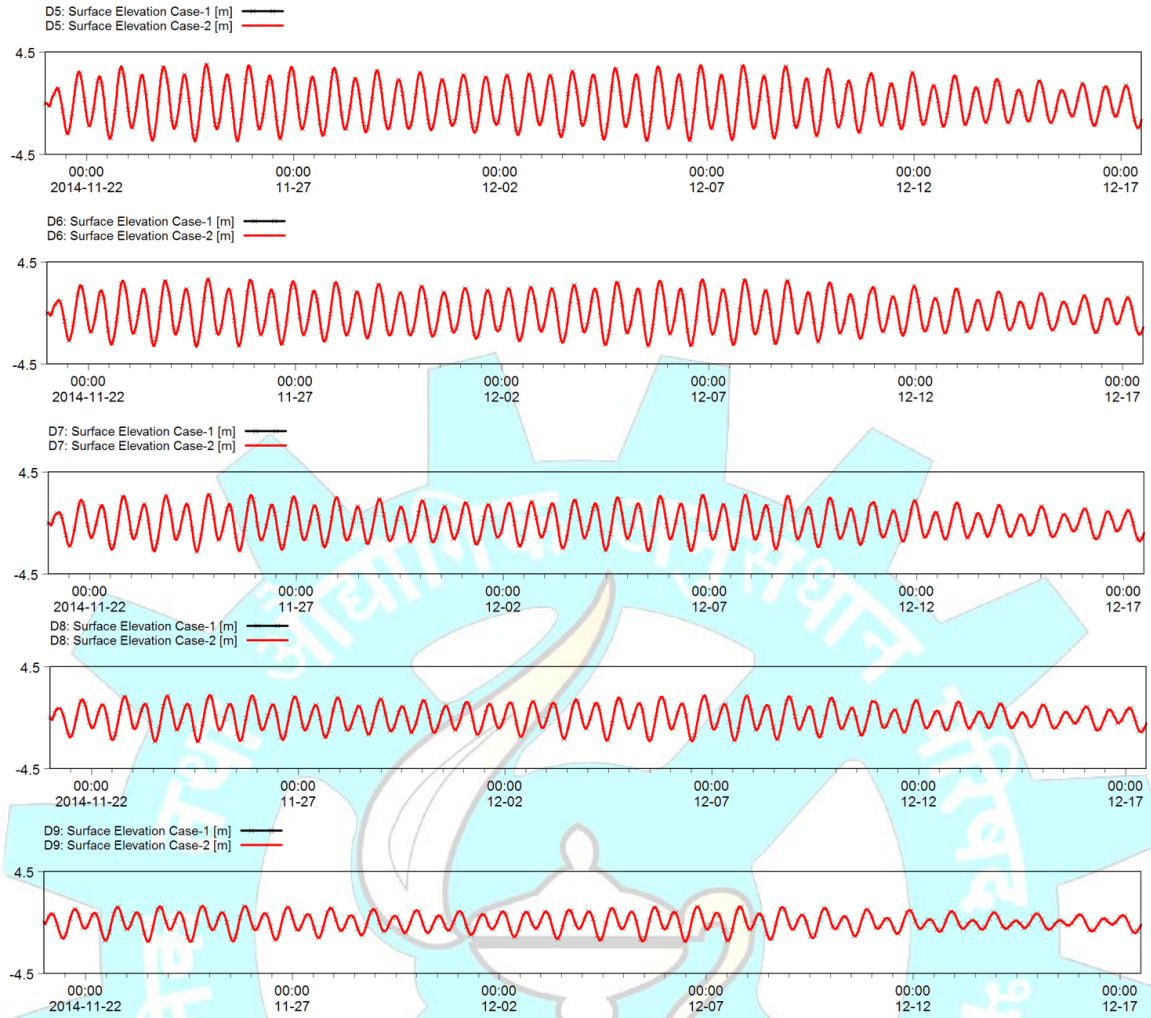

Fig. 4.63. Plot showing variation of surface elevation at points D5 to D9 along 10m contour for Case-1(Base), Case-2(with coastal road)

Fig. 4.64. Plot showing variation of surface elevation at points T11 to T13 along transect T1 for Case-1(Base), Case-2(with coastal road)

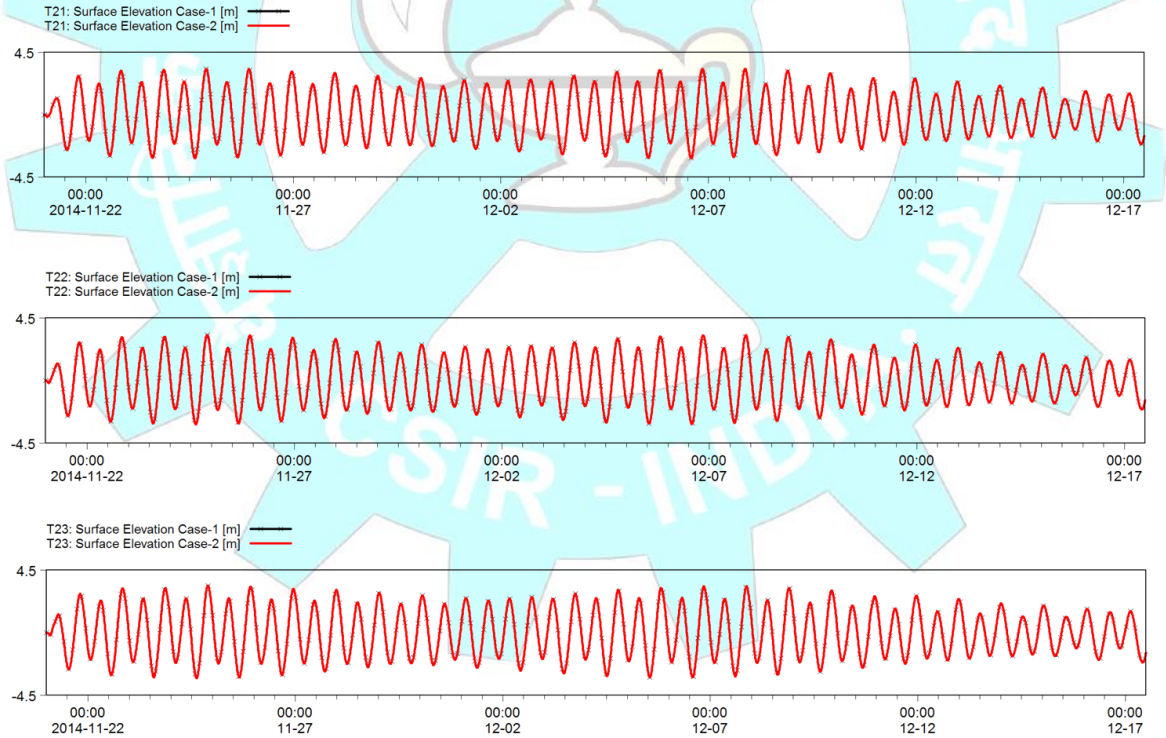

Fig. 4.65. Plot showing variation of surface elevation at points T21 to T23 along transect T2 for Case-1(Base), Case-2(with coastal road)

Fig. 4.66. Plot showing variation of surface elevation at points T31 to T33 along transect T3 for Case-1(Base), Case-2(with coastal road)

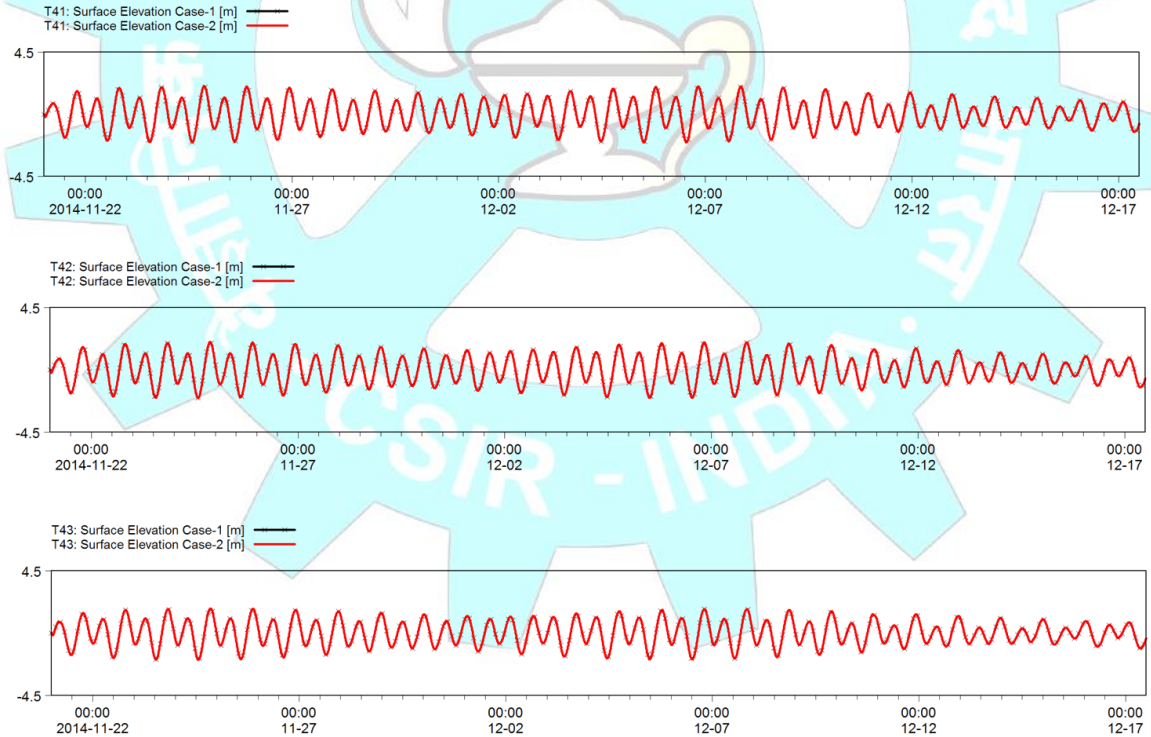

Fig. 4.67. Plot showing variation of surface elevation at points T41 to T43 along transect T4 for Case-1(Base), Case-2(with coastal road)

Chapter 5

5 CONCLUSIONS

5.1 Conclusions

The extreme values of storm surges, tsunami amplitudes, and significant wave heights are estimated for 19 points in the near shore region along the coastal road. From these 19 points the ranges of extreme values are presented in these conclusions. The conclusions from this study based on numerical model studies are:

- The design wave heights, storm surge elevation and tsunami amplitudes for the study region were estimated using various numerical models. The tidal range was taken from the available literature.
- The maximum storm induced wave height in the near shore region is estimated to be 4.89m in 20 m water depth for the 1982 cyclone. The maximum storm surge estimated for a cyclonic storm passed close to Mumbai coast is 1.5m for the 2001 cyclone. The tsunami amplitudes for an input earthquake magnitude of 9Mw earthquake are estimated to vary between 0.48m and 0.73m along the coastal road.
- Based on long term wave hindcast data combined with storm waves, the design wave height at 20 m depth for 1in100 year return period is estimated as 7.2m while along coastal road project the design wave heights varied between 0.5m and 1.9m.
- The hydrodynamics off the Mumbai coast ascertained through measurements and validated numerical models. The numerical models used in the study provide reliable and reasonable results pertaining to hydrodynamics of the region. The comparison of flow vectors and flow along the transect points showed that there is no significant change in flow conditions due to coastal road facilities.
- The difference in near shore morphology changes between the base case and the final coastal road alignment case, based on numerical model studies, is observed to be insignificant.

5.2 Recommendations

- During the coastal road construction activities, it is likely that there would be changes in the local flow conditions. These changes would stabilise once the construction activity ceases.
- In order to keep a check on the changes in the tidal elevations, wave and flow conditions, it is essential to continuously monitor the hydrodynamics and water quality parameters before starting, as well as during the project execution phase and further for a period of 2 years after completion of project.

- Necessary precautions should be taken so as to minimise the turbidity of the coastal waters during the reclamation and/or other offshore/coastal construction activities.
- Periodic monitoring of the sandy beaches and the shoreline should be carried out through cross-section profiles measurements and shoreline change studies so that a record of status of the coast before, during and after the project is available.

END OF THE DOCUMENT